MASTER OF PHILOSOPHY

Mathematical modelling of negative feedback signal transduction processes

Aldakheel, Sahar Ahmed Aziz

Award date:
2014

Awarding institution:
University of Dundee

MASTER OF PHILOSOPHY

Mathematical modelling of negative feedback signal transduction processes

Sahar Ahmed Aziz Aldakheel

2014

University of Dundee

Mathematical Modelling of Negative Feedback Signal Transduction Processes

By

Sahar Ahmed Aziz Aldakheel

A Thesis submitted for the degree of Master of Philosophy

Division of Mathematics

University of Dundee

Dundee

January 2014

To my husband
To my son (Ahmed)

Contents

Acknowledgements

My sincere thanks go to Professor M.A.J. Chaplain for accepting me as a PhD student, giving me the best opportunity to challenge myself and teaching me the most advance techniques in Mathematical Biology; for his outstanding supervision, his endless support, endless patience and the encouragement, and also for the proofreading of this thesis and teaching me how to write in a scientific way. Many thanks also to Marc Sturrock for endless help and encouragement.

My warmest thanks go to my parents for their love, support and encouragement. To everyone in my family, thank you very much for your support. Finally, I would like to thank my husband Saleh for pointing me in the right direction before I came to the UK and his encouragement, endless help and for his astonishing company.

This work was sponsored by Ministry of Higher Education , Riyadh, Saudi Arabia.

Declaration

I declare that the following thesis is my own composition and that it has not been submitted before in application for a higher degree.

Sahar Aldakheel

Certification

This is to certify that Sahar Aldakheel has complied with all the requirements for the submission of this Master of Philosophy thesis to the University of Dundee.

Prof. Mark Chaplain

Abstract

Many important processes in cells are controlled by extracellular signals which are caused by many different chemical signals from their surrounding. Cells have the capability to react to signal transduction in an appropriate way, such as activate the response of intracellular molecules, which is mainly governed by proteins reacting with each other.

Intracellular signalling networks are mainly based on kinases and phosphatases, enzymes which control phosphorylation and dephosphorylation of other enzymes in the cellular surrounding to the nucleus.

In this thesis we present mathematical models for negative feedback signal transduction processes. Signal transduction pathways are often equipped with negative feedbacks. Negative feedback loops are important components that exhibit oscillations in concentrations of the substances involved, both temporally and spatially. These feedbacks constitute a major research for targeted therapies in cancer treatment, drug action and cause cross-activation of other pathways. Specifically, we investigate systematically how the negative feedback structure of the signal transduction network can transmit information despite noise in protein levels. In this thesis, we consider mathematical models of the Hes1, Hes1-Stat3 and p53-Mdm2 pathways.

In chapter 3, we have undertaken a detailed study of the previous work done in the field.

Building on this previous work, we derive mathematical models (systems of partial differential equations) to capture the evolution in space and time of the key variables in the Hes1 and p53-Mdm2 systems. Computational simulations allow us to show that our reaction-diffusion models are able to produce sustained oscillations both spatially and temporally. The simulations of our models also allow us to calculate a diffusion coefficient range for the variables in each mRNA and protein, as well as ranges for other key parameters of the models. Also, we have carried out simulations under different conditions such as considering a time delay in the protein diffusion process from nucleus to the cytoplasm, varying the thickness of the nucleus membrane which slows down diffusion in a cell. Our results have extended and generalized previous work in this area.

All the mathematical models in this thesis use the numerical analysis of nonlinear partial differential equations and computational simulations to obtain insight into the underlying biological systems. The systems of nonlinear partial differential equations were solved numerically using one of the MATLAB, COMSOL and URDME software packages.

Publications

1. M. Sturrock, A. Hellander, S. Aldakheel, L. Petzold, M.A.J. Chaplain. (2013) The role of dimerisation and nuclear transport in the Hes1 gene regulatory network. *Bull. Math. Biol.* DOI 10.1007/s11538-013-9842-5

Chapter 1

Introduction

Signal transduction plays a vital role in many intracellular processes such as eukaryotic chemotaxis, polarity generation, cell division. The correct localisation of transcription factors is vitally important for the proper functioning of many intracellular signalling pathways. Experimental data has shown that many pathways exhibit oscillations in concentrations of the substances involved, both temporally and spatially. Negative feedback loops are important components of these oscillations, providing fine regulation for the factors involved. Negative feedback loops controlling the concentrations of key intracellular proteins are prevalent in a diverse range of important cellular processes. Mathematical models can help us to better understand these interactions. In this thesis we consider mathematical models of two such pathways: Hes1 and p53-Mdm2.

The chapters of the thesis are organised as follows:

Chapter 2 is a biological overview of the cell cycle and intracellular signal transduction pathways, in particular, negative feedback systems. The aim of this chapter is to give some basic information of the main components of the cell cycle, the important processes of transcription and translation, a description of some important transcription factors (p53, STAT3, Hes1 and the interactions among them), tumour suppressor genes and cancer.

In chapter 3, we present a literature review of the modelling of a number of specific intracellular and intercellular processes in time. One set of efforts has dealt with modeling the fundamental regulatory activity of the cell, controlled at the level of enzymes and genes. Also the models discuss the significance of oscillatory motion in relation to the organization of cellular processes in time, the feedback of cellular signaling processes using theoretical methods for analysing the occurrence of stable oscillations and the arrangement of control interactions by computer simulations. In addition, we review the models which analyse the spatio-temporal interactions within a cell using spatio-temporal models of genetic control by including diffusion in the cytoplasm and time delays.

Another set of modelling efforts has focussed on the Hes1 network. These studied the modelling of transcriptional negative feedback loops and the dynamics of Hes1 oscillations considering the transcription factors and showed that reaction-diffusion models of the hes1 system are able to produce sustained oscillations both spatially and temporally. Also, we review some models of the STAT pathway and analyse the signal transduction performed by the various STAT proteins.

Other studies have examined spatial effects in signalling which had been hitherto studied only in purely temporal settings: these include studies of spatial effects in the oscillating system of p53-Mdm2 and exploring the mechanisms of DNA-damage response to p53 and their possible relevance to apoptosis. The last set of modelling efforts has focussed on studying the equilibrium state(s) of negative feedback systems and investigated the existence of Hopf bifurcations for such systems

We will consider intracellular negative feedback loops specifically those involving transcription factors, critical contributors to cellular homeostasis and, when dysfunctional, to disease processes. Most previous mathematical models examining intracellular negative feedback systems have taken a simplified approach using ordinary differential equations (ODEs) and have not considered the different spatial structures within a cell. Such ODE models have used delays to account for the processes of transcription, translation and transport within the cell. However, in this thesis, we consider modelling the spatial interactions explicitly, using partial differential equation (PDE) models, with the knowledge that the localisation of certain proteins is critical for normal cellular functioning. As such, we consider mathematical models of two such pathways - the Hes1 and p53-Mdm2 systems. Building on previous mathematical modelling approaches, we derive systems of partial differential equations to capture the evolution in space and time of the variables in the Hes1-Stat3 and p53- Mdm2 systems. Therefore, in Chapter 4, we begin by considering a simple example of a feedback inhibition system, namely that of Hes1 mRNA and Hes1 protein. We present a mathematical model of this system, showing how our model builds on previous work to reflect the biology in greater depth and present our computational simulation results.Theoretical studies have shown that network time delays due to the processes of transcription and translation and protein dimerisation are key regulators of the dynamics of the Hes1 feedback loop. Also, we present the P53-Mdm2 a mathematical model of this system, showing how our model builds on previous work.

Then in Chapter 5, we expand the study of the Hes1 ODE system by consecrating the spatio-temporal dynamic model by building the PDE model. Theoretical studies have shown how diffusion might play a role in modulating or affecting the response. The results are based on numerical and analytical work, some of which is detailed in the Appendix. we conclude with a synthesis of the results. W show that the protein Stat3 plays a central role in maintaining the segmentation clock and include the Stat3 negative feedback loop in our model. We show that the Hes1 oscillations depend on cyclic changes in the phosphorylation of the protein Stat3, since phosphorylated Stat3 (pStat3) increases the degradation rate of Hes1. Our extended Stat3-Hes1 model system has been studied under different conditions such as varying the nuclear membrane thickness, including noise in the diffusion term, considering some spatial “holes” in the cytoplasm and the affect of convection on the model system.

In chapter 6, we consider the p53-Mdm2 system, where localisation of proteins is of particular importance since it has implications for cancer. Again we develop a mathematical model and show that network time delays due to the processes of transcription and translation of the dynamics of the p53-Mdm2 feedback system are very important. Alsowe studiy P53-Mdm2 model system under different conditions such as varying the nuclear membrane thickness and including noise in the diffusion term.

Through computational simulations in chapter 5 and 6, we show that our reaction-diffusion models are able to produce sustained oscillations both spatially and temporally, accurately reflecting experimental evidence and advancing previous models. The simulations of our models also allow us to calculate a diffusion coefficient range for the variables in each mRNA and protein system, as well as ranges for other key parameters of the models, where sustained oscillations are observed.

In the final chapter of the thesis, chapter 7, we conclude with a discussion of our results and an indication of future work in this area.

Chapter 2

Biological Background

2.1 Introduction

In this chapter, the biology of signal transduction and the intracellular network would be reviewed . The focus points would involve the biology of the cell cycle, the important processes of transcription and translation, the role of transcription factors (p53, Stat3, Hes1 and the interactions among them), tumour suppressors and cancer. The concept of negative feedback systems would be introduced.

2.2 Signal Transduction.

Effective control of cellular behaviors has serious implications in the study of biological processes and disease. The living cell can be viewed as a complex system of interacting networks. These networks can be roughly divided into three types, signal transduction, metabolic networks and regulatory networks.

All organisms have the dynamic ability to coordinate constantly their activities with environmental changes. The function of communicating with the environment is called signal transduction which is achieved through a number of pathways that receive and process signals originating from the external environment, from other cells within the organism and also from different regions within the cell (Istvan Petak and Kopper. 2006).

signal transduction depends on molecular circuits. These molecular circuits detect, amplify, and integrate diverse external signals to generate responses. Signal transduction occurs when an extracellular signalling molecule binds to the cell surface where receptor activate as sequence of the passive diffusion of the ligand through the plasma membrane . In turn, this receptor trigger intracellular molecules creating a response inside the cell when the ligands pass through the nuclear membrane into the nucleus, enabling gene transcription and protein synthesis.

There are four stages in this process:

1– Membrane receptors transfer information from the environment to the cell's interior. A few nonpolar signal molecules are able to diffuse through the cell membranes and, hence, enter the cell, they can bind to proteins that interact directly with DNA and modulate gene transcription. Thus, a chemical signal enters the cell and directly alters gene expression patterns. However, most signal molecules are too large and too polar to pass through the membrane. Thus, the molecules information must be transmitted across the cell membrane (often referred to as the ligand) without the molecules themselves entering the cell. The interaction of the ligand and the receptor alters the tertiary or quaternary structure of the receptor, including the intracellular domain. The information embodied by the presence of the ligand, often called the primary messenger (Berg JM 2002).

2– Changes in the concentration of small molecules called Second messengers, that relay information from the receptor-ligand complex. The use of second messengers has several consequences on the cell. they can influence gene expression and other processes after they diffuse to the nucleus, also amplified significantly in the generation of second messengers. Thus, a low concentration of signal in the environment can yield a large intracellular signal and response (Berg JM 2002).

The regulation of gene expression is achieved through genetic regulatory systems structured by networks of interactions between DNA, RNA, proteins and small molecules where the majority of those molecules are proteins. It is known and understood that the processes of transcription and translation control the level of gene expression (Alam-Nazki and Krishnan 2012). As most genetic regulatory networks of interest involve many components connected through interlocking positive and negative feedback loops (Davidson 2005; DeJong 2002). Gene regulatory networks have an important role in every process of life, including cell differentiation, metabolism, the cell cycle and signal transduction (Karlebach and Shamir. 2008).

3– Protein phosphorylation is a common means of information transfer. Many second messengers elicit responses by activating protein kinases. This protein kinase and others are the link that transduces changes in the concentrations of free second messengers into changes in the covalent structures of proteins (Berg JM 2002).

4– The signal is terminated. Protein phosphatases are one mechanism for the termination of a signaling process. After a signaling process has been initiated and the information has been transduced to affect other cellular processes, the signaling processes must be terminated. Without such termination, cells lose their responsiveness to new signals. Moreover, signaling processes that fail to be terminated properly may lead to uncontrolled cell growth and the possibility of cancer propagation (Berg JM

2002).

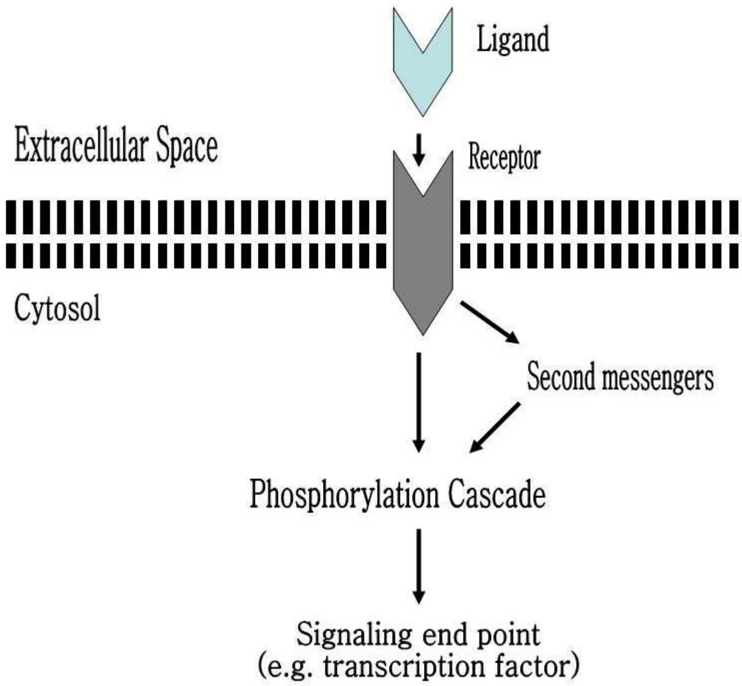

Figure 2.1: *A schematic diagram of a simplified transduction signal pathway.*

2.3 Transcription and Translation

The process of creating RNA from DNA is called *transcription*. During transcription, an RNA polymerase (enzyme) binds to a specific region of DNA known as a promoter and reads the DNA sequence resulting in an antiparallel RNA strand (complementary) which has Uracil (U) instead of Thymine (T) in the template DNA. The new strand of RNA is called messenger RNA (mRNA). The process of transcription can be divided into 5 stages: pre-initiation, initiation, promoter clearance, elongation and termination (Solomon et al. 2007). In eukaryotes, RNA polymerase can not recognize the promoter sequence directly. Instead, transcription factors (proteins) mediate the binding of RNA polymerase. So after certain transcription factors bind to the promoter, the RNA polymerase binds to the promoter (Ouhammouch et al. 2003). All of these events occurs in the *nucleus*. Mature mRNA molecules are transported to the cytoplasm where *translation* take place. Translation is the process of transforming mRNA (produced by transcription) to produce protein by the ribosome. Once the ribosome complex (rRNA and proteins) bind to a specific region of mRNA and start to scan the mRNA, each nucleotide of mRNA is translated to one amino acid (Stryer and Lubert 2002) (see Figure 2.2).

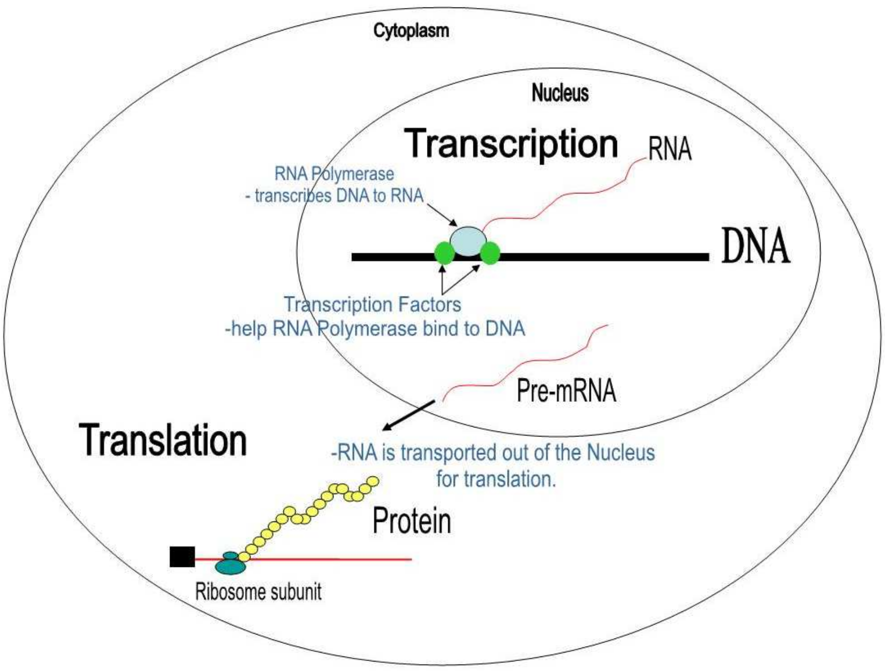

Figure 2.2: *A schematic diagram of transcription and translation. RNA polymerase bind to gene promoter and begins to scan DNA sequence to generate complementary RNA-in the nucleus. The mRNA is then transported to the cytoplasm where ribosomes binds and read through to produce protein.*

2.4 Transcription Factors

Transcription factors (TFs) are proteins that bind to a specific DNA sequence in order to increase or decrease mRNA production. They might function alone or in a complex as an activator or repressor.

2.4.1 Hes1–STAT3 interactions

The Hairy and Enhancer of Split homologue 1 protein (Hes1) is a transcription factor that belongs to the family of basic helix-loop-helix (bHLH) Transcriptional suppressors. Hes proteins consist of three evolutionarily conserved domains: the bHLH, Orange, and WRPW domains (Dawson et al. 1995). In general Hes proteins suppress transcription. The Hes1 protein plays crucial roles in controlling the proliferation of neuronal, endocrine, T-lymphocyte progenitor cells during development and differentiation (Kamakura et al. 2004).

It has been found that Hes1 can repress its own expression through direct binding to its own promoter (i.e. a negative feedback loop (cf. Figure 2.3). Activation of Hes1 promoter leads to the production of both Hes1 mRNA and protein. The latter then binds to a DNA sequence on the Hes1 promoter and represses Hes1 gene expression. Due to the instability of both Hes1 mRNA and Hes1 protein, they disapper after repression. Degradation of Hes1 protein relieves negative autoregluation, permitting the next round of Hes1 expression (Kobayashi and Kageyama 2011).

Signal transducers and activators of transcription proteins (STATs) are a family of latent cytoplasmic transcription factors that are activated in response to extracellular stimuli. They were first discovered in interferon (IFN) regulated gene transcription, specifically Stat 1 and Stat2 (Schindler et al. 992b). Today seven STAT members have

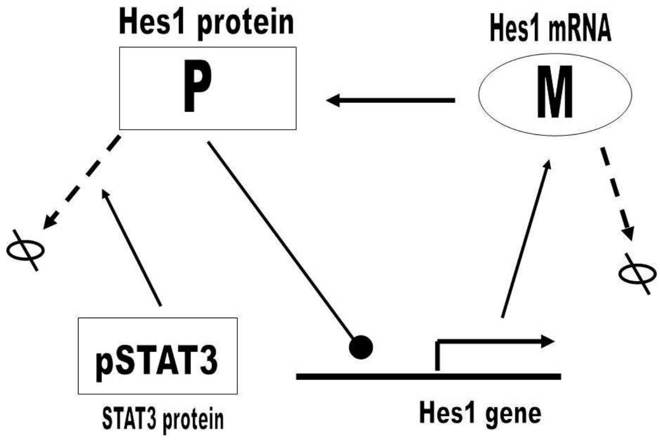

Figure 2.3: *Schematic diagram showing that the basic Hes1 negative feedback loop is driven externally by cyclic changes in the level of phosphorylated Stat3 (pStat3), which regulates the degradation rate of Hes1 protein.*

been identified in mammalian cells: Stat1, Stat2, Stat3, Stat4, Stat5a, Stat5b and Stat6, ranging in size from 750-850 amino acids.

Stat3 was initially identified as the acute-phase response factor (APRF), activated by interleukin-6, (IL-6). It was further shown that Stat3 activation occurred in the cytoplasm, that Stat3 phosphorylation was essential and that Stat3 binds to IL-6 response elements of various acute-phase protein genes (e.g., the alpha2-macroglobulin, fibrinogen, and alpha1-acid glycoprotein genes) (Wegenka et al. 1993).

In response to growth factors, cytokines and tyrosine kinases, STATs are phosphorylated and form homo-dimers that translocate from the cytoplasm to the nucleus to act as transcription activators. In normal cells, activation of STAT3 is transient, because of proteins that act as negative regulators such as suppressors of cytokine signalling, (SOCS), but in cancer cells STAT3 is constitutively activated. STAT3 is activated in many human cancers and plays an important role in the activation of genes encoding apoptosis inhibitors, cell-cycle regulators as well as inducers of angiogenesis (Jing and Tweardy 2005).

Stat3, the cytoplasmic transcription factor is activated by the JAK2 (Janus Kinase 2 gene provides instructions for making protein that promotes the growth and division of cells) and the phosphration process to be translocated to the nucleus and acts like transcriptional factor in the nucleus. The main step of this process is shown in Figure 2.4. Where the inactive JAK are attached to the cytoplasmic domain cytokine receptors. Then, the cytokine molecule bind to association of cytokine receptors this leading to activate JAKs which cause phosphorylation of tyrosine residues in cytoplasmic proteins of the receptors. After that, the phosphotyrosine complexes one the receptors bind to STAT proteins this lead to phosphorylates STAT proteins. Then, it dissociate from the receptor and the binds to one other. The STAT dimer migrates to the nucleus then bind to the promoter region of cytokine responsive gene where it is activate gene transcription.

It has been demonstrated that both active Notch and notch effectors (Hes1 and Hes5) are involved in STAT3 activation. Hes1 and Hes5 proteins bind to JAK2 and STAT3, facilitating the formation of the JAK2-STAT3 complex and STAT3 phosphorylation activation (Kamakura et al. 2004). Research papers presented the first evidence for crosstalk between two major signal transduction pathways, Notch-Hes and JAK-STAT3-Hes1 and other Hes protein expression induced by the activation of Notch receptors. Hes proteins bind to STAT3 directly inducing phosphorylation.

The Notch signaling pathway regulates cell differentiation by the intercellular communication between cells. Notch protein spans the cell membrane with part of it inside and part outside. Ligand transmembrane proteins, binding to the extracellular domain, induce proteolytic cleavage and release of the intracellular domain, which enters the cell nucleus to modify gene expression (Oswald F 2001).

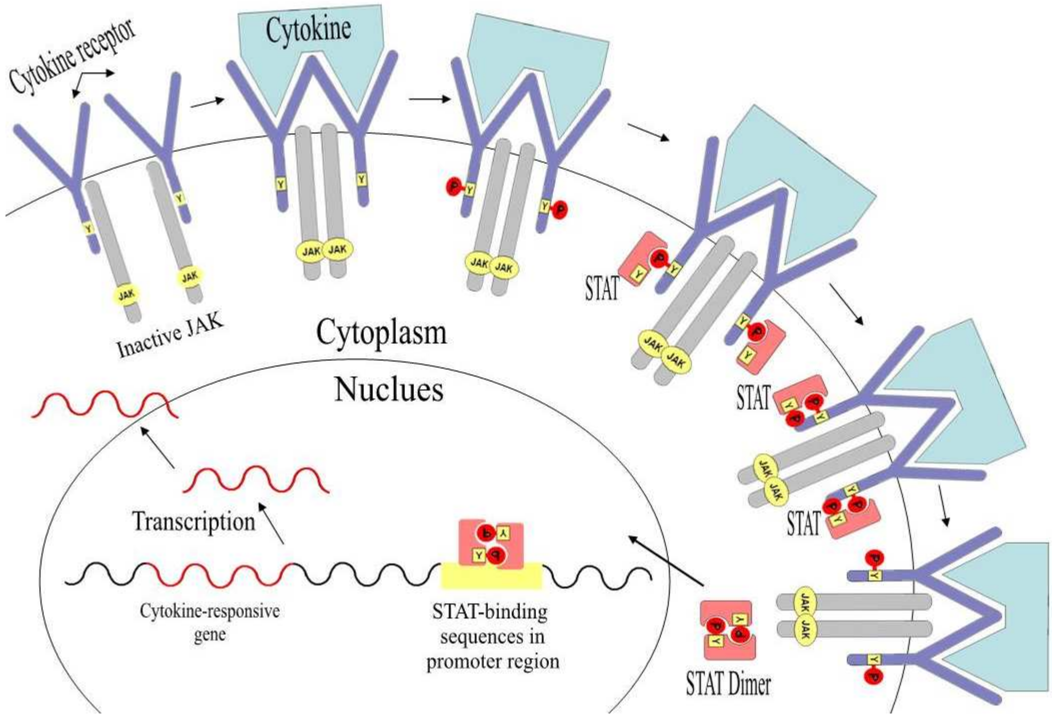

Figure 2.4: *Schematic diagram showing the Cytokine signaling and the activating of STAT transcription.*

In early stage, the development of the nervous system produces proneural genes such as Ngn2 which induces the expression of Notch ligands such as Deltalike1 (DLL1) which activate Notch signaling in neighboring cells forming the Notch domain (NICD). Then, Notch domain move from the transmembrane region to the nucleus where it forms NICD complex then induces expression of the basic helix-loop-helix factors Hes1 and Hes5which repress expression of proneural genes and Notch ligands.

Microarray analysis with cultured fibroblasts identified the signal transducer, the activator of transcription (Stat3) and the suppressor of cytokine signaling (Socs3) system as novel oscillators. Janus kinase activates Stat3 by phosphorylation, and phosphorylated Stat3 (Stat3-P) forms a dimer that enters the nucleus and activates expression of target genes such as Socs3. Socs3 in turn inhibits phosphorylation of Stat3, forming a negative feedback loop. This negative feedback loop induces oscillations in the formation of Stat3-P and in the expression of Socs3 Fig 2.5. Especially, Stat3-P and Socs3 oscillations are coupled with Hes1 oscillation as shown in (Fig 2.5). Stat3-Socs3 oscillations also inhibits Hes1 oscillation. suggesting that the Stat3-Socs3 pathway regulates oscillatory expression of Hes1 in the developing nervous system. Hes1 is required for phosphorylation of Stat3, suggesting that Hes1 oscillations and Stat3-Socs3 oscillations depend on each other (Ryoichiro and Imayoshi 2008).

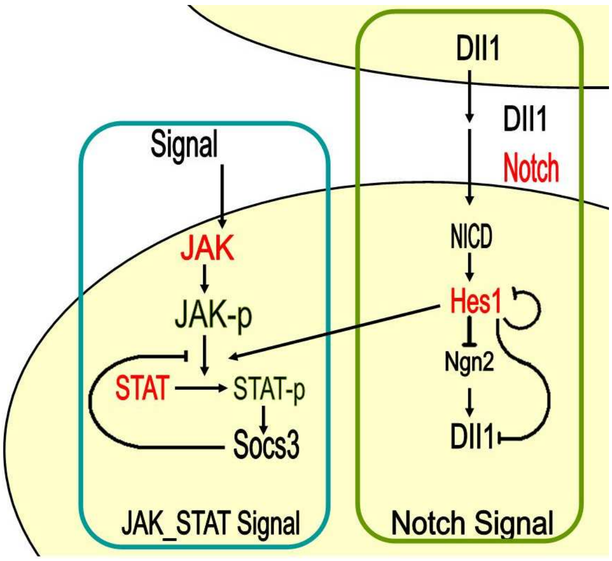

Figure 2.5: *Schematic diagram showing the oscillator network in neural progenitors. Hes1 expression oscillates owing to negative feedback. Formation of phosphorylated (-p) Stat3 and expression of Socs3 also oscillate owing to negative feedback. Hes1 oscillation and Stat3-Socs3 oscillations seem to depend on each other. Hes1 oscillation then induces Ngn2 and DII1 oscillations, which in turn activate Notch signaling in neighboring cells.*

Hes1 expression is downregulated during early G1 phase, where, Hes1 is also known to promote G1 phase progression by downregulating cyclin-dependent kinase inhibitors. Thus, Hes1 both promotes and inhibits the cell cycle. Hes1 oscillation is required for efficient cell proliferation and differentiation of neural progenitors. The negative feedback loop of Hes1 was proposed by Yoshiura et al. (2007). The negative feedback is driven by the level of phosphorylated Stat3 which in turn causes Hes1 degradation. Using mouse fibroblasts after serum stimulation, the results of Yoshiura et al. (2007)

showed that in the absence of STAT3 signalling, Hes1 protein is stabilized. Conversely, when p-Stat3 formation is constitutively up-regulated, Hes1 protein is abolished. The latter observation would support the existence of a negative feedback loop of Hes1-STAT3 (Yoshiura et al. 2007).

2.4.2 p53–Mdm2 interactions

p53 is a tumour suppressor protein that plays a crucial role in the regulation of cell cycle, apoptosis, senescence and DNA repair (Fridman and Lowe 2003; Vousden and Lu 2002). Mutant p53 genes cause approximately 50% of human cancers (Hainaut and Hollstein 2000; Feki and Irminger-Finger 2004). The progression of the cell cycle phases are monitored at certain check points via intracellular negative signals to make sure that a cell replicates without mistakes. If, however, an error occurs during cell replication, the regulatory proteins are activated (O'Connell and Cimprich 2005). p53 activation results in cell cycle arrest at G1 or G2, by stimulating some inhibitory protein such as CKI (Lozano and Zambetti 2005). However, if DNA damage is irreparable, p53 stimulates programmed cell death (apoptosis) (Hengartner 2000).

The murine double minute oncogene expressed protein, Mdm2, is an important negative regulator of the p53 protein. It has been found that mutated p53 in many cancers is accompanied by an over-expression of Mdm2 protein (Kussie et al. 1996). In normal conditions, the Mdm2 protein concentration is very low. There are 3 mechanisms by which Mdm2 inhibits p53 (Vassilev et al. 2004). First, Mdm2 can bind to the p53 transactivation domain, preventing p53 to activate genes expressing proteins for DNA repair or directing it to apoptosis. Second, Mdm2 is involved in exporting p53 from the cell nucleus. Moreover, Mdm2 may attach to p53 as ubiquitin results upon p53 degradation. After DNA damage, p53 is activated by protein kinases which phosphorylate p53. Phosphorylation of the p53 protein prevents the Mdm2-p53 complex formation and p53 concentration builds up in the cell. Once the damage is repaired, phosphorylation of p53 by protein kinases stops and the Mdm2-p53 complex is reformed (Li et al. 2003).

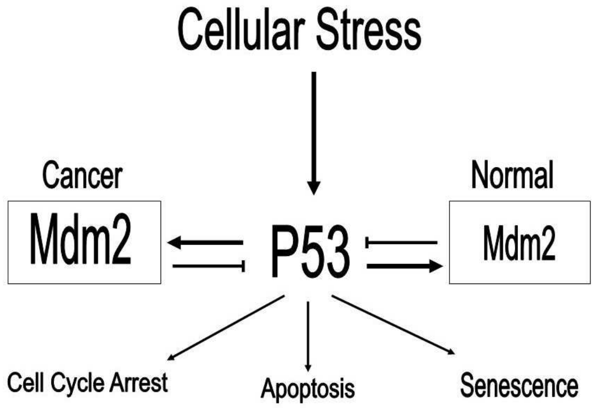

Figure 2.6: *Schematic diagram showing mechanisms of cellular stress, e.g., DNA damage, telomere erosion, hypoxia, or oncogene expression, which can activate the p53 response pathway. The p53-Mdm2 autoregulatory feedback loop governs the level of p53. Over-expression of Mdm2 in human cancer, e.g., gene amplification of Mdm2, targets p53 for ubiquitin-dependent proteolytic degradation to disable the p53 network.*

2.4.3 Tumour suppressors (inhibitors)

Tumour suppressor genes encode proteins which protect cells from cancer. There are two families of genes: the cip/kip family and INK4a/ARF. Both groups prevent the progression of the cell cycle and the formation of tumours. For example, p21, p27 and p57 are members of the cip/kip family. They can bind to cyclin-cdk complexes causing them to be inactivated, and hence, preventing the cell from from leaving the G1 phase of the cell cycle. The p161NK4a protein belongs to the INK4a/ARF family. This protein binds to CDK4 and arrests the cell in the G1 phase of the cell cycle.

2.5 The Cell Cycle

The cell cycle is a critical regulator of the processes of cell proliferation and growth as well as of cell division after DNA damage. The cell cycle also serves to protect the cell from DNA damage (Schwartz and Shah 2005).

Cell division is a very important process in all living organisms. During the division of a cell, DNA replication and cell growth also take place to ensure correct division. These cells divide once in approximately every 24 hours and cell division properly lasts for only about an hour. However, this duration of cell cycle can vary from organism to organism and also from cell type to cell type.

The cell cycle is divided into two basic phases, Interphase (resting phase) is the phase between two successive M phases where it lasts more than 95% of the duration of cell cycle and M Phase (Mitosis phase) which is representing the phase when the actual cell division or mitosis occurs.

The interphase is the time during which the cell is preparing for division by undergoing both cell growth and DNA replication in an orderly manner. It is divided into three further phases. First, G1 phase (Gap 1) G1 phase corresponds to the interval between mitosis and initiation of DNA replication. During G1 phase the cell is metabolically active and continuously grows but does not replicate its DNA. Then, S phase (Synthesis) or synthesis phase marks the period during which DNA synthesis or replication takes place. During this time the amount of DNA per cell doubles. However, there is no increase in the chromosome number, so the number of chromosomes at S will remains the same number of the chromosome in phase G1. Finally, G2 phase (Gap 2) During the G2 phase, proteins are synthesised in preparation for mitosis while cell growth continues.

Some cells exhibit division because they have been lost as result of injury or cell death, they exit G1 phase to enter an inactive stage called quiescent stage (G0) of the cell cycle. Cells in this stage remain metabolically active but no longer proliferate.

M phase is the most dramatic period of the cell cycle. The mitosis has been divided into four stages of nuclear division. First, Prophase which is the first stage of mitosis follows the S and G2 phases of interphase where new DNA molecules formed. In the prophase, the proteinaceous components of the cell cytoplasm help to attache the two chromatids together to form compact mitotic chromosomes. Cells at the end of prophase, do not show golgi complexes, endoplasmic reticulum, nucleolus and the nuclear envelope. Then, Metaphase where the complete disintegration of the nuclear envelope marks the start of the second phase of mitosis, hence the chromosomes are spread through the cytoplasm of the cell, and the condensation of chromosomes is completed. At this stage, chromosome is made up of two sister chromatids, which are held together by the centromere. Hence, the metaphase is characterised by all the chromosomes coming to lie at the equator with one chromatid of each chromosome connected by its kinetochore to spindle fibres from one pole and its sister chromatid connected by its kinetochore to spindle fibres from the opposite pole. After that, Anaphase, At the onset of phase, each chromosome arranged at the metaphase plate is splited simultaneously and the two daughter chromatids begin their migration towards the two opposite poles. Where each chromosome moves away from the equatorial plate. Finally, Telophase, At the beginning of the final stage of mitosis, i.e., telophase, the chromosomes that have reached their respective poles decondense and lose their individuality. Also, Nuclear envelope assembles around the chromosome clusters and golgi complex and ER reform.

The timing and order of cell cycle events are monitored during cell cycle checkpoints that occur at the G1/S phase boundary, in S phase, and during the G2/M phases. These checkpoints ensure that critical events in a particular phase of the cell cycle are completed before a new phase is initiated, thereby preventing the formation of genetically abnormal cells. Cell cycle progression can be blocked at these checkpoints in response to the status of both the intracellular and extracellular environment. Damaged cells are eliminated through the process of apoptosis. Thus as a cell progresses through the cell cycle, it must determine whether to complete cell division, arrest growth to repair cellular damage, or undergo apoptosis if the damage is too severe to be repaired or if the cell is incapable of repairing the DNA. It is at the checkpoints that the cell determines which of these options is suitable (King and Cidlowski 1998).

Two types of protein are considered to be the most crucial regulatory molecules of the cell cycle: cyclins and cyclin-dependent kinases (CDK). They control switching from G1 to S or G2 to M. Cdk itself adds phosphate to a variety of proteins for the activation or inactivation protein in question which in turn coordinates entry into the next phase. In response to extracellular signals (e.g. growth factors), cyclin D activates expression of cyclin E protein which binds to cdk2 leading the cell to move from G1 to S-phase. Cyclin B binds to cdk1 allowing the cell to transition from G2 to M-phase. Once the nuclear envelope breaks down, the cyclin B-cdk complex becomes inactivated and the cell exits M-phase (Robbins et al. 2004). Targeting CDKs would recapitulate cell cycle checkpoints that would necessarily limit a tumor cells ability to cycle, and this may then facilitate the induction of apoptosis (Schwartz and Shah 2005).

During cell division a number of important cell cycle proteins are synthesized periodically dependent on transcription. Often the function of tumor suppressors like p53 is to arrest cell division and to send a damaged cell into apoptosis. The group is working on identifying transcriptional targets of p53. Thereby they discovered new signaling pathways leading to cell cycle arrest and apoptosis (Katrien Vermeulen and Bockstaele

2003).

This great interest in apoptosis is due to the recognition that many diseases involve too much apoptosis or too little apoptosis. Many toxins and other cellular stresses can also trigger apoptosis. Apoptosis is associated with a distinct set of biochemical and physical changes involving the cytoplasm, nucleus and plasma membrane. Early in apoptosis, the cells round up, losing contact with their neighbors, and shrink (Lawen 2003).

Apoptosis and proliferation are intimately coupled. Some cell-cycle progression is regulated by positive and negative signals where the cell cycle regulators can influence both cell division and programmed cell death. A perfect control of cell division is important for avoiding the development of cancer. The linkage of cell cycle and apoptosis has been recognized for c-Myc, p53, pRb, Ras, PKA, PKC, Bcl-2, NF-κB, CDK, cyclins and CKI. A direct link between cell cycle and apoptosis may be supposed from the fact that a number of similar morphological features exist between mitosis and apoptosis. Mitosis and apoptosis share common morphological features such as cell shrinkage, chromatin condensation and membrane blebbing (Katrien Vermeulen and Bockstaele 2003).

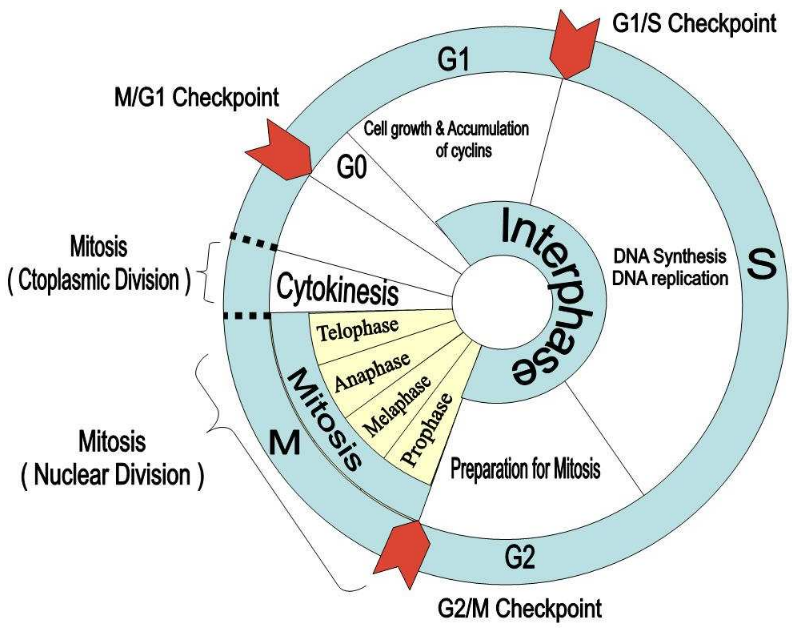

Figure 2.7: *Schematic diagram of the cell cycle. M = Mitosis, G1 = Gap 1, G2 = Gap2, S = Synthesis.*

2.5.1 Cancer

The term “cancer” is actually a broad group of diseases which may be described as *out-of-control cell growth*. Cancer cells divide and grow uncontrollably. There are two types of tumours – benign tumours and malignant tumours. In benign tumours, the appearance of cells is often quite normal, but they divide more rapidly than normal. Benign tumours do not invade neighbouring tissues and do not lead to metastasis (the spread of a tumour from one organ to other non-adjacent organs.). These tumours usually do not grow beyond 1-2 mm^3 due to the lack of oxygen and nutrients.

On the other hand, malignant tumours, or cancers, display two life-threatening phenomena – angiogenesis and metastasis. Angiogenesis is a process by which the tumour cells induce blood vessels to provide them with the required nutrients needed for tumour expansion. Metastasis is the process of the growth and development of secondary tumours at distant locations in the host to the primary tumour.

A recent seminal paper identified six key aspects of cancer, now known as "hallmarks", which distinguish it from normal cells/tissue involving: self-sufficiency in growth signals, limitless replicative potential, evasion of apoptosis, tissue invasion and metastasis, insensitivity to growth-inhibitory signals and sustained angiogenesis (Hanahan and Weinberg 2000). The recent advancements in cancer genomics has made it clear that different transcriptional factors such as p53, stat1 and hes1, have unique roles in tumour development and suppression. So the possibility to use these factors as biomarkers, tumour suppressors and gene therapy agents for cancer management is attracting the attention of scientists and clinicians. However, these therapies are still in their early stages of development. Hence, for the development of comprehensive cancer management and anticancer therapies, a better understanding of these transcriptional factors is required. The studies on p53, stat1 and hes1 in the present thesis aims to provide a better understanding of the relationship between cancer and normal cells.

Chapter 3

Mathematical Modelling of Negative Feedback Systems

In this chapter we review some of the work done in the theoretical modelling of negative feedback systems (e.g. Hes1, p53-Mdm2) and other relevant studies. Most of the dynamic models which represent the fundamental regulatory activity of the cell are controlled at the level of the gene and proteins. It is important to understand the cellular organization and the dynamic activity of the molecular control processes involved in these feedback systems and gene regulatory networks since concentration levels in such systems are known to undergo oscillatory behaviour.

3.1 Ordinary Differential Equation Models

Perhaps the first theoretical investigation into such intracellular regulatory networks was that of Goodwin (1965) who studied the type of periodic behaviour which can arise in model systems incorporating the essential control features of enzymatic regulatory processes and discussed the significance of oscillatory motion in relation to the organization of cellular processes in time.

The mode of Goodwin (1965) considered the interactions between enzymes Y_i and their mRNA X_i in a negative feedback loop which lead to set of equations describing the dynamic of this system as follows:

$$\begin{aligned}\frac{dX_i}{dt} &= \frac{\alpha_i}{A_i + k_i Y_i} - b_i\\ \frac{dY_i}{dt} &= \alpha_i X_i - \beta_i\end{aligned}$$

The above system of equations $i = 1, 2, 3...$ define what Goodwin (1965) termed a non-linear biochemical oscillator. As result of this work, Goodwin (1965) reported that the majority of enzymes in a cell are being synthesised at any one time and their synthesis and activity are regulated by negative feedback control processes.

Goodwin (1965) also described the interactions in some intracellular processes where one molecular species has a repressive effect on another. This feedback systems was represented mathematically by the following system of equations:

$$\begin{aligned}\frac{dX_1}{dt} &= \frac{\alpha_1}{A_1 + k_{11}Y_1 + k_{12}Y_2} - b_1\\ \frac{dY_1}{dt} &= \alpha_1 X_1 - \beta_1\\ \frac{dX_2}{dt} &= \frac{\alpha_2}{A_2 + k_{21}Y_1 + k_{22}Y_2} - b_2\\ \frac{dY_2}{dt} &= \alpha_2 X_2 - \beta_2\end{aligned}$$

The result of this study showed that the cell employs non-linear interactions between control circuits to achieve the organization of biochemical processes in a temporal domain, where the behaviour of the oscillations is completely coherent and the slower oscillation is driven by the faster one.

In this paper, Goodwin (1965) also investigated a special class of oscillations of negative feedback control processes in the more general type of system where damping, oscillations and limit cycle are expected. The system of equations which was studied was the following:

$$\begin{aligned}\frac{dX_1}{dt} &= \frac{\alpha_1}{A_1+k_1Z_1}-b_1X_1\\ \frac{dY_1}{dt} &= \mu_1X_1-\beta_1Y_1\\ \frac{dZ_1}{dt} &= \gamma_1Y_1-\delta_1Z_1\end{aligned}$$

These equations consider for the first time the concept of delay due to the diffusion of molecules, the concept of "precursors" and the notion of a metabolic sequence. From these studies the oscillatory behaviour which is expected to be a very important dynamic feature of cellular control processes were predicted and it was shown that the oscillations can arise at different levels of cellular organization.

Griffith (1968a) observed that the theoretical method for analysing the circumstances for occurrence of stable oscillations and the arrangement of control interactions was computational simulations. He considered the Goodwin (1963, 1965) model given schematically by $G+mR=GR_m$ where $R=$ Repressor, combining with a gene G. The proportion of time G is active is given by, $p=\frac{1}{1+kx^m}$, where the parameter $m\to\infty$.

Griffith used standard techniques to examine the stationary points of the system ($M^{'}$ = $E^{'}$ = 0) and their (linear) stability, and the analysis showed that were are no limit cycles. He also studied the three variable case given by M_0 = βE_0, E_0 = γP_0, $\alpha\beta\gamma P_0(1+P_0^m)$

= 1. He reported that the absence of limit cycles in the two variables case should still hold, whilst in three variable case, it would be surprising if limit cycles appeared for very low values of m.

In a second paper, Griffith (1968b) discussed equations similar to those discussed in Part I. He considered $G + mI = GIm$ where I is a so-called inducer for metabolite P. The time for which the gene G is active is given by, $P = \frac{Kx^m}{1+kx^m}$, where $K =$ equilibrium constant.

Once again he is carrying out a linear stability analysis of the steady-states of the systems, the same general behaviour to the previous model was observed.

Freeman (2000) observed that the intercellular communication that regulates cell fate during animal development must be precisely controlled to avoid dangerous errors. Both positive and negative feedback loops play vital roles in dynamic regulation of developmental signalling. In this paper, he analysed the temporal control of signalling, and spatial control by feedback. He also analysed the integration of feedback events in pattern formation. It was observed that positive and negative feedback can establish left–right asymmetry. It was reported that while positive feedback can contribute distinct signals, negative feedback can restrict the ligand range. He also reported that negative feedback generates stability.

Ciliberto et al. (2005) observed that oscillations can arise from a combination of positive and negative feedbacks or from a long negative feed back loop alone. In their study they developed a mathematical model of p53 oscillations based on positive and negative feedback in the p53 / Mdm2 network. According to the model, the system reacts to DNA damage by moving from a stable steady state into a region of stable limit cycles.

They observed certain points in their model as follows:

1. p53/Mdm2 network responds to environmental stress such as gamma irradiation by generation of pulses of p53. The oscillations produced increased with increasing stress.

2. In their model p53 level is kept low by degradation induced by Mdm2. The simulated DNA damage by increasing Mdm2 degradation in nucleus.

3. They also inferred that the model can be used to formulate two experiments that might discriminate whether oscillations are based on negative feedback look alone or on a combination of positive and negative feedback loops.

Geva-Zatorsky et al. (2006) studied oscillations in the p53-Mdm2 system considering negative and positive feedbacks and the mechanism of oscillations of p53-Mdm2, the variability in p53 pulses and the potential function of p53 oscillations there. The authors also studied the dynamics of the p53-Mdm2 feedback loop in individual cells.

Zhang et al. (2007) made an analytical report exploring the mechanisms of DNA-Damage Response to p53 pulses and their possible relevance to apoptosis. They constructed models at protein level, with the following assumptions:

1. Transcriptional regulation is replaced by regulation corresponding to protein synthesis using a Hill function given by
$H(x) = \frac{x^n}{J^n + x^n}$, with Transcription Factor [TF] = x. They formulated models combining

positive and negative feedback loops. They compared the dynamics of the following models using

$$G(u,v,q,r) = \frac{2ur}{(v-u+v.q+u.r)+\sqrt{(v-u+v.q+u.r)^2-4u.r(r-u)}}$$

2. Heaviside function with

$$H(x) = \begin{cases} 1, x > 0 \\ 0, x \leq 0 \end{cases}$$

They evaluated the DNA damage and degradation rate constants using

$$\begin{aligned} \frac{d(DNAdamage)}{dt} &= -k_{repair}.H(DNAAdvantage) \\ k_{d_2} &= k_{d_2}(1+DNAAdvantage) \\ k_{d53} &= kd_{53}+k_{d53}.G[(Mdm2^*, \theta, \frac{J_1}{P(53^*)}, \frac{J_2}{P(53^*)}] \end{aligned}$$

where, $(Mdm2^*) = (MdM2_{nuc})$ and $P(53^*) = [P53]$

Using the above three equations, the models were organised to evaluate $\frac{d(P53)}{dt}$, $\frac{d(MdM2_{cyt})}{dt}$, $\frac{d(Mdm2_{nuc})}{dt}$ for the given steady state values. They generalised the model of Ciliberto et al. (2005). They observed that in contrast to the jumping of parameter values between steady-state and robust oscillatory state, the models proposed by them reflected that the onset of oscillations is difficult. They observed that the model is consistent with experimental observation and p53 phosphorylation.

Bose and Ghosh (2007) have given an overview of their studies on the $p53-Mdm2$ network and the associated pathways from a systems biology perspective. They discuss a number of key predictions, related to some specific aspects of cell-cycle arrest and cell death, which could be tested in experiments. They describe the mathematical models developed by them to study the p53-mediated cell cycle arrest and apoptosis. We discuss briefly the major results obtained and point out their experimental relevance. They considered the cell-cycle arrest, as the cell-cycle is an example of a dynamical system in which events unfold as a function of time.

They inferred that there is a marked difference in the apoptotic response of cancer cells with normal Mdm2 expression and Mdm2 over-expression when treated with nutlin, an inhibitor of the p53-Mdm2 interaction. They also inferred that low levels of caspase-3 cannot bring about cell death. The amount of p21, the transcription of which is activated by p53, appears to be a crucial factor in determining the cell fate.

Zeiser et al. (2007) described a model for the Hes1 oscillator considering the transcription factor for a single binding site described by

$$\begin{aligned} 2X &= \frac{k_d}{k_{-d}} X_2 \\ X_2 + B_0 &= \frac{k_1}{k_{-1}} B_1 \end{aligned}$$

with k_1, k_{-1} being association and dissociation constants respectively. They attempted to estimate the Hill coefficient in the switch of a Hes1 oscillator and suggested a model of the autoregulative network. They used the Goodwin system and found sustained oscillations.

Puszynski et al. (2009) designed model for crosstalk between p53 and the NF-κB system and anti-apoptotic functions of NF-κB combining their stochastic models of NF-κB and p53 system. Their main assumption was $I_\alpha B_\alpha$ and A_{20} transcription rates are proportional to $\frac{b_1}{b_1+p53_{p_m}}$, where p_m is the amount of active nuclear p53.

3.2 Delay Differential Equation Models

Monk (2003) reported oscillatory expression of Hes1, p53, NF-κB driven by transcriptional time delays. Representing Hes1 mRNA by M(t) and Hes1 protein by P(t), he considered the system:

$$\begin{aligned}\frac{dM}{dt} &= \alpha_m G[P(t)-\tau] - \mu_m M(t)\\ \frac{dP}{dt} &= \alpha_p M(t) - \mu_p P(t)\end{aligned}$$

where μ_m, μ_p = rate of degradation of mRNA and Hes1, α_m = basal rate of transcript initiation and
$G[P(t-\tau] = \frac{1}{1+(P(t-\tau)/P_0)^n}$, where P_0 = concentration of Hes1. He also assumed the following:

(1) The translation is non-saturating; (2) movement of Hes1 between the cytoplasm and nucleus is neglected and (3) the delay takes a discrete value τ.

Bernard et al. (2006) studied transcriptional feedback loops and the role of Gro/TLE1 in Hes1 Oscillations, inspired by the experiments on oscillatory dynamics due to Hes1, p53 and NF-KB. They studied the effects of Hes1 factor. They considered the model of Jensen et al, Monk and Lewis which is describing the cellular concentration of Hes1 mRNA representing the cellular concentration of Hes1 protein. They also considered an additional influencing factor namely, the Gro/TLE1 protein, activated through Hes1-induced hyper-phosphorylation.

Momiji and Monk (2008) developed a more detailed model of the Hes1 circuit of Monk (2003), incorporating nucleo–cytoplasmic transport. They showed that differential protein stability can increase the amplitude of Hes1 oscillations but that the resulting expression profiles do not fully match experimental data. They considered the delay differential equation system.

They observed that the models represent Hes1 auto-repressive feedback loop in a simple manner representing transcription, translation repression and degradation represented mathematically as if they take place in a single spatially homogeneous cellular compartment. In order to consider additional known bio-chemical processes, they observed their model of the Hes1 network incorporates the key features of Hes1 dynamics, although it does not take into account the interaction of Hes1 with other biochemical species. They also studied the external driving of Hes1 oscillations by STAT2 phosphorylation. They considered the model of Yoshiura et al. (2007) and extended the model to study a three component Hes1 Model.

Nikol'skii and Vasilenko (2000) analyse the signal transduction performed by proteins of the STAT (Signal transducer and activators of transcription) family. They observed that the STAT Protein activator develops in two steps - first there occur phosphorylation of tyrosine, then that of serine also located in the C-terminal part of the molecule.

They reported that unlike other short-lived transcription factors, STAT proteins have a long half-life. It is also reported that the activated STAT molecules are inactivated by Cytokines and growth factors that activate STAT Proteins. They concluded that the main feature allowing proteins of the STAT family to be united into single group was their combination of two functions - the signal and transcriptional ones. The participation of the signal transduction demonstrate once more inter connection of all cellular process.

Bar-Or et al. (2000) reported the generation of oscillations by the p53-Mdm2 feedback loop. Assuming that the p53 concentration obeys the kinetic equation:

$$\frac{d(P53)}{dt} = source_p 53 - p53(t) Mdm2(t) degradation(t) - dP53P53(t)$$

where $source_p53$ = synthesis rate of p53 protein and the last term reflecting Mdm2 independent mechanism for kinetics governing the Mdm2 concentration was given by

$$\frac{d(Mdm2)}{dt} = p1 + p2_{max} \frac{I(t)^m}{k^n{}_m + I(t)^n} - dMdm2.Mdm2(t)$$

where I is the Intermediary given by,

$$\frac{d(I)}{dt} = activity p53(t) - k_{delay} I(t)$$

where $activity = \frac{Gsignal(t)}{1+C_2 Mdm2P53}$, where the activating signal was given by, $\frac{d(signal)}{dt} = -repair.signal(t)$.

Using the model, they reported consistency with computer simulations and observed that a delay in p53-dependent induction of Mdm2 is a pre-requisite for oscillatory behaviour and the length of delay determines period of oscillations.

Mihalas et al. (2006) studied the following system:

$$\begin{aligned}
x_1'(t) &= 1 - b_1 x_1(t) \\
y_1'(t) &= x_1(t) - (a_1 + a_{12} y_2(t-\tau)) y_1(t) \\
x_2'(t) &= f(y_1(t-\tau)) - b_2 x_2(t) \\
y_2'(t) &= x_2(t) - (a_2 + a_{21} y_1(t-\tau)) y_2(t)
\end{aligned}$$

where $f : R \to R$, the Hill function, is given by

$$f(x) = \frac{x^n}{a + x^n}$$

$n \in N^+$, $a > 0$, and all parameters are less than or equal to 1.

They studied the equilibrium state of the system and investigated the existence of Hopf bifurcation for the system using time delay and analysed the direction of Hopf bifurcation by normal form theory.

Sturm and Weber (2008) discuss the use of generic methods to reduce the questions on the existence of Hopf bifurcations in parameterized polynomial vector fields to quantifier elimination problems over the reals combined with simplification techniques available in REDLOG. Using generic methods to reduce the Hopf bifurcation problem to a quantifier, elimination available in REDLOG, one can construct most of the results given in the literature within less than a minute of computation time.

Shi-Wei et al. (2007) propose a statistical signal response model to describe the different oscillatory behaviour in a biological network motif, exploiting the non-linear dynamics in the negative feedback loop. The delay is chosen as a bifurcation model, the existence of Hopf bifurcation and the stability of the periodic solutions of the model equations with the centre manifold theorem and the normal form they are discussed. It is studied that there is a periodic solution born in a Hopf bifurcation beyond a critical time delay and this bifurcation phenomenon may be important to elucidate the mechanism of oscillatory activities in regulatory biological networks.

In this study, exploiting an auto-regulatory negative feedback loop, a statistical model of the p53–Mdm2 negative feedback system, with the aim of describing the different dynamical oscillatory behaviour of protein levels - both in individual and at population cells in a self-consistent way. This is elucidated through the equations:

$$\begin{aligned}\frac{d(Xt)}{dt} &= AX(t) + BX(t-\tau) + F \\ A &= (-\alpha p(1-r_0 p)M - \mu p - \alpha p(1-rp)P\end{aligned}$$

It is assumed that under normal conditions, the amount of p53 protein in the cell is kept low by the genetic metric in Mdm2 and p53 itself. When cells are exposed to damaging agents, it increases suddenly and this is followed by a cascade of events, through the modification of the binding properties of Mdm2.

Thus the authors state that:

(i) The p53 and Mdm2 leave their basal levels $P(0)$ and $M(0)$ and increase, with p53 followed by Mdm2.

(ii) After some time, due to negative feedback mechanism decreases its own along with the level of Mdm2 and enter a stationary level (p^*, M^*).

(iii) When the signal is completely resolved, the p53-Mdm2 loop returns to the normal case and the levels of p53 and Mdm2 to their basal values.

3.3 Partial Differential Equation Models

Building on the model of Mahaffy and Pao (1984), Busenberg and Mahaffy (1985) considered a class of models based on the theory of Jacob and Maned (genetic repression for control of biosynthesis and pathways in cells) including both spatial diffusion and time delays. Based on Goodwin's assumptions, they considered the following system:

$$\begin{aligned}
\frac{du_1(t)}{dt} &= f(v_1(t) - b_1 u_1(t) + a_1 \int_{-\partial\omega} [u_2(x_1(t) - u_1(t)] dS_\omega \\
\frac{dv_1(t)}{dt} &= -b_2 v_1(t) + a_2 \int_{-\partial\omega} [V_2(x_1(t) - V_1(t)] dS_\omega \\
\frac{\partial u_2(x,t)}{\partial t} &= D_1 \Delta u_2(x_1 t) - b_1 u_2(x_1 t)
\end{aligned}$$

and

$$\frac{\partial v_2(x,t)}{\partial t} = D_2 \Delta v_2(x_1 t) - b_2 u_2(x_1 t) + C_0 u_{2t}(x),$$

where $x \in \omega$, with boundary conditions,

$$\frac{\partial u_2(x,t)}{\partial t} = -\beta_1[u_2(x_1t - u_1t]$$

and

$$\frac{\partial v_2(x,t)}{\partial t} = -\beta^*[v_2(x_1t) - v_1(t)D_2\Delta v_2(x_1t) - b_2u_2(x_1t) + C_0u_{2t}(x),$$

$$\frac{\partial u_2(x,t)}{\partial t} = \frac{\partial v_2(x,t)}{\partial t} = 0$$

with the constants b_i = Kinetic Rates of decay, a_i = rates of transfer, D_i = Diffusion Coefficients, C_0 = production rate of repressor;

$v_1(t), u_2(x)$ = Delayed concentrations having discrete delays or a distributed delay, given by,

$$Z_{it} = \int_{-r}^{0} Z_i(t+\theta)d\eta(\theta)$$

with $\int_{-r}^{0} d\eta(\theta)$ = 1. Also β_1 and β_1^* are Fick's Law constants.

They obtained Differential Equation with one delays describing well mixed compartment system. From the above equations, they reduced the two compartment diffusion model to a system of delay differential equations. They established that the model reduces to a well mixed two compartment model when the Diffusivity tends to ∞.

Brown and Kholodenko (1999) first estimated the relative steady state gradient for a protein located exclusively on the cell membrane. They reported that the absolute concentration and gradients depend on kinase activity. They concluded that if the kinase and phosphatase of a protein are spatially separated in a cell, then large spatial gradients of the phospho-protein are inevitable, which has important implications in cell-signalling.

Rangamani and Iyengar (2006) analysed the spatio-temporal representations of dynamic cellular phenomena and how these models can be used to understand biological specificity in functional response. They studied the direct interaction networks. They observed that if the reaction is an enzyme catalysed reaction, where there is no change in the enzyme, the rate of reaction can be formulated using Michaelis–Menten Kinetics. They analysed chemical kinetics using ODEs and PDEs derived from the biochemical reaction system:

$$A + B \rightleftharpoons^{k_1}_{k_2} C$$

where the rate of the forward reaction = $k_1[A][B]$ and the rate of the backward reaction = $k_2[C]$. Net reaction rate = forward rate - backward rate.

They studied the temporal dynamics of the system by analysing the system of ODEs and further they analysed the spatio-temporal dynamics from the system of reaction–diffusion equations. For estimating the diffusion coefficients of the various species, they considered the Stokes' and the Wilke–Chang.

Gordon et al. (2009) reported the Spatio-Temporal Modelling of P53-Mdm2 Oscillatory system, investigating the spatial effects. Their spatial model accounts for both negative feedback and transcriptional delay. Considering p53 and Mdm2 with the six kinetic interactions namely: (1) basal p53 synthesis, (2) Mdm2 independent p53 degradation, (3) Mdm2-mediated P53 elimination, (4) basal p53-independent Mdm2 synthesis, (5) p53-induced Mdm2 synthesis and (6) Mdm2 degradation.

Sturrock et al. (2011) derived systems of partial differential equations to capture the evolution in space and time of the variables in the Hes1 and p53-Mdm2 systems. Through computational simulations they show that their reaction-diffusion models are able to produce sustained oscillations both spatially and temporally, accurately reflecting experimental evidence and advancing previous models. The simulations of our models also allow us to calculate a diffusion coefficient range for the variables in each mRNA and protein system, as well as ranges for other key parameters of the models, where sustained oscillations are observed. Finally, by exploiting the explicitly spatial nature of the partial differential equations,they manipulate mathematically the spatial location of the ribosomes, thus controlling where the proteins are synthesized within the cytoplasm. The results of their simulations predict an optimal distance outside the nucleus where protein synthesis should take place in order to generate sustained oscillations.

They inferred that the simulation results of our models have demonstrated the existence of oscillatory dynamics in negative feedback systems both for relatively simple (Hes1) and more complex (p53-Mdm2) pathways and have been able to focus on reactions occurring both in the cell nucleus and in the cytoplasm. The main advantage of using systems of PDEs to model intracellular reactions is that the PDEs enable spatial effects to be examined explicitly.

Cangiani and Natalini (2010) had earlier considered a spatio-temporal model for protein transport along microtubules, but not applied to negative feedback systems. This work was extended by Sturrock et al. (2012) to account for the effect of the nuclear membrane, active transport and cell shape on the observed oscillations.

Shymko and Glass (1974) studied spatial switching with two localised but chemically coupled catalytic sites and analysed the dependence of stability of the steady state. They considered the following equations:

$$\frac{\partial \psi}{\partial t} + F(\psi) - D \bigtriangledown^2 \psi = G(\psi)\Delta(r)$$

where ψ(r,t) is the vector of concentrations. The dependence for synthesis of chemical species was found through

$$f_A(\psi) = \frac{b + (\psi + \theta)^n}{1 + (\psi + \theta)^n}$$

where $b < 1$. They showed that the qualitative dynamics of chemical systems with a spatially heterogeneous catalyst depends in a fundamental way on the relative locations of the catalytic sites.

3.4 Analytical and Stochastic Models

Finally we note that recently there has been some work done in attempting to solve models of a canonical gene regulatory network – the "self-repressing gene" (i.e. the Hes1 system) – using analytical techniques. Several papers have adopted a stochastic approach and constructed a so-called "Master Equation" for such systems (Hornos et al. 2005; Ramos et al. 2011; Grima et al. 2012; Miekisz and Szymańska 2013) governing the probabilities $f_i(n,t)$, $i = 0,1$ (gene off or on) that there are n protein molecules in the system at time t and the gene (DNA) is in the state i. Using generating function techniques exact analytical solutions have been found for the steady-state problem and also the time-dependent problem, providing information on the total number of protein molecules in the system. However, we note that such models are highly theoretical and rather abstract, treating the distinct processes of transcription and translation as one, and ignoring all spatial effects.

3.5 Summary

Since the seminal work of Goodwin (1965) there have been many papers on gene regulatory networks (intracellular negative feedback systems) adopting a range of different modelling approaches and using different mathematical techniques – ordinary differential equations, delay (ordinary) differential equations and some with partial differential equations.

For the remainder of this thesis, we will use systems of partial differential equations to model in an explicitly spatial way several key gene regulatory networks which have been implicated in cancer – in particular, the Hes1 system and the p53-Mdm2 system.

Chapter 4

A Spatio-temporal Mathematical Model of the Hes1 and p53-Mdm2 Gene Regulatory Networks

4.1 A Spatio-Temporal Mathematical Model of the Hes1 System

4.1.1 Introduction

In this chapter we give an overview of a novel model by Sturrock et al. (2011) which developed the original model of Monk (2003). We will subsequently extend this model in chapter 5 and chapter 6 for Hes1 dimerization, stat3 and p53-Mdm2.

The Hes1 system is one of the most investigated feedback inhibition systems involving the transcription factor *Hairy Enhancer of Split 1* (Hes1) (Monk 2003). Hes1 transcription factor is a protein that is encoded by the Hes1 gene and a member of the Hes family of proteins which are basic helix-loop-helix (bHLH)-type transcriptional repressors that possess the bHLH domain in the N-terminal region for DNA binding. Hes1 has been shown to influence of nervous and digestive systems partially through the Notch signalling pathway by repressing bHLH activators. Hence, it is a primary target of Notch signalling and regulates many biological events by negatively regulating transcription of tissue-specific transcription factor (Ohsako et al. 1994).

HES1 also plays an important role in the Notch signalling pathway, (Shimojo et al. 2008). In the absence of Notch signalling, Hes1 expression is inhibited. After Notch signals have been processed within the cell, the plasma membrane releases the intracellular domain of Notch, which moves to the nucleus where it associates with RBPJ forming a complex that lead to activates Hes1 expression. Notch signalling activates Hes1 expression where HES1 has been shown to target Notch ligands such Dll1, Jagged1 (Jag1), and Neurogenin-2 (Ngn2) (Kageyama 1999).

Also, Hes1 can repress its own production by directly binding to N-box target sequences in its own promoter and represses the transcription of hes1 mRNA, thus forming a negative feedback loop, which produces oscillations in Hes1 gene expression. The interaction of the Hes1 system is similar to the generic example of a negative feedback loop with variable X and Y (see Figure 4.1). An increase in X causes Y to increase, which in turn results in the inhibition of X. After X begins to decrease Y levels will diminish, and this allows X to increase again. The repetition of this process produces oscillations in X and Y. Figure 4.2 shows that Hes1 follows the same process to produce oscillations, where Hes1 protein is produced by Hes1mRNA and then goes on to inhibit its own mRNA and so forth, with the result that the system oscillates with period of around 120 minutes. Hes1 oscillations are important for the maintenance and proliferation of neural stem cells under the control of Notch signalling (Baek et al. 2006).

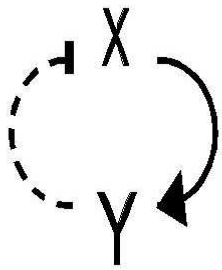

Figure 4.1: *A generic negative feedback loop.*

4.2 A Mathematical Model of the Hes1 System

Mathematical modelling of intracellular regulatory systems has developed since it began in 1965 with the work of Goodwin (1965). Monk (2003) was the first to consider biological data to develop a mathematical model of the Hes1 system. The basic reaction kinetics for this system modelled using ordinary differential equations are as follows:

$$\frac{d[M]}{dt} = \frac{\alpha_M}{1+(\frac{[P]}{\hat{p}})^h} - \mu_M[M] \tag{4.1}$$

$$\frac{d[P]}{dt} = \alpha_P[M] - \mu_P[P] \tag{4.2}$$

where $[M]$ and $[P]$ are the concentrations of Hes1 mRNA and Hes1 protein, respectively.

The first term on the right hand side of Eq.(4.1) is a Hill function which decreases as the protein concentration increases, modelling repression by the Hes1 protein. The parameter α_M is the rate of transcript initiation in the absence of Hes1 protein and $\widehat{p}$ is the concentration of Hes1 and h is a Hill coefficient. The second term represents the natural degradation of the Hes1 mRNA with parameter μ_M.

The first term on the right hand side of Equation (4.2) is the Hes1 protein production term from translation of Hes1 mRNA with parameter α_P and the second term represents Hes1 protein degradation with parameter μ_P.

A standard mathematical analysis shows that two-component models with negative feedback cannot have stable self-sustained oscillations (Bernard et al. 2006). In order to model the intracellular processes, Monk (2003) introduced a time-delay to equations (4.1), (4.2) to account for the processes of transcription and translation, and obtained sustained oscillations.
The two-compartment model for Hes1-mRNA self-repression with time-delay can be written as a system of delay differential equations (DDEs):

$$\frac{d[M]}{dt} = \frac{\alpha_M}{1+(\frac{[P(t-\tau_M)]}{\widehat{p}})^h} - \mu_M[M] \tag{4.3}$$

$$\frac{d[P]}{dt} = \alpha_P[M(t-\tau_P)] - \mu_P[P] \tag{4.4}$$

where τ_M and τ_P are the transcriptional and translational delays, respectively.

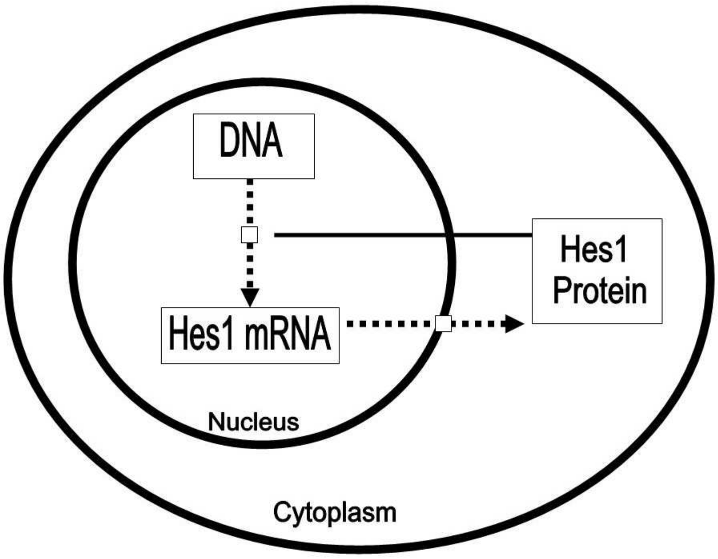

Figure 4.2: *A schematic diagram of the Hes1 gene regulatory network. hes1 mRNA is transcribed in the nucleus. It is then exported to the cytoplasm where translation into Hes1 protein occurs. hes1 mRNA is then inhibited in the nucleus by its own protein. This is one of the simplest examples of a negative feedback loop.*

A Time Delay Model

We here turn our attention to time delay in the transcription and translation processes. Many physiological systems which operate by feedback mechanisms have time delays occurring during the main process of receiving the effect and the physiological response. Therefore a time delay is a natural occurrence due to the finite transmission speed of matter, energy and information (Yutaka and Shinji 2011).

A time delay exists in the Hes1 system if any of the processes inside the cell take longer than others. For example, a time delay could exist in the mRNA transcription or in the protein translation or it could be in both.

We rewrite the system of equations (4.1), (4.2) considering the time delay first caused by the delay in mRNA transcription, then by the delay in protein degradation and finally by both interaction, transcription and production. Then we will study the system numerically using the parameter values in Table 1 to show the effect of the time delay on the oscillations.

Table 4.1: *List of parameter values*

Parameters	Values
α_M	1
α_P	1
μ_M	0.1
μ_P	1
τ_M	20
τ_P	20
h	5
$\widehat{p}$	1

For a delay caused in the protein production by the mRNA, in the cytoplasm which may coursed by the interaction of the Hes1 with other intracellular proses such as the activation of JAK-STAT interaction or by the activating Notch signalling.
To study the delay in protein production, equations (4.1), (4.2) become:

$$\frac{d[M]}{dt} = \frac{\alpha_M}{1+(\frac{[P]}{\widehat{p}})^h} - \mu_M[M] \tag{4.5}$$

$$\frac{d[P]}{dt} = \alpha_P[M(t-\tau_P)] - \mu_P[P] \tag{4.6}$$

If the delay was in the mRNA transcription then we have the following equations:

$$\frac{d[M]}{dt} = \frac{\alpha_M}{1+(\frac{[P(t-\tau_M)]}{\widehat{p}})^h} - \mu_M[M] \tag{4.7}$$

$$\frac{d[P]}{dt} = \alpha_P[M] - \mu_P[P] \tag{4.8}$$

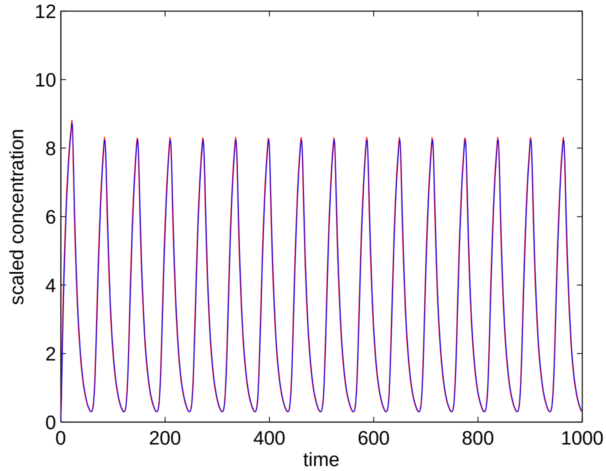

Figure 4.3: *Plot of Hes1 mRNA (red) and Hes1 protein (blue) concentrations against time with delay parameter $\tau = 20$. Computational simulation of the model with delay in Hes1 protein production, system of equations (4.5),(4.6). Oscillations are observed in the concentrations of both hes1 mRNA and HES1 protein.*

Finally, if the delay was a result of both processes of mRNA transcription and protein production, the equations are as follows:

$$\frac{d[M]}{dt} = \frac{\alpha_M}{1+(\frac{[P(t-\tau_M)]}{\widehat{p}})^h} - \mu_M[M] \tag{4.9}$$

$$\frac{d[P]}{dt} = \alpha_P[M(t-\tau_P)] - \mu_P[P] \tag{4.10}$$

We solve the systems of equations numerically using the parameter values in Table 1 and, as expected, we obtain oscillations in both hes1 mRNA and Hes1 protein levels. Figures 4.3, 4.4 and 4.5 show the oscillation of the concentrations of Hes1 mRNA and Hes1 protein vary over time. By comparing Figures 4.3, 4.4 and 4.5, we see that oscillatory dynamics are sustained steady and the delay does not caused big different on the oscillation. However, mRNA transcription delay has slightly delay on the protein production in Fig 4.4 comparing to the delay caused by the protein production itself

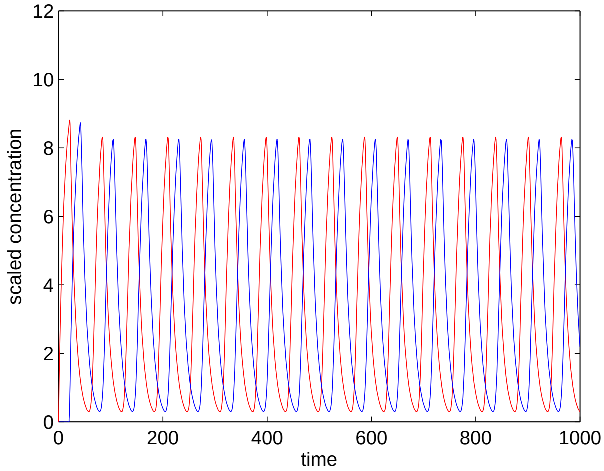

Figure 4.4: *Plot of Hes1 mRNA (red) and Hes1 protein (blue) concentrations against time with delay parameter* $\tau = 20$*. Computational simulation of the model with delay in hes1 mRNA transcription, system of equations(4.7),(4.8). Oscillations are observed in the concentrations of both hes1 mRNA and HES1 protein.*

in Fig 4.3, while Fig 4.5 shows the oscillation takes more time for the mRNA and the protein to shift between the cytoplasm and the nucleus.

4.3 The Hes1 Spatio-temporal Mathematical Model

We now extend the previous models and consider spatial interactions within the cell as shown in Figure 4.6. We consider the nucleus and cytoplasm as two spatial compartments separated by the nuclear membrane (in all subsequent analysis and models, zero flux boundary conditions are imposed on all species at the cell membrane). Also, we couple the reaction kinetics from ODE model (4.1), (4.2) with diffusion to model the protein and mRNA transport within the cell.

Hes1 transcription occurs in the nucleus to produce hes1 mRNA which then transfers

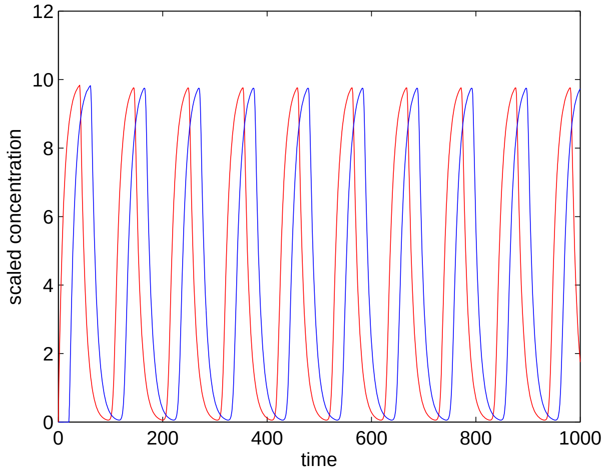

Figure 4.5: *Plot of Hes1 mRNA (red) and Hes1 protein (blue) concentrations against time with delay parameter* $\tau = 20$. *Computational simulation of the model with delay in both hes1 mRNA transcription and Hes1 protein production, system of equations(4.9,4.10). Oscillations are observed in the concentrations of both hes1 mRNA and HES1 protein.*

to the cytoplasm where Hes1 protein synthesis occurs. We assume that the mechanism governing the spatial movement of the mRNA and the protein between the nucleus and the cytoplasm is diffusion.

The system of equations of the spatio-temporal evolution of hes1 mRNA and Hes1 protein is now:

$$\frac{\partial [M_n]}{\partial t} = D_{M_n}\nabla^2[M_n] + \frac{\alpha_M}{1+(\frac{[P_n]}{\hat{p}})^h} - \mu_M[M_n], \tag{4.11}$$

$$\frac{\partial [M_c]}{\partial t} = D_{M_c}\nabla^2[M_c] - \mu_M[M_c], \tag{4.12}$$

$$\frac{\partial [P_c]}{\partial t} = D_{P_c}\nabla^2[P_c] + \alpha_P[M_c] - \mu_P[P_c], \tag{4.13}$$

$$\frac{\partial [P_n]}{\partial t} = D_{P_n}\nabla^2[P_n] - \mu_P[P_n], \tag{4.14}$$

where $[M_n]$,$[M_c]$, $[P_n]$ and $[P_c]$ are the concentration of the nuclear and the cytoplasmic hes1 mRNA and the nuclear and the cytoplasmic Hes1 protein respectively. $[D_i]$ denote the diffusion coefficients for each species.

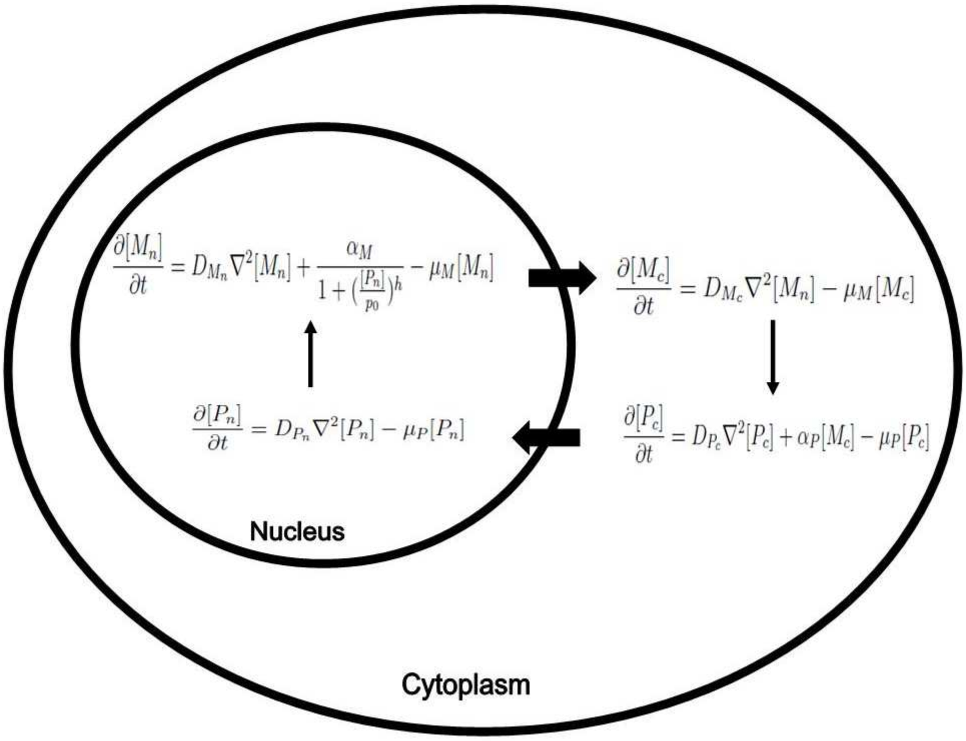

Figure 4.6: *Schematic diagram showing how the spatial interactions between hes1 mRNA and Hes1 protein are modelled. hes1 mRNA is produced in the nucleus (transcription), then exported across the nuclear membrane into the cytoplasm where it is translated into protein, i.e., transcription occurs exclusively in the nucleus and translation/synthesis occurs exclusively in the cytoplasm. Hes1 protein is then imported back across the nuclear membrane to the nucleus where it inhibits the production of its own mRNA, i.e., a negative feedback loop exists.*

Continuity of flux boundary conditions across the nuclear membrane allow import and export of hes1 mRNA and Hes1 protein, while zero flux boundary conditions at the outer cell membrane ensure that all molecules remain within the cell.

$$
\begin{aligned}
D_{M_n}\frac{\partial[M_n]}{\partial n} &= D_{M_c}\frac{\partial[M_c]}{\partial n} \; and \; [M_n]=[M_c] \; at\; the\; nuclearmembrane \qquad (4.15)\\
D_{P_n}\frac{\partial[P_n]}{\partial n} &= D_{P_c}\frac{\partial[P_c]}{\partial n} \; and \; [P_n]=[P_c] \; at\; the\; nuclearmembrane \qquad (4.16)\\
\frac{\partial[M_c]}{\partial n} &= 0, \; at\; the\; cell\; membrane \qquad (4.17)\\
\frac{\partial[P_c]}{\partial n} &= 0, \; at\; the\; cell\; membrane \qquad (4.18)
\end{aligned}
$$

Equations (4.11)–(4.14) represent a system of reaction-diffusion equations modelling the spatio-temporal evolution of the Hes1 system. The same reaction kinetics from the ODE model (4.1), (4.2) are retained but are now also coupled with diffusion to model explicitly protein and mRNA transport within a cell, i.e., molecules move from the nucleus to the cytoplasm and cytoplasm to nucleus across the nuclear membrane. The PDE system reflects the reality that mRNA is transcribed from DNA exclusively in the nucleus and that protein is translated from mRNA exclusively in the cytoplasm, i.e., there are production terms only for $[M_n]$ (in Eq. (4.11)) and $[P_c]$ (in Eq. (4.13)). Finally, we make the assumption that the translation of proteins from mRNA in the cytoplasm occurs some distance away from the nucleus and outside the endoplasmic reticulum (ER), since proteins produced in the ER are mainly either exported to the exterior of the cell or transported to other membrane structures such as the Golgi apparatus, lysosomes and endosomes(Alberts et al. 1994), (**?**).

In order to model this, we modify Equation (4.13) as follows:

$$
\frac{\partial[P_c]}{\partial t} = D_{P_c}\nabla^2[P_c] + H_1(x,y)\alpha_P[M_c] - \mu_P[P_c] \qquad (4.19)
$$

where $H_1(x,y)$ is a Heaviside function localising the protein production whose specific form will be given after the nondimensionalisation of the system. The $H_1(x,y)$ function takes the is value zero (0) in a region just outside the nucleus, meaning there is no protein synthesis in this ER region. In a region further away from the nucleus (outside the ER) the function takes the value one (1), in the region of the cytoplasm where we assume the translation of protein occurs.

We nondimensionalise Equations (4.11), (4.12), (4.14) and (4.19) with scaling variables as follows (see Appendix A):

$$
\begin{aligned}
\overline{[M_n]} &= \frac{[M_n]}{m_0}\ ,\ \overline{[M_c]} = \frac{[M_c]}{m_0}\ ,\ \overline{[P_n]} = \frac{[P_n]}{p_0}\ ,\ \overline{[P_c]} = \frac{[P_c]}{p_0} \\
\bar{t} &= \frac{t}{\tau}\ ,\ \overline{X} = \frac{x}{L}\ ,\ \overline{Y} = \frac{y}{L} \qquad (4.20)
\end{aligned}
$$

where $[m_0]$,$[p_0]$ are reference concentration, τ is reference time, and L is a reference length. Using this scaling Equations (4.11), (4.12), (4.14) and (4.19) become:

$$\frac{\partial[\overline{M_n}]}{\partial\bar{t}} = D^*_{M_n}\nabla^2\overline{[M_n]} + \frac{\alpha^*_M}{1+(p^*\overline{[P_n]})^h} - \mu^*_M[\overline{M_n}] \qquad (4.21)$$

$$\frac{\partial[\overline{M}_c]}{\partial\bar{t}} = D^*_{M_c}\nabla^2[\overline{M}_c] - \mu^*_M[\overline{M}_c] \qquad (4.22)$$

$$\frac{\partial[\overline{P}_c]}{\partial\bar{t}} = D_{P_c}\nabla^2[P_c] + H_1(x,y)\alpha_P[M_c] - \mu_P[P_c] \qquad (4.23)$$

$$\frac{\partial[\overline{P}_n]}{\partial\bar{t}} = D^*_{P_n}\nabla^2[\overline{P}_n] - \mu^*_P[\overline{P}_n] \qquad (4.24)$$

where

$$
\begin{aligned}
D_{M_n}^* &= \frac{\tau D_{M_n}}{L^2}\ ,\ D_{M_c}^* = \frac{\tau D_{M_c}}{L^2}\ ,\ D_{P_n}^* = \frac{\tau D_{P_n}}{L^2}\ ,\ D_{P_c}^* = \frac{\tau D_{P_c}}{L^2} \\
\alpha_M^* &= \frac{\tau \alpha_M}{m_0}\ ,\ \alpha_P^* = \frac{\tau \alpha_P}{p_0} \\
\mu_M^* &= \tau \mu_M\ ,\ \mu_P^* = \tau \mu_P\ ,\ p^* = \frac{p_0}{\widehat{p}}
\end{aligned} \tag{4.25}
$$

and

$$
H_1(\overline{x},\overline{y}) = \begin{cases} 0, & \text{if } \frac{\overline{x}^2}{2} + \overline{y}^2 \leq 0.25, \\ 1, & \text{if } \frac{\overline{x}^2}{2} + \overline{y}^2 > 0.25. \end{cases}
$$

We apply zero initial conditions, zero-flux boundary condition at the cell membrane and flux continuity boundary conditions across the nucleus membrane:

$$
[\overline{M}_n] = [\overline{M}_c] = [\overline{P}_n] = [\overline{P}_c] = 0,\ at\ t = 0 \tag{4.26}
$$

$$
D_{M_n}^* \frac{\partial [\overline{M}_n]}{\partial n} = D_{M_c}^* \frac{\partial [\overline{M}_c]}{\partial n}\ and\ [\overline{M}_n] = [\overline{M}_c]\ at\ the\ nuclearmembrane \tag{4.27}
$$

$$
D_{P_n}^* \frac{\partial [\overline{P}_n]}{\partial n} = D_{P_c}^* \frac{\partial [\overline{P}_c]}{\partial n}\ and\ [\overline{P}_n] = [\overline{P}_c]\ at\ the\ nuclearmembrane \tag{4.28}
$$

$$
\frac{\partial [\overline{M}_c]}{\partial n} = 0,\ at\ the\ cell\ membrane \tag{4.29}
$$

$$
\frac{\partial [\overline{P}_c]}{\partial n} = 0,\ at\ the\ cell\ membrane \tag{4.30}
$$

Due to a lack of experimental data, we take reference concentrations to be $[m_0]$=0.05μM and $[p_0]$=1μM. Figures 4.7, 4.8 show the computational simulation results of Equations (4.21)-(4.24), where oscillations in concentrations are observed with a period of oscillation of approximately 200 time units. Knowing that the period of oscillation of Hes1 is approximately 2hours (Hirata et al. 2003) we can estimate the reference time τ as follows: 200τ =2 h which means τ= 36 s.

To obtain the value of the variable L we used 2-dimensional cell domain with length of 30μM to represents both the nucleus and cytoplasm where the nucleus has a major axis of length 0.8 units and minor axis of length 0.5 units and the cytoplasm has a major axis of length 3 units and a minor axis of length 2 units. Hence, the non-dimensional cell width is equal to 3 L = 30μM so, the reference length L=10μM.

Parameter Estimation

The following parameter values were used in our simulations of the non-dimensional Hes1 system:

$$\begin{aligned} D^*_{M_n} = D^*_{M_c} = D^*_{P_n} = D^*_{P_c} = 7.5 \times 10^{-4} \\ \alpha^*_M = 1\ ,\ \alpha^*_P = 2\ ,\ h = 5\ ,\ p^* = 1\ ,\ \mu^*_M = \mu^*_P = 0.03 \end{aligned} \tag{4.31}$$

From (4.19) and (4.25) we calculate the dimensional parameter values as follows:

$$
\begin{aligned}
D_{M_n} &= \frac{L^2 D^*_{M_n}}{\tau} = 2.08 \times 10^{-11} cm^2 s^{-1} \\
so: D_{M_n} &= D_{M_c} = D_{P_n} = D_{P_c} = 2.08 \times 10^{-11} cm^2 s^{-1} \\
\alpha_M &= 1.39 \times 10^{-9} M s^{-1},\ \alpha_P = 1.11 s^{-1} \\
\mu_M &= \mu_P = 8.33 \times 10^{-4} s^{-1},\ h = 5,\ p_0 = 1 \times 10^{-6} M
\end{aligned}
$$

We carried out a number of simulations on the Hes1 system (4.21)-(4.24) to obtain the range of diffusion coefficients for which we observe oscillations (all other parameters remain unchanged). The system exhibits oscillations when the mRNA and the protein diffusion coefficients have a value in the range 1.67×10^{-11} to $9.72 \times 10^{-11} cm^2 s^{-1}$. We have also calculated a range of mRNA degradation rates: $1.67 \times 10^{-4}$to $1.17 \times 10^{-3} s^{-1}$, protein degradation rates 1.94×10^{-4} to $1.06 \times 10^{-3} s^{-1}$ and Hill coefficients $h \geq 4$ for which the system exhibits oscillations.

4.3.1 Computational Simulation Results

We solve the system (4.21)-(4.24) numerically using COMSOL/FEMLAB package which uses the finite element technique. Triangular basis elements and Lagrange quadratic basis functions along with a backward Euler time-stepping method for integrating the equations were used in all simulations.

Figure 4.7 shows the total concentrations of hes1 mRNA and Hes1 protein over time in the nuclear compartment, while Figure 4.8 shows the total concentrations in the cytoplasm.

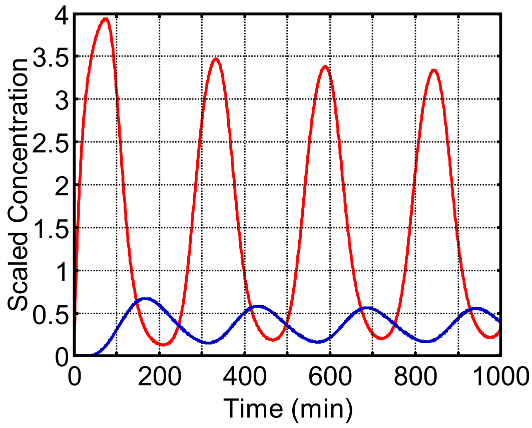

Figure 4.7: *Plot of the concentrations of hes1 mRNA (red) and Hes1 protein (blue) in the nucleus over time. The period of oscillations is approximately 120 min*

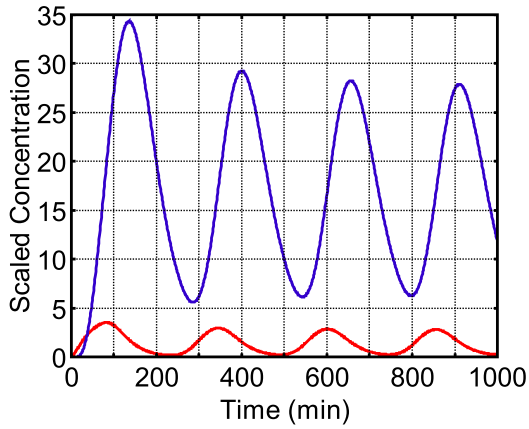

Figure 4.8: *Plot of the concentrations of hes1 mRNA (red) and Hes1 protein (blue) in the cytoplasm over time. The period of oscillations is approximately 120 min*

The plots presented in Figures 4.9 and 4.10 show how the hes1 mRNA and Hes1 protein concentrations vary spatially as well as temporally within the cell. The mRNA is produced inside the nucleus and by $t = 60$ min has started to cross the nuclear membrane to enter the cytoplasm (Figure 4.9). In the cytoplasm the mRNA is translated into protein, which then diffuses back into the nucleus and represses the production of its own mRNA $t = 120min$. The mRNA concentration has clearly depleted by $t = 120$ min, reflecting the period of the temporal oscillation seen in Figures 4.7, 4.8. As can

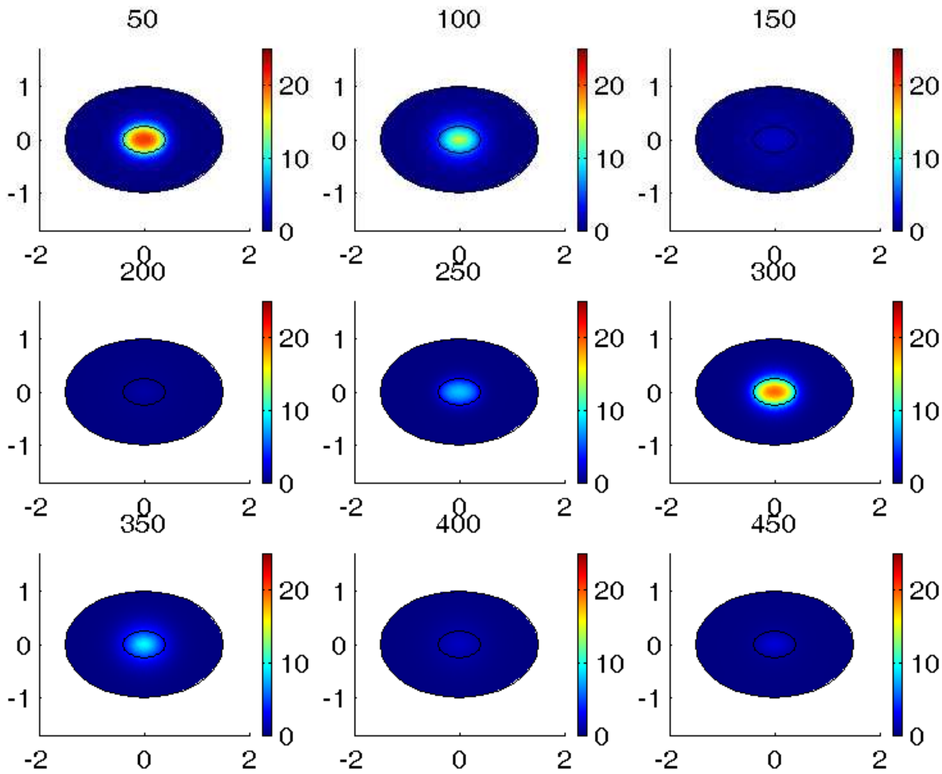

Figure 4.9: *Plots showing the spatio-temporal evolution of hes1 mRNA concentration within the cell from times t=0 to 480 min at 60 min intervals. The concentration oscillates in both time and space. Parameter values as per (25).*

be seen from Figure 4.10, there is a delay in the rise of protein concentration after $t = 0$ as it takes time for the mRNA to be produced and exported to the cytoplasm. By $t = 60$ min the protein levels have clearly risen in the cytoplasm and have reached the nucleus. At $t = 120$ min the protein concentration has decreased significantly, due to the inhibition of mRNA transcription by the protein.

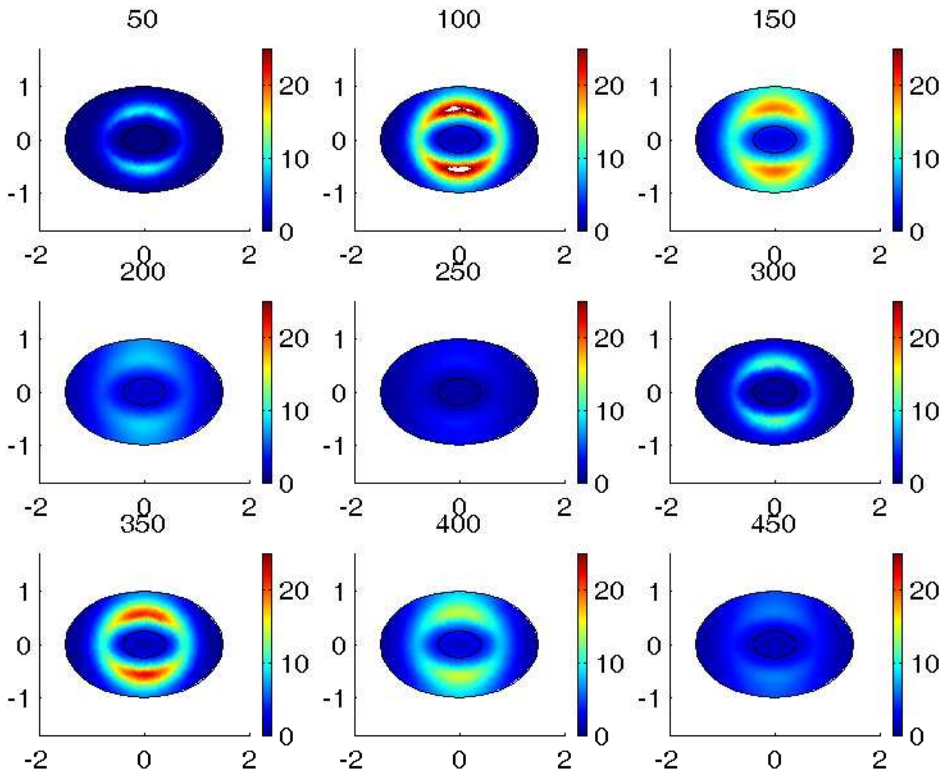

Figure 4.10: *Plots showing the spatio-temporal evolution of Hes1 protein concentration within the cell from times t=0 to 480 min. The concentration oscillates in both time and space. Parameter values as per (25).*

4.4 A Spatio-Temporal Mathematical Model of the P53-Mdm2 System

4.4.1 Introduction

p53 is known as protein 53 or tumour protein 53 (on account of its molecular weight). The p53 gene was identified in 1979 by Arnold Levine, David Lane and Lloyd Old, but in 1989 it found its role in the cell as a tumour suppressor gene (Lane and Crawford 1979). It plays an important role in multicellular organisms where it is a transcription factor that regulates the cell cycle, functions as a tumour suppressor and is involved in preventing cancer. Mutations that inactivate p53 function have been detected in more than 50% of human cancers (Bennett et al. 1999).

In normal unstressed cells the concentration level and activity of p53 are low, whereas the concentration of p53 increases and is negatively regulated in response to stress signals such as DNA damage due to Mdm2 induced degradation.

The regulation of the p53 protein by mdm2 goes through four successive phases of the standard eukaryotic cell cycle including, mitosis (M phase), gap1 (G1 phase), synthesis (S phase) and gap2 (G2 phase). There are several nuclear proteins involved in the regulation of DNA replication during the cell growth (Alberts et al. 1994). The p53 tumour suppressor protein is one of the most important nuclear proteins involved in growth arrest, apoptosis and DNA repair (Melino et al. 2003). In normal unstressed cells, the levels of p53 protein are sustained at low levels via interaction with other protein such as MDM2 (murine double minute 2). Once the levels of p53 protein increases, for example after DNA damage, it acts as a transcription factor, inducing the expression of several genes such as Bax (apoptosis inducer), p21 WAF1, which induces growth arrest (Freedman and Levine 1998). Upon several types of stresses, the p53 pathway has been divided into five stages, the stress signals which activate p53 pathway, detection and interpretation of the upstream signals by the upstream mediators, interaction of p53 with several proteins which lead to its stability, transcriptional activation and protein-protein interactions and the final outcome, growth arrest , apoptosis or DNA repair (Levine et al. 2006). As mentioned previously, in normal conditions, the level of p53 protein is down-regulated through its interaction with mdm2 protein which enhances p53 degradation in the cytoplasm or via a p53-mdm2 complex in the nucleus, preventing p53 to activate transcription (Thut et al. 1997). Specifically, p53 protein utilizes its NH2-terminal domain to activate its own transcription. The mdm2 binds to this region blocking this ability (Lu and Levine 1995). The mdm2 protein has the ability to shuttle between the nucleus and cytoplasm due to the NES sequence (Roth et al. 1998). Its activity is essential for shuttling p53 to the cytoplasm for degradation by cytoplasmic proteasomes. Figure 4.11 summarizes regulation of the p53 by the mdm2 in normal cells. The ability of mdm2 protein to shuttle p53 from the nucleus to the cytoplasm was proposed by Freedman and Levin, (1998). In a later model, mdm2, p53,CRM1,and RanGTP form a ternary complex in the nucleus Figure 4.12. This triggers transportation of the complex through the nuclear pore to the cytoplasm where p53 protein is degraded while the mdm2 protein is returned to the nucleus.

Following DNA damage, p53 protein is stabilized and activated as a transcription factor that induces expression of several genes. It has been demonstrated that after DNA damage, the ability of mdm2 to down-regulate p53 either via degradation or by forming a complex to prevent transcription were lost although high levels of mdm2 were observed (Landers et al. 1997).

The tumour suppressor protein p53 has been observed in a wide variety of human cancers. Loss of p53 gene from chromosome 17 was reported in several cancers (Vogelstein et al. 1988). Another study showed that the p53 gene contains point mutations in the lung cancer (Takahashi et al. 1989). The inactivation of p53 could be caused in several ways: mutation occurrence found in 50% of human cancers. Some viruses such as SV40, HPV or adenoviruses encode proteins that inhibit p53 protein. In both cases of inflammatory breast cancer and neuroblastoma, the accumulation of p53 protein in the cytoplasm was reported. The accumulation of mdm2 protein in some types of cancers was observed.

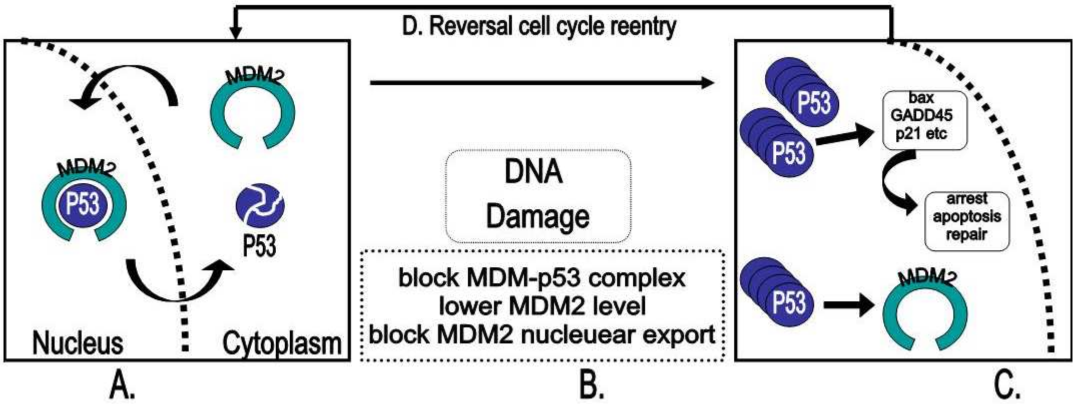

Figure 4.11: *A model of the regulation of the p53 protein by the mdm2 protein. (A) To prevent p53 transcription in the nucleus, mdm2 binds to p53 protein. utilizing RanGTP-dependent pathway, mdm2 shuttle p53 from nucleus to cytoplasm for degradation by proteasomes. (B) After DNA damage, mdm2 becomes inactive via blocking p53-mdm2 complex formation, lower mdm2 levels and blocking mdm2 nuclear transportation. (C) p53 remains active as transcription factor and tumour suppression in the nucleus in order to cause growth arrest or apoptosis. (D) After the DNA is repaired mdm2 become active again, practicing its function as autoregulatory protein controlling p53 in the nucleus (Adapted from Freedman and Levine, 1999).*

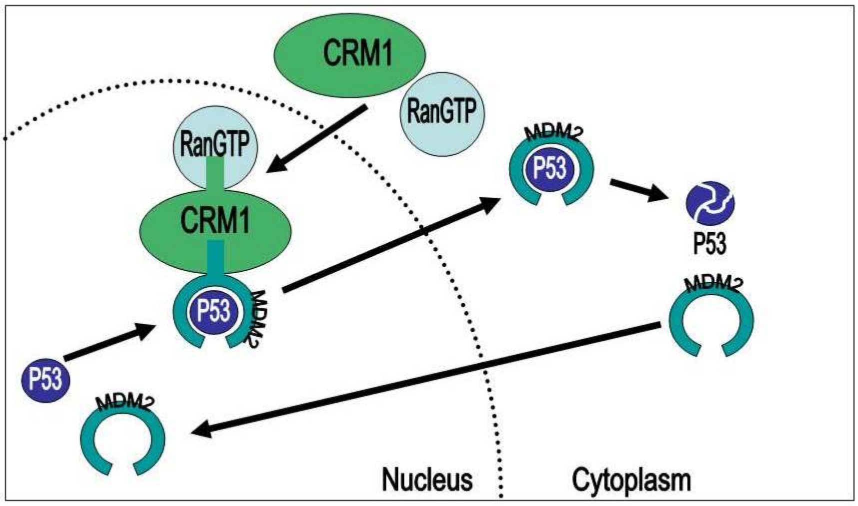

Figure 4.12: *A model for the transportation of p53 from the nucleus to the cytoplasm by mdm2. It is believed that mdm2, p53, CRM1 and RanGTP form complex that trigger transportation of p53 to the cytoplasm. The mdm2 then is separated from p53 and is returned the nucleus (Adapted from Freedman and Levine, 1998)*

4.5 Mathematical Modelling of the p53-Mdm2 System

Mdm2 functionally interacts with many proteins involved in the control of cell proliferation and survival. Mdm2 acts as a direct negative regulation of p53. This occurs through two main mechanisms: first, transcriptional activation of p53; second, targeting p53 for modification and degradation (Manfredi 2010).

The basic interaction between p53 and Mdm2 creates a negative feedback which is shown in the schematic digram in Figure 4.13.

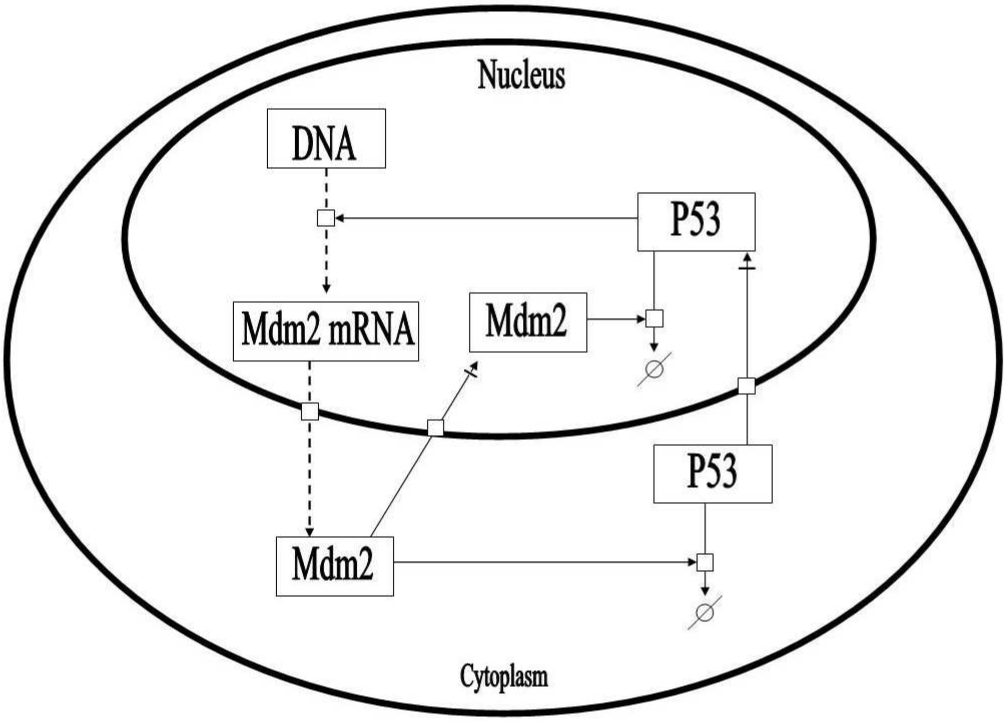

Figure 4.13: *A schematic representation of the p53-Mdm2 model.*

We begin by looking at the fundamental reaction kinetics of the system. Denoting the concentrations of p53, Mdm2 and Mdm2 mRNA by $[p], [M]$ and $[Mm]$, respectively, the ODE system below is formulated to capture the interactions depicted in Figure 4.13:

$$\frac{d[P]}{dt} = \beta - (\mu + \nu(\frac{[M]^{h1}}{\widehat{M}^{h1} + [M]^{h1}}))[P] \tag{4.32}$$

$$\frac{d[Mm]}{dt} = \alpha + \eta(\frac{[P]^{h2}}{\widehat{P}^{h2} + [P]^{h2}}) - \phi[Mm] \tag{4.33}$$

$$\frac{d[M]}{dt} = \gamma[Mm] - \rho[M] \tag{4.34}$$

where $[P], [Mm]$ and $[M]$ are the concentration of p53, Mdm2 mRNA and Mdm2 protein, respectively.

The first ODE equation (4.32) for p53 has β as a production term of p53 followed by a natural degradation term of rate μ, and ν a degradation term of Mdm2. The second ODE (4.33) for Mdm2 mRNA, has a production rate α, followed by η a production term of p53, and finally ϕ degradation rate. The final ODE (4.34) is for the Mdm2 protein, which has γ a production rate of Mdm2 mRNA and ρ a degradation rate. $\widehat{M}$ and $\widehat{p}$ are activation thresholds, and h1 and h2 are Hill coefficients.

Table 4.2: *Parameters value*

Parameters	Values	Parameters	Values
β	10	μ	0.00025
ν	64	α	0.00235
η	40	ϕ	0.8
γ	01	ρ	3
A	0.05	B	1.066
h1	1	h2	50

We are going the study the system (4.32), (4.33) and (4.34) numerically using the parameter values in Table (4.2) to show the oscillations of the system.

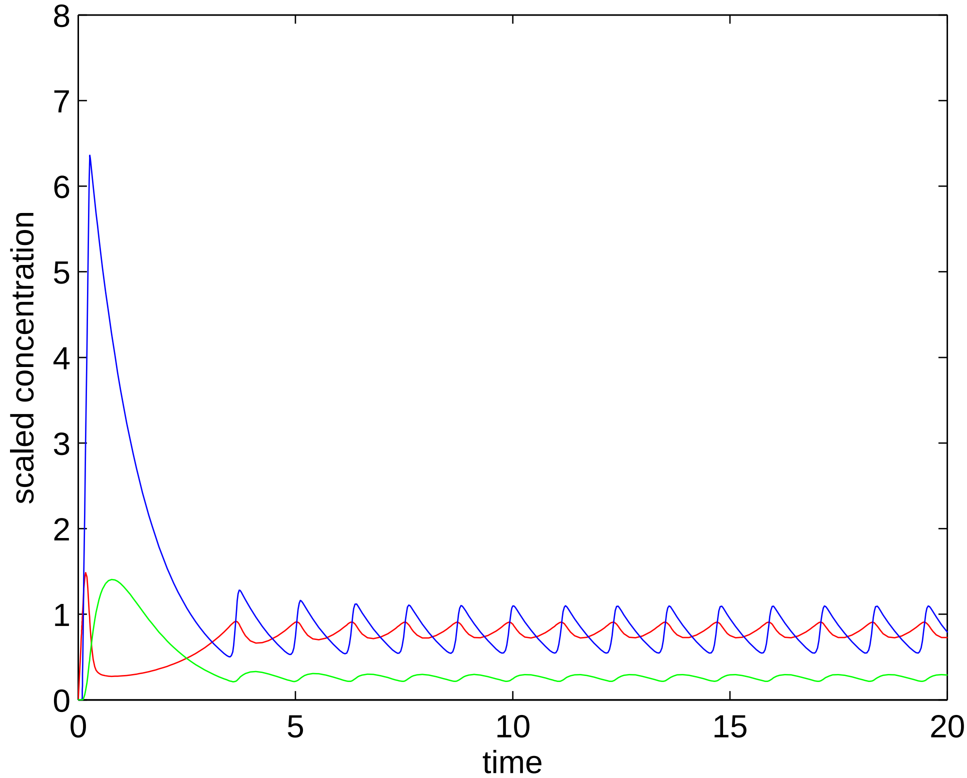

Figure 4.14: *Plot of p53 (red), Mdm2 mRNA (blue) and Mdm2 protein (green) concentrations against time with no delay. Computational simulation of the model with parameter values in Table (4.2).*

Figure 4.14 shows the simulation of the p53-Mdm2 model without a time delay.

4.5.1 A Model with Time Delay

A time delay exists in the system if any of the processes inside the cell take longer than others. For example, a time delay could exist in the protein transcription or in the mRNA translation or it could be in both. As before with the Hes1 system, Monk (2003) added a delay to account for transcript elongation, splicing, processing and export.

Following Monk (2003), we rewrite the equation system (4.32), (4.33) and (4.34) considering the time delay firstly caused by the delay in mRNA transcription, then by the delay in protein degradation and finally by both of the delays. Then we are going the study the system numerically using the parameter values in Table 4.2 to show the effect of the time delay on the system.

If the delay is associated with p53, equations (4.11), (4.12) and (4.13) become:

$$\frac{d[P]}{dt} = \beta - (\mu + \nu(\frac{[M]^{h1}}{\widehat{M}^{h1} + [M]^{h1}}))[P] \tag{4.35}$$

$$\frac{d[Mm]}{dt} = \alpha + \eta(\frac{[P(t-\tau)]^{h2}}{\widehat{P}^{h2} + [P(t-\tau)]^{h2}}) - \phi[Mm] \tag{4.36}$$

$$\frac{d[M]}{\partial dt} = \gamma[Mm] - \rho[M] \tag{4.37}$$

If the delay was in the Mdm2 mRNA transcription then we would have the following equations:

$$\frac{d[P]}{dt} = \beta - (\mu + \nu(\frac{[M]^{h1}}{\widehat{M}^{h1} + [M]^{h1}}))[P] \tag{4.38}$$

$$\frac{d[Mm]}{dt} = \alpha + \eta(\frac{[P]^{h2}}{\widehat{P}^{h2} + [P]^{h2}}) - \phi[Mm] \tag{4.39}$$

$$\frac{d[M]}{\partial dt} = \gamma[Mm(t-\tau)] - \rho[M] \tag{4.40}$$

If the delay was associated with the Mdm2 protein then we would have the following equations:

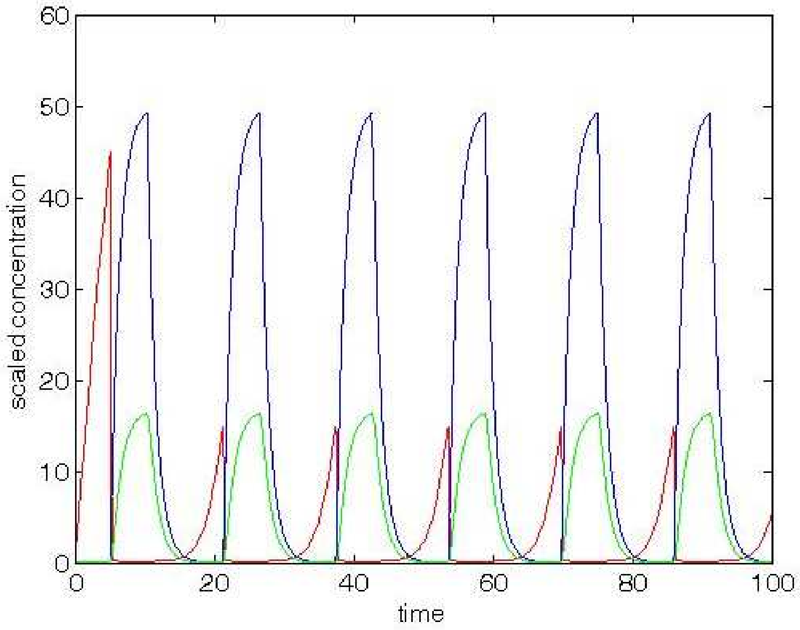

Figure 4.15: *Plot of p53 (red), Mdm2 mRNA (blue) and Mdm2 protein (green) concentrations against time with tau = 5. Computational simulation of the model with delay in p53 protein degradation. System of equations (4.35), (4.36) and (4.37) with parameters values in Table (4.2).*

$$\frac{d[P]}{dt} = \beta - (\mu + \nu(\frac{[M(t-\tau)]^{h1}}{\widehat{M}^{h1} + [M(t-\tau)]^{h1}}))[P] \quad (4.41)$$

$$\frac{d[Mm]}{dt} = \alpha + \eta(\frac{[P]^{h2}}{\widehat{P}^{h2} + [P]^{h2}}) - \phi[Mm] \quad (4.42)$$

$$\frac{d[M]}{\partial dt} = \gamma[Mm] - \rho[M] \quad (4.43)$$

We solve the systems of equations numerically using the parameter values in Table 4.2. As expected, we obtain oscillations from the negative feedback system.

It is clear that the concentrations of the variables reach higher levels compared with the result of the oscillation in Fig 4.14. Figure 4.15 shows the result of the equations

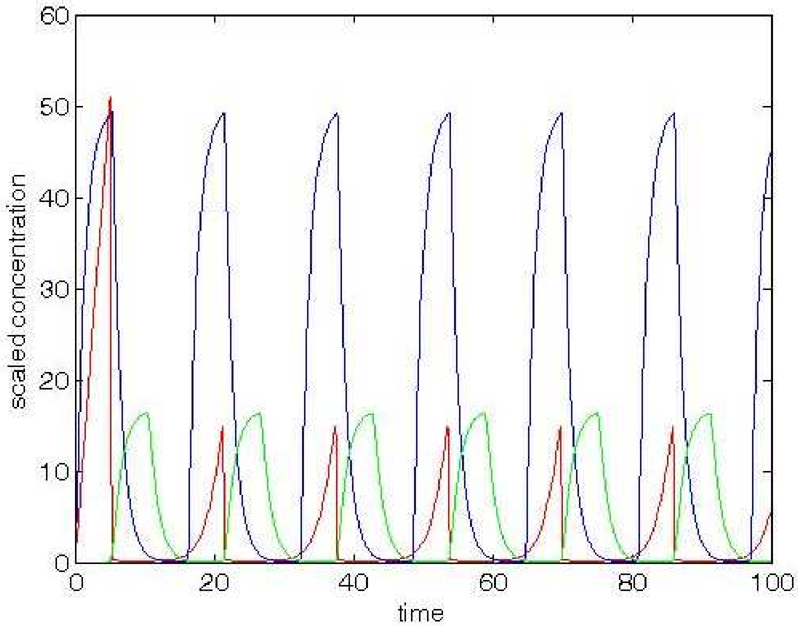

Figure 4.16: *Plot of p53 (red), Mdm2 mRNA (blue) and Mdm2 protein (green) concentrations against time with delay $\tau = 5$. Computational simulation of the model with delay in Mdm2 mRNA degradation. System of equations (4.38), (4.39) and (4.40) with parameters value in Table (4.2).*

(4.35), (4.36) and (4.37) when we consider the time delay through the p53 degradation process. Mdm2 mRNA takes more time to diffuse between the two domains (nucleus, cytoplasm) thus its concentration is higher than the concentration of the other components.

Figure 4.16 shows the result of the equations (4.38), (4.39) and (4.40) when we consider the time delay through the Mdm2 mRNA degradation process. p53 takes more time to diffuse between the two domains thus its concentration is higher than the concentration of the other components whereas the Mdm2 mRNA diffuses faster.

In Figure 4.17, the result of the equations (4.41), (4.42) and (4.43) simulation when we

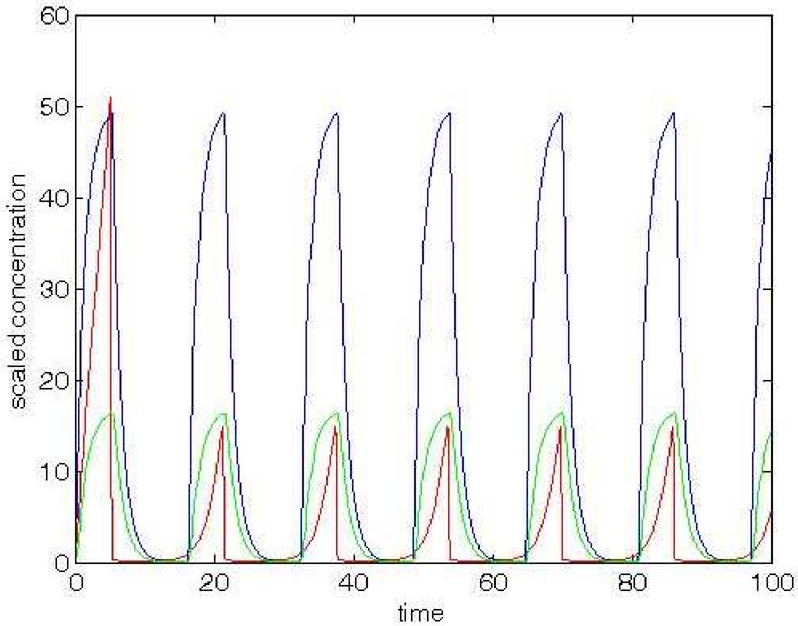

Figure 4.17: *Plot of p53 (red), Mdm2 mRNA (blue) and Mdm2 protein (green) concentrations against time with delay $\tau = 5$. Computational simulation of the model with delay in Mdm2 protein degradation System of equations (4.41), (4.42) and (4.43) with parameter values in Table (4.2).*

consider the time delay through the Mdm2 protein degradation process are given. It shows the Mdm2 protein diffusion is following the p53 diffusion while it is not in other figure. So adding the time delay has quickened the Mdm2 protein shuttle between the nucleus and the cytoplasm.

Chapter 5

A Spatio-temporal Mathematical Model of the Hes1 System Incorporating Dimerization

The chapter can be broadly organized into three parts. In the first part of this chapter we extend the ODE model analysed in (Momiji and Monk 2008) by building the PDE model for Hes1 dimeraization system and run the simulation for the model. Then, in the second part, we present the ODE model of Stat3 and extend the model by considering diffusion (i.e. a PDE model) and run the simulation of the model. Finally we analysed the impact of the Stat3 PDE model on the Hes1 PDE model in the first part and examined the effects on the model such as varying nuclear membrane thickness, adding diffusion noise, and adding convection (modelling molecular transport along microtubules) to the model.

5.1 Introduction

We start this chapter by developing the previous model to include the effect of Hes1 dimeraization. In order to do this, we first consider the delay ODE model of Momiji and Monk (2008).

Oscillations in molecular species concentration levels are the sign of complex genetic regulatory network involving a negative feedback loop. it plays an important role in wide rang of cellular phenomena. Many of the biological processes involve transcriptional oscillations which depends on a segmentation clock to organise transcriptional oscillations in complex networks of interactions (Momiji and Monk 2008). The oscillatory expression of Hes1 has been shown to be involved in the segmentation clock.

The model in Equations (4.1) and (4.2) in chapter 4 encodes the Hes1 feedback loop in simple manner, representing only transcription, translation and degradation. However, there are several other important biochemical processes involved in the Hes1 feedback loop. Momiji and Monk (2008) used experimental biological data to develop a more detailed Hes1 model to generate protein oscillation. Momiji and Monk (2008) consider seven biochemical prosses such as transcription, translation, repression, degradation, protein shuttling and protein dimerisation.

Figure 5.1 represents schematically the mass action kinetics for the main processes involved in the more complex Hes1 feedback circuit as it is presented in Momiji and Monk (2008).

We sumraize the intracelullar processes involved in the Hes1 feedback loop.

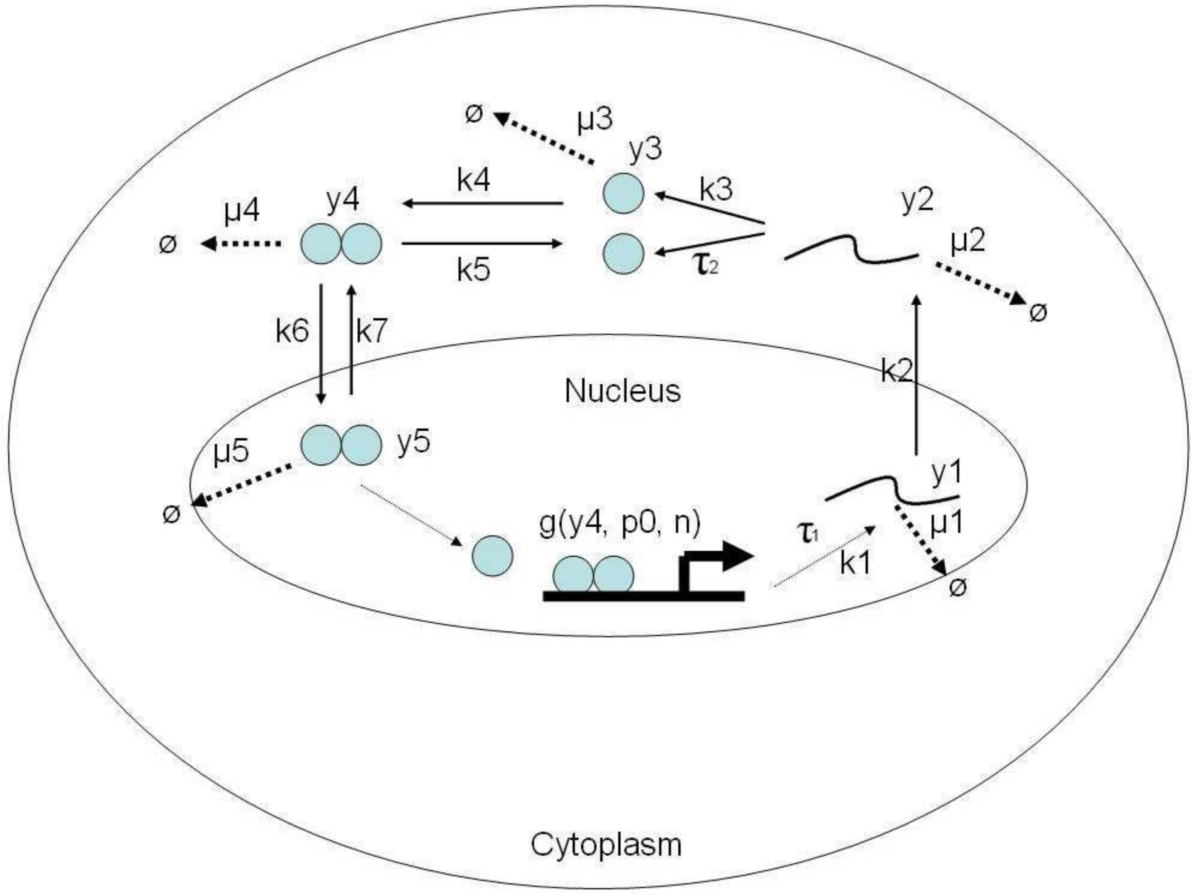

Figure 5.1: *Schematic diagram illustrating the more detailed biochemical processes associated with the Hes1 feedback network.*

(1) Transcription: the hes1 gene is transcribed in the nucleus to produce nascent hes1 mRNA, which is then spliced and processes prior to export from the nucleus. This linear elongation process involves a time delay (Mahaffy and Pao 1984).

(2) Nuclear export of mRNA: mature mRNA is transported out of the nucleus to the cytoplasm.

(3) Translation: hes1 mRNA is translated to produce monomeric Hes1 protein molecules.

Table 5.1: *List of parameters values used the model of Momiji and Monk (2008)*

Parameters	Values
μ_1	0.03
μ_2	0.03
μ_3	0.3
μ_4	0.03
μ_5	0.03
k1	10
k2	1
k3	10
k4	0.01
k5	0.001
k6	10
k7	0
τ_1	14
τ_2	2
n	5
p_0	1250

(4) Protein dimerisation: two Hes1 protein monomers can bind to form a Hes1 homodimer.

(5) Nucleo-cytoplasmic shuttling: Hes1 dimers can shuttle between the cytoplasm and the nucleus.

(6) Transcriptional repression: Hes1 dimers bind to specific sequences in the promoter region of the hes1 gene, resulting in a reduction in the rate of hes1 transcription (Takebayashi et al. 1994).

(7) Degradation: both hes1 mRNA and Hes1 protein are unstable, having half lives of around 20–25 min (Hirata et al. 2003).

Momiji and Monk (2008) build a simple model using the mass action kinetics to represent the circuit mathematically by a five-variable system as follows:

$$
\begin{aligned}
\frac{d[y_1]}{dt} &= -(\mu_1+k_2)[y_1]+k_1[\frac{1}{1+(\frac{p}{p_0})^n}][[y_5](t-\tau_1)] && (5.1)\\
\frac{d[y_2]}{dt} &= -\mu_2[y_2]+k_2[y_1] && (5.2)\\
\frac{d[y_3]}{dt} &= -\mu_3[y_3]+k_3[y_2](t-\tau_2)-2k_4[y_3]^2+2k_5[y_4] && (5.3)\\
\frac{d[y_4]}{dt} &= -(\mu_4+k_5+k_6)[y_4]+k_4[y_3]^2+k_7[y_5] && (5.4)\\
\frac{d[y_5]}{dt} &= -(\mu_5+k_7)[y_5]+k_6[y_4] && (5.5)
\end{aligned}
$$

where y_1-y_5 represent the concentrations of mRNA in the nucleus, mRNA in the cytoplasm, Hes1 monomer in the cytoplasm, Hes1 dimer in the cytoplasm, and Hes1 dimer in the nucleus, respectively. μ_1-μ_5 are the linear degradation rates of the corresponding components; k_1-k_7 are rates of mRNA production, mRNA export, protein production, dimerisation, dimer dissociation, protein import, and protein export, respectively; τ_1 and τ_2 are the time delays in transcription and translation.

Then, Momiji and Monk (2008) solve the five equation system using the parameter listed in Table (5.1) to prove that the model have sustained oscillation solution with a period of 120min.

5.2 The Spatio-temporal Model

We now extend the above model and consider spatial interactions within the cell:

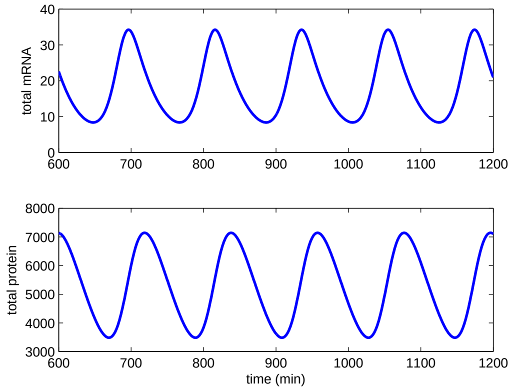

Figure 5.2: *Representative oscillatory profiles of Hes1 mRNA and Hes1 protein resulting from a simulation of the model using the parameters listed in Table 5.1.*

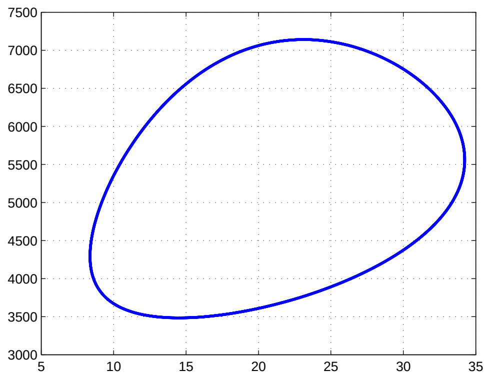

Figure 5.3: *Plot showing the limit cycle obtained from the 5-variable model.*

$$\frac{\partial[y_{1n}]}{\partial t} = D_{y_{1n}}\nabla^2[y_{1n}] - \mu_1[y_{1n}] + k_1\left[\frac{1}{(1+\alpha[y_{4n}])^n}\right], \tag{5.6}$$

$$\frac{\partial[y_{1c}]}{\partial t} = D_{y_{1c}}\nabla^2[y_{1c}] - \mu_1[y_{1c}], \tag{5.7}$$

$$\frac{\partial[y_{3c}]}{\partial t} = D_{y_{3c}}\nabla^2[y_{3c}] - \mu_3[y_{3c}] + k_3[y_{1c}] - 2k_4[y_{3c}]^2, \tag{5.8}$$

$$\frac{\partial[y_{4c}]}{\partial t} = D_{y_{4c}}\nabla^2[y_{4c}] - \mu_4[y_{4c}] + k_4[y_{3c}]^2, \tag{5.9}$$

$$\frac{\partial[y_{4n}]}{\partial t} = D_{y_{4n}}\nabla^2[y_{4n}] - \mu_4[y_{4n}], \tag{5.10}$$

where, y_{1n}, y_{1c}, y_{3c}, y_{4c} and y_{4n} represent Hes1 mRNA in the nucleus, mRNA in the cytoplasm, Hes1 monomer in the cytoplasm, Hes1 dimer in the cytoplasm and Hes1 dimer in the nucleus respectively. μ_1, μ_3 and μ_4 are the liner degradation of Hes1 mRNA, Hes1 monemar and Hes1 dimer respectively. Also, k_1, k_3, k_4 and α are the rate of mRNA production hes1 protein production, dimer formation and Hes1 protein production respectively.

As previously the continuity of flux boundary conditions for the nucleus membrane allow import and export of mRNA and the protein and zero flux boundary condition at the cytoplasm membrane to ensure that all molecules remain within the cell membrane i.e.

$$
\begin{aligned}
D_{y_{1n}}\frac{\partial[y_{1n}]}{\partial n} &= D_{y_{1c}}\frac{\partial[y_{1c}]}{\partial n} \textit{ and } [y_{1n}]=[y_{1c}] \textit{ at the nuclear membrane} && (5.11)\\
D_{y_{3c}}\frac{\partial[y_{3c}]}{\partial n} &= 0 \textit{ and } [y_{3c}]=0 \textit{ at the nuclear membrane} && (5.12)\\
D_{y_{4n}}\frac{\partial[y_{4n}]}{\partial n} &= D_{y_{4c}}\frac{\partial[y_{4c}]}{\partial n} \textit{ and } [y_{4n}]=[y_{4c}] \textit{ at the nuclear membrane} && (5.13)\\
\frac{\partial[y_{1c}]}{\partial n} &= 0, \textit{ at the cell membrane} && (5.14)\\
\frac{\partial[y_{3c}]}{\partial n} &= 0, \textit{ at the cell membrane} && (5.15)\\
\frac{\partial[y_{4c}]}{\partial n} &= 0, \textit{ at the cell membrane} && (5.16)
\end{aligned}
$$

Equations (5.6)–(5.10) represent a system of reaction-diffusion equations modelling the spatio-temporal evolution of the more detailed Hes1 system. The same reaction kinetics from the ODE model of Momiji and Monk (2008) are retained but are now also coupled with diffusion to model explicitly protein and mRNA transport within a cell, i.e., molecules move from the nucleus to the cytoplasm and cytoplasm to nucleus across the nuclear membrane. The PDE system reflects the reality that mRNA is transcribed from DNA exclusively in the nucleus and that protein is translated from mRNA exclusively in the cytoplasm. Finally, we make the assumption that the dimerization of proteins in the cytoplasm occurs some distance away from the nucleus and it takes more time for the Hes1 dimer protein to shuttle to the nucleus.

$$
\frac{\partial[y_{3c}]}{\partial t} = D_{y_{3c}}\nabla^2[y_{3c}] - \mu_3[y_{3c}] + k_3 H_1(x,y)[y_{1c}] - 2k_4[y_{3c}]^2 \qquad (5.17)
$$

where $H_1(x,y)$ is a function localising the protein production whose specific form will be given after the nondimensionalisation of the system.

We nondimensionalise Equations (5.6), (5.7), (5.9), (5.10) and (5.18) with scaling variables as follows (see appendix C):

$$
\begin{aligned}
[y_{1n}^*] &= \frac{[y_{1n}]}{y_0} \;,\; [y_{1c}^*] = \frac{[y_{1c}]}{y_0} \;,\; [y_{3c}^*] = \frac{[y_{3c}]}{y_0} \;,\; [y_{4n}^*] = \frac{[y_{4n}]}{y_0} \;,\; [y_{4c}^*] = \frac{[y_{4c}]}{y_0} && (5.18)\\
t^* &= \frac{t}{\tau}, X^* = \frac{x}{L}, Y^* = \frac{y}{L} && (5.19)
\end{aligned}
$$

where $[y_0]$ is reference concentration, τ is reference time, and L is a reference length. Using this scaling Equations (5.6), (5.7), (5.9), (5.10) and (5.18) become:

$$
\begin{aligned}
\frac{\partial [y_{1n}]^*}{\partial t^*} &= D^*_{y_{1n}} \nabla^2 [y_{1n}]^* - \mu_1^* [y_{1n}]^* + k_1^* \left(\frac{1}{1+\alpha^* [y_{4n}]^*} \right) && (5.20)\\
\frac{\partial [y_{1c}]^*}{\partial t^*} &= D^*_{y_{1c}} \nabla^2 [y_{1c}]^* - \mu_1^* [y_{1c}]^* && (5.21)\\
\frac{\partial [y_{3c}]^*}{\partial t^*} &= D^*_{y_{3c}} \nabla^2 [y_{3c}]^* - \mu_3^* [y_{3c}]^* + k_3^* H_1(x,y) [y_{1c}]^* - 2k_4^* [y_{3c}]^{*2} && (5.22)\\
\frac{\partial [y_{4c}]^*}{\partial t^*} &= D^*_{y_{4c}} \nabla^2 [y_{4c}]^* - \mu_4^* [y_{4c}]^* + k_4^* [y_{3c}]^{*2} && (5.23)\\
\frac{\partial [y_{4n}]^*}{\partial t^*} &= D^*_{y_{4n}} \nabla^2 [y_{4n}]^* - \mu_4^* [y_{4n}]^* && (5.24)
\end{aligned}
$$

where

$$
\begin{aligned}
\frac{\tau}{L^2} D_{y_{1n}^*} \cdot y_0 &= D^*_{y_{1n}} \;,\; \frac{\tau}{L^2} D_{y_{1c}^*} \cdot y_0 = D^*_{y_{1c}} \;,\; \frac{\tau}{L^2} D_{y_{3c}^*} \cdot y_0 = D^*_{y_{3c}}\\
\frac{\tau}{L^2} D_{y_{4n}^*} \cdot y_0 &= D^*_{y_{4n}} \;,\; \frac{\tau}{L^2} D_{y_{4c}^*} \cdot y_0 = D^*_{y_{4c}} \;,\; \alpha y_0 = \alpha^*\\
\tau \mu_1 &= \mu_1^* \;,\; \tau \mu_3 = \mu_3^* \;,\; \tau \mu_4 = \mu_4^*\\
\frac{\tau k_1}{y_0} &= k_1^* \;,\; \tau k_3 = k_3^* \;,\; \tau y_0 k_4 = k_4^* && (5.25)
\end{aligned}
$$

and

$$H_1(x,y) = \begin{cases} 1, & \text{if } x^2+y^2 \geqslant 0.3, \\ 0, & \text{if } x^2+y^2 < 0.3. \end{cases}$$

We apply zero initial conditions, zero-flux boundary conditions at the cell membrane and flux continuity boundary conditions across the nucleus membrane:

$$\begin{aligned}
[y_{1n}]^* &= [y_{4n}]^* = [y_{1c}]^* = [y_{3c}]^* = [y_{4c}]^* = 0,\ at\ t = 0 && (5.26)\\
D^*_{y_{1n}} \frac{\partial [y_{1n}]^*}{\partial n} &= D^*_{y_{1c}} \frac{\partial [y_{1c}]^*}{\partial n}\ and\ [y_{1n}]^* = [y_{1c}]^*\ at\ the\ nuclear\ membrane && (5.27)\\
D^*_{y_{4n}} \frac{\partial [y_{4n}]^*}{\partial n} &= D^*_{y_{4c}} \frac{\partial [y_{4c}]^*}{\partial n}\ and\ [y_{4n}]^* = [y_{4c}]^*\ at\ the\ nuclear\ membrane && (5.28)\\
D^*_{y_{1c}} \frac{\partial [y_{1c}]^*}{\partial n} &= 0\ and\ [y_{1c}]^* = 0\ at\ the\ nuclear\ membrane && (5.29)
\end{aligned}$$

$$\begin{aligned}
\frac{\partial [y_{1c}]^*}{\partial n} &= 0,\ at\ the\ cell\ membrane && (5.30)\\
\frac{\partial [y_{3c}]^*}{\partial n} &= 0,\ at\ the\ cell\ membrane && (5.31)\\
\frac{\partial [y_{4c}]^*}{\partial n} &= 0,\ at\ the\ cell\ membrane && (5.32)
\end{aligned}$$

We take reference concentrations to be $[y_0]$=1μM. Figures 5.2, 5.3 show the simulations results of Equations (5.20)–(5.24). It was recognisable that a period of oscillation was approximately 225 time units. Hence, knowing that the period of oscillation of Hes1 is approximately 2h (Hirata et al. 2003), we have the reference time τ as follows: 225τ = 2h which means τ= 32s (see appendix C).

To obtain the value of the variable L, we used 2-dimensional cell with length of $30\mu M$ to represents both the nucleus and cytoplasm where the nucleus has a major axis of length 0.8 units and minor axis of length 0.5 units and the cytoplasm has a major axis of length 3 units and a minor axis of length 2 units. Hence, the non-dimensional cell width is equal to 3 L = $30\mu M$ so, the reference length L=$10\mu M$.

Parameter Estimation

The following parameter values were used in our simulations of the non-dimensional Hes1 system:

$$\begin{aligned} D^*_{y_{1n}} &= D^*_{y_{1c}} = D^*_{y_{3c}} = D^*_{y_{4n}} = D^*_{y_{4c}} = 7.5 \times 10^{-4} \\ \mu^*_1 &= \mu^*_3 = \mu^*_4 = 0.03 \\ k^*_1 &= k^*_3 = k^*_4 = 5 \\ \alpha^* &= 1\ ,\ n^* = 5 \end{aligned} \tag{5.33}$$

From 4.57 and 4.65 we calculate the dimensional parameter values (see appendix C):

$$\begin{aligned} D_{y^*_n} &= \frac{L^2 D^*_{y_n}}{\tau} = 2.34 \times 10^{-11} cm^2 s^{-1} \\ D_{y^*_{1n}} &= D_{y_{1c}*} = D_{y_{3c}*} = D_{y_{4n}*} = D_{y_{4c}*} = 2.34 \times 10^{-11} cm^2 s^{-1} \\ \mu_1 &= \mu_3 = \mu_4 = 9.4 \times 10^{-4} s^{-1} \\ k_1 &= k_3 = k_4 = 1.56 \times 10^{-4} \\ \alpha &= 1 M s^{-1}. \end{aligned} \tag{5.34}$$

5.2.1 Computational Simulation Results

Once again we solved PDE system (5.20)–(5.24) numerically using the finite element software COMSOL (Triangular basis elements and Lagrange quadratic basis functions along with a backward Euler time-stepping method for integrating the equations were used in all simulations). Figure 5.4 shows the total concentrations of hes1 mRNA, Hes1 protein dimers and Hes1 protein over time in the cytoplasm, while Figure 5.5 shows the total concentrations in the nucleus over time. Both sets of results show oscillatory dynamics of the Hes1 system. The plots presented in Figs. 5.6 and 5.7 show how the hes1 mRNA and protein concentrations vary spatially as well as temporally within the cell. The mRNA is produced inside the nucleus and by t = 50 min has started to cross the nuclear membrane to enter the cytoplasm (Fig. 5.6). In the cytoplasm the mRNA is translated into protein, then two Hes1 protein monomers bind to form a Hes1 dimer which then diffuses back into the nucleus and represses the production of its own mRNA (t=250 min). The mRNA concentration has clearly depleted by t=120 min, reflecting the period of the temporal oscillation seen in Figs. 5.4, 5.5.

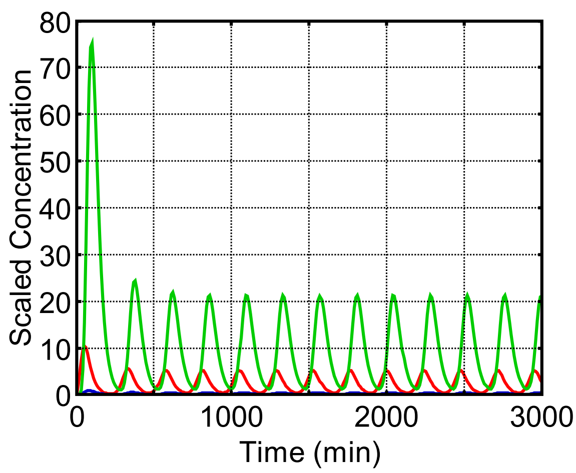

Figure 5.4: *Plot of the concentrations of Hes1 mRNA (red), the Hes1 protein dimers (blue) and Hes1 protein (green) in the cytoplasm over time. The period of oscillations is approximately 120 min*

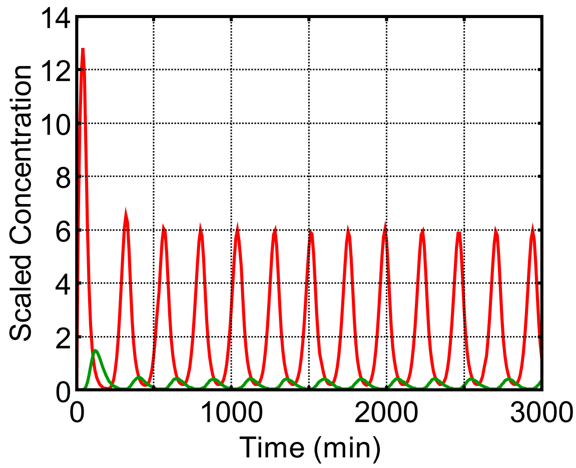

Figure 5.5: *Plot of the concentrations of hes1 mRNA (red) and Hes1 protein (green) in the nucleus over time. The period of oscillations is approximately 120 min*

5.3 External driving of Hes1 oscillation by Stat3 Phosphorylation

5.3.1 The Stat3 System

Stat3 (Signal Transducer and Activator of transcription) is a member of STATs proteins that mediate cellular responses to different cytokines and growth factors. The activation of STATs by tyrosine phosphorylation cytokines or growth factors bind to the cell receptors. Once tyrosine phosphorylated, two STAT monomers form dimers. The dimers then translocate to the nucleus and bind to specific region of the target gene (Smithgall et al. 2000). Stat3 protein regulates gene expression involved in cell proliferation, survival and self-renewal (Walker et al. 2011).

It was shown in previous study that formation of Stat3-P is inhibited in the absence of Hes1, suggesting that Stat3-Socs3 oscillations and Hes1 oscillation depend on each other. So, Hes proteins bind to JAK2 and Stat3 resulting of Stat3 phosphorylation and activation. Phosphorylated Stat3 was detected only in the cells expressing Hes1, but

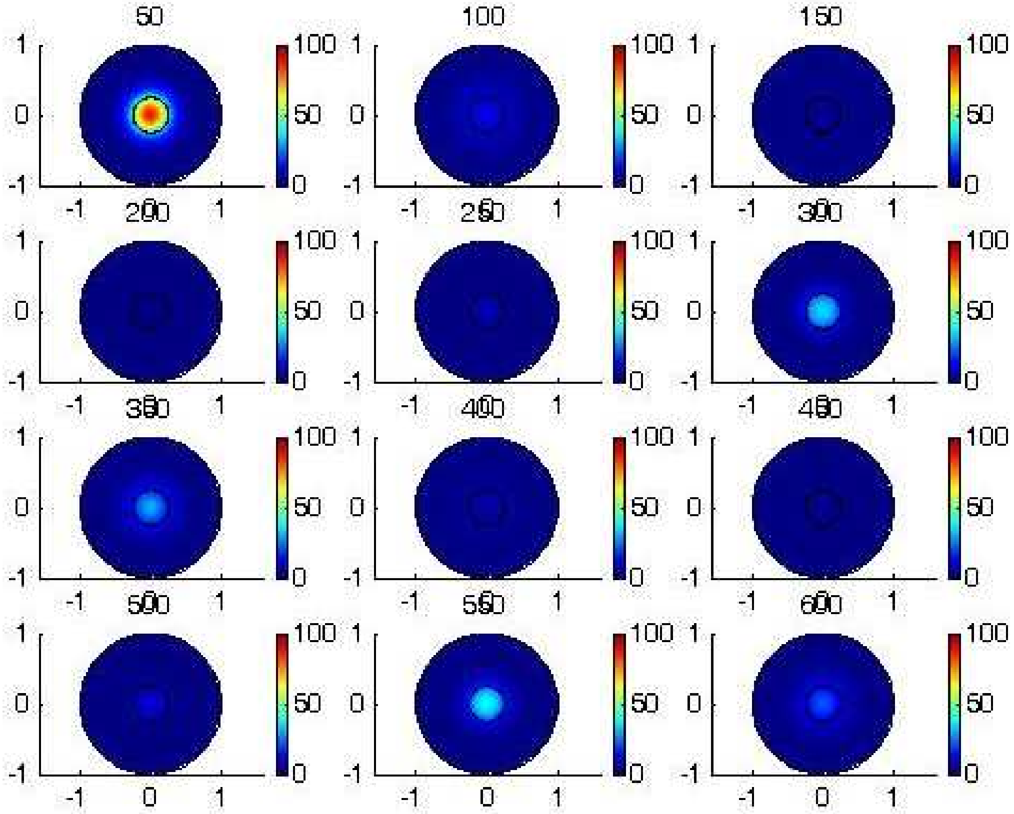

Figure 5.6: *Plots showing the spatio-temporal evolution of hes1 mRNA concentration within the cell from times t = 0 to 450 min at 50 min intervals. The concentration oscillates in both time and space. Parameter values as per (5.33).*

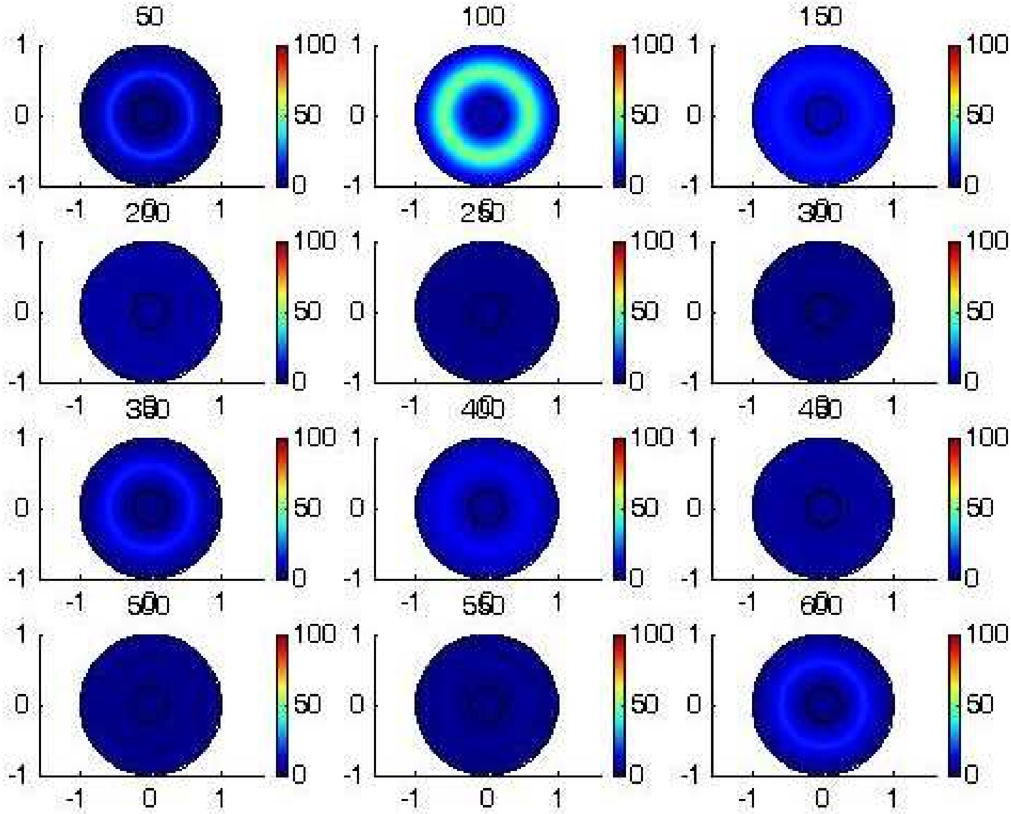

Figure 5.7: *Plots showing the spatio-temporal evolution of Hes1 Protein concentration within the cell from times t = 0 to 450 min at 50 min intervals. The concentration oscillates in both time and space. Parameter values as per (5.33).*

not the surrounding cells where Hes1 expression markedly increases the level of tyrosine phosphorylation of endogenous Stat3. Suppression of Hes1 expression reduces Stat3 phosphorylation (Kamakura et al. 2004). It has been found that Hes1 represses its own expression by binding to its own promoter. Also, phosphorylated Stat3 (Stat3-P) induces suppression of cytokine signaling 3 (Socs3) expression, Socs3 inhibits phosphorylation of Stat3 and negatively regulates it, forming a negative feedback loop. Thus, the Stat-Socs pathway is regulated by its own negative feedback loop, in a similar manner to Hes1 (Yoshiura et al. 2007). Interestingly, inhibition of Stat3-Socs3 oscillations blocks Hes1 oscillation, suggesting that Stat3- Socs3 signalling regulates oscillatory versus persistent Hes1 expression (Yoshiura et al. 2007) (see Fig 5.9).

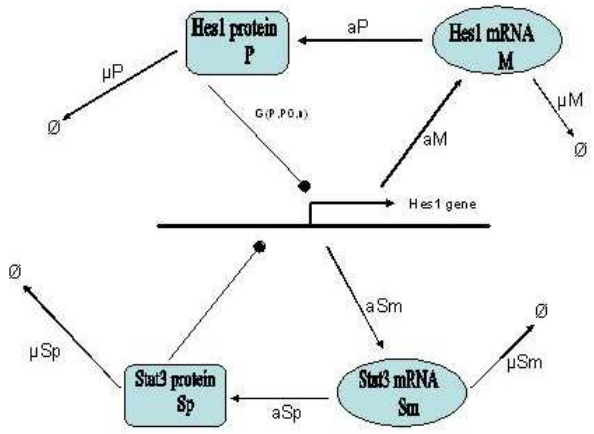

Figure 5.8: *Schematic diagram showing the similarity between the negative feedback loops in the Hes1 and Stat3 systems.*

5.3.2 The Stat3 Mathematical Model

To formulate the mathematical model of the intracellular regulatory system of the Stat3 negative feedback loop, we follow the same steps as in previous sections when deriving the model of the Hes1 system. We suggest that Stat3 oscillatory expression plays a central role in maintaining the segmentation clock. Stat3 represses the transcription of its own gene through direct binding to regulatory sequences in the Stat3 promoter. The basic interactions of this system (see Fig. 5.8 and 5.10), Stat3 protein is produced by Stat3 mRNA and then goes on to inhibit its own mRNA and so forth, with the result that the system oscillates with a period of around 120 min.

The equations governing the concentrations of Stat3 mRNA and protein respectively are:

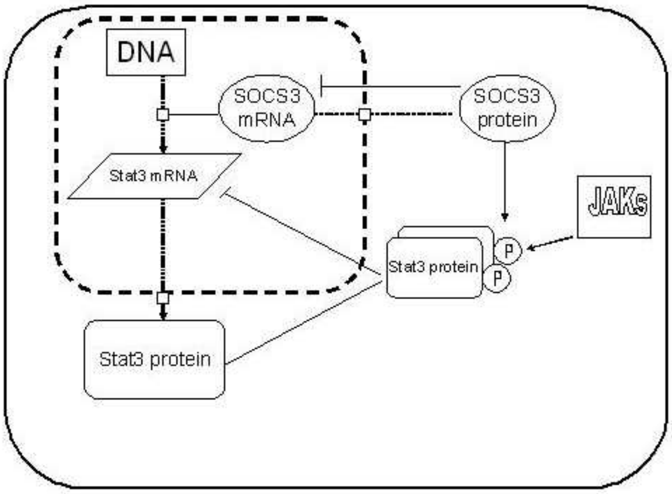

Figure 5.9: *Schematic diagram showing the constitutive activation of Stat3 by the cytokine receptor JAK which phosphorylates Stat3, which is then dimerized and translocated to the nucleus where it regulates gene expression. Stat3 signalling is phosphorylation-regulated by SOCS3.*

$$\frac{dSm}{dt} = \frac{\alpha_{Sm}}{1+(Sp/P_0)^n} - \mu_{Sm}Sm, \tag{5.35}$$

$$\frac{dSp}{dt} = \alpha_{Sp}Sm_c - \mu_{Sp}Sp, \tag{5.36}$$

where [Sm] and [Sp] are the concentration of Stat3 mRNA and Stat3 protein, respectively.

The first term on the right hand side of Eq.(5.35) is a Hill function which decreases as the protein concentration increases, modelling repression by the Stat3 protein. The parameter α_{Sm} is the rate of transcript initiation in the absence of Stat3 protein and p_0 is the concentration of Stat3 and n is a Hill coefficient. The second term represents the natural degradation of the Stat3 mRNA with parameter μ_{Sm}.

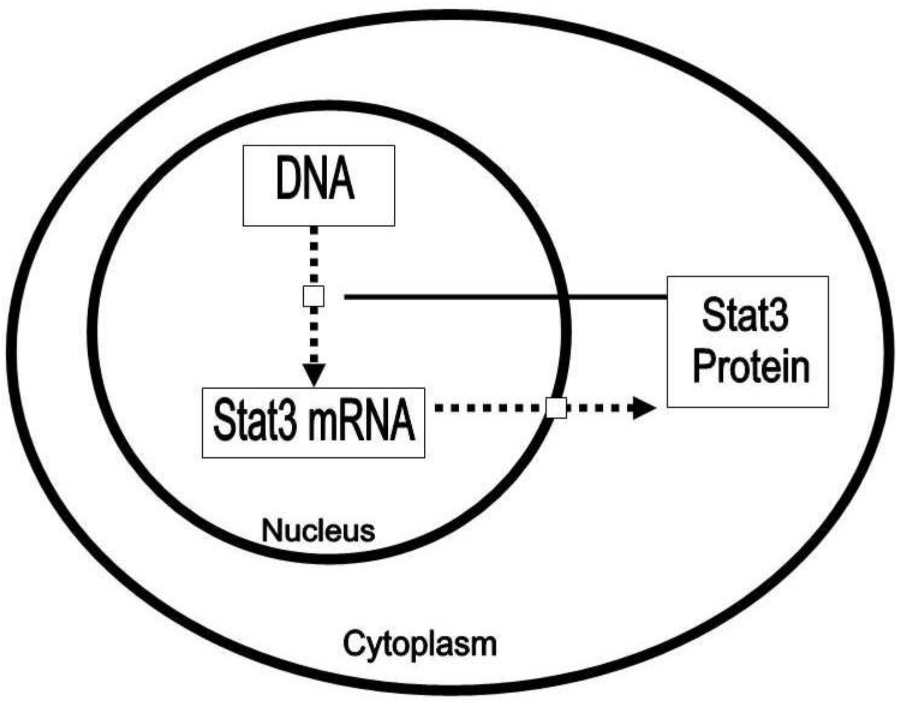

Figure 5.10: *A schematic representation of the Stat3 model*

The first term on the right hand side of Eq.(5.36) is Stat3 protein production term from translation of Stat3 mRNA with parameter α_{Sp} and the second term represents Stat3 protein degradation with parameter μ_{Sp}.

We now extend the above ODE models and consider spatial interactions within the cell. As previously, we consider the nucleus and cytoplasm as two distinct spatial compartments and the cytoplasm enclosed within the outer cell membrane. Transcription occurs exclusively in the nucleus and protein synthesis occurs exclusively in the cytoplasm.We assume that the main mechanism governing the spatial movement of mRNA and protein between the nucleus and cytoplasm is diffusion. Denoting by [Smn], [Smc] and [Spn], [Spc] the concentrations of nuclear and cytoplasmic Stat3 mRNA and nuclear and cytoplasmic Stat3 protein, respectively, the system of equations describing the spatio-temporal evolution of Stat3 mRNA and Stat3 protein concentrations is now

$$\frac{\partial Sm_n}{\partial t} = D_{Sm_n}\nabla^2 Sm_n + \frac{\alpha_{Sm}}{1+(Sp/P_0)^n} - \mu_{Sm}Sm_n, \tag{5.37}$$

$$\frac{\partial Sm_c}{\partial t} = D_{Sm_c}\nabla^2 Sm_c - \mu_{Sm}Sm_c, \tag{5.38}$$

$$\frac{\partial Sp_c}{\partial t} = D_{Sp_c}\nabla^2 Sp_c + \alpha_{Sp}Sm_c - \mu_{Sp}Sp_c, \tag{5.39}$$

$$\frac{\partial Sp_n}{\partial t} = D_{Sp_n}\nabla^2 Sp_n - \mu_{Sp}Sp_n. \tag{5.40}$$

We apply zero initial conditions, zero-flux boundary condition at the cell membrane and flux continuity boundary conditions across the nucleus membrane:

$$\begin{aligned}
D_{Sm_n}\frac{\partial[Sm_n]}{\partial n} &= D_{Sm_c}\frac{\partial[Sm_c]}{\partial n} \; and \; [Sm_n]=[Sm_c] \; at\ the\ nuclearmembrane\\
D_{Sp_n}\frac{\partial[Sp_n]}{\partial n} &= D_{Sp_c}\frac{\partial[Sp_c]}{\partial n} \; and \; [Sp_n]=[Sp_c] \; at\ the\ nuclearmembrane\\
\frac{\partial[Sm_c]}{\partial n} &= 0,\; at\ the\ cell\ membrane\\
\frac{\partial[Sp_c]}{\partial n} &= 0,\; at\ the\ cell\ membrane
\end{aligned} \tag{5.41}$$

5.3.3 Computational Simulation Results

As in the case of the Hes1 system, we solved the PDE system (5.37)-(5.40) numerically using the parameter values in table (5.2). Fig 5.11 shows the total concentrations of Stat3 mRNA and Stat3 protein over time in the nuclear compartment, while Fig 5.12 shows the total concentrations in the cytoplasm. Both sets of results show oscillatory dynamics of the Stat3 system.

Table 5.2: *Parameters value used in the computational simulations of the PDE model*

Parameters	Values
μ_1	0.03
μ_2	0.03
α_1	1
α_2	1
n	5
p_0	1

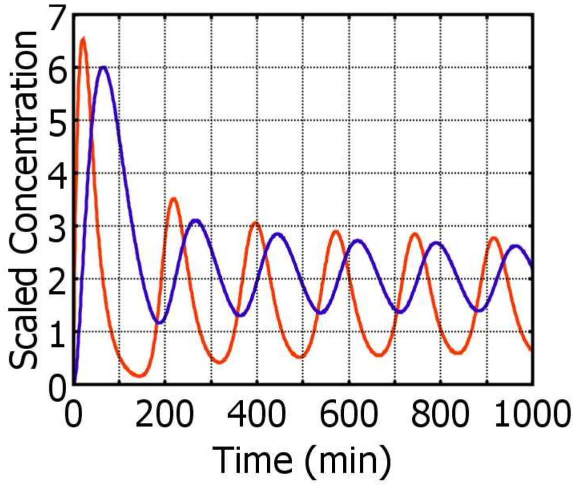

Figure 5.11: *Plot of the concentration of Stat3 mRNA (red) and Stat3 protein (blue) in the nucleus over time.*

5.4 A Model of the Hes1-Stat3 system

As result of the study of the post translation oscillation of Stat3 phosphorylation and its negative feedback loop which revealed a potential mechanism underlying the dependency of Hes1 oscillation on the Stat3 phosphorylation oscillations, Momiji and Monk (2008) incorporated these new features to study a Hes1 model which is based around two components, then formulated a new ODE model including Hes1 dimerisation and

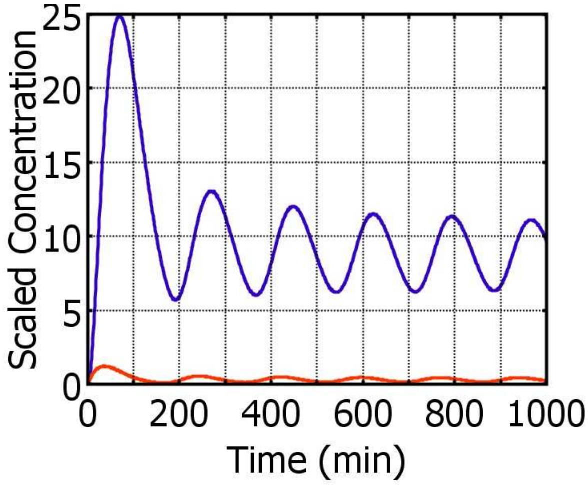

Figure 5.12: *Plot of the concentration of Stat3 mRNA (red) and Stat3 protein (blue) in the cytoplasm over time.*

time delays.

In this section we formulate the model in a different way while still incorporating the time delay and Hes1 dimerisation.

$$
\begin{aligned}
\frac{\partial y_{1n}^*}{\partial t^*} &= D_{y_{1n}}^* \nabla^2 y_{1n}^* - \mu_1^* y_{1n}^* + k_1^* \left(\frac{1}{(1+\alpha 1^* y_{4n}^*)^{n1}} \right) \\
\frac{\partial y_{1c}^*}{\partial t^*} &= D_{y_{1c}}^* \nabla^2 y_{1c}^* - \mu_1^* y_{1c}^* \\
\frac{\partial y_{3c}^*}{\partial t^*} &= D_{y_{3c}}^* \nabla^2 y_{3c}^* - \mu_3^* y_{3c}^* + k_3^* H_1(x,y) y_{1c}^* - 2k_4^* y_{3c}^{*2} \\
\frac{\partial y_{4c}^*}{\partial t^*} &= D_{y_{4c}}^* \nabla^2 y_{4c}^* - \mu_4^* y_{4c}^* + k_4^* y_{3c}^{*2} \\
\frac{\partial y_{4n}^*}{\partial t^*} &= D_{y_{4n}}^* \nabla^2 y_{4n}^* - \mu_4^* y_{4n}^* \\
\frac{\partial y_{5n}}{\partial t} &= D_{y_{5n}} \nabla^2 y_{5n} + \frac{\alpha 5}{1+(y_{6n}/P_0)^{n2}} - \mu_5 y_{5n} \\
\frac{\partial y_{5c}}{\partial t} &= D_{y_{5c}} \nabla^2 y_{5c} - \mu_5 y_{5c} \\
\frac{\partial y_{6c}}{\partial t} &= D_{y_{6c}} \nabla^2 y_{6c} + \alpha 6 y_{6c} - \mu_6 y_{6c} \\
\frac{\partial y_{6n}}{\partial t} &= D_{y_{6n}} \nabla^2 y_{6n} - \mu_6 y_{6n} \qquad (5.42)
\end{aligned}
$$

Where, y_{1n}, y_{1c}, y_{3c}, y_{4c}, y_{4n}, y_{5n}, y_{5c}, y_{6n} and y_{6c} represent Hes1 mRNA in the nucleus, mRNA in the cytoplasm, Hes1 monomer in the cytoplasm, Hes1 dimer in the cytoplasm, Hes1 dimer in the nucleus, Stat3 mRNA in the nucleus and Stat3 protein in the cytoplasm, respectively. μ_1^*, μ_3^* and μ_4^* are the liner degradation of Hes1 mRNA, Hes1 monomer and Hes1 dimer respectively. Also, k_1^*, k_3^*, and k_4^* are the rate of mRNA production, hes1 protein production and dimer formation rate, respectively. Also α_1^*, α_5^*, α_6^* and n the prouduction of Hes1 mRNA in apsent of Hes1 protein, the rate of Stat3 mRNA transcript, Stat3 protein production term and a Hill coefficient, respectively.

Momiji and Monk (2008) showed a 120 min period oscillation in the level of phosphorylation of the Stat3 protein which was shown to be necessary for the observed

Table 5.3: *Parameters value*

Parameters	Values	Parameters	Values
p_0	1	k1	2
μ_1	0.03	k3	5
μ_3	0.03	k4	2
μ_4	0.03	α_1	7
μ_5	0.03	α_5	1
μ_6	0.03	α_6	1
n1	2	n5	5

transcriptional Hes1 oscillations. Oscillation of Stat3 phosphorylation is driven by a negative feedback loop involving Stat3 and Socs3 oscillation, and Hes1 oscillations depend on the Stat3 phosphorylation oscillations (Yoshiura et al. 2007).
We ran numerical simulations of the Hes1-Stat3 system model using the parameter values in table (5.3) to examine if there is any affect of each system on the other's oscillation when it does not have any time-dependent effects.

Figure 5.13 shows that Stat3 negative feedback oscillates and does not show any effect caused by the Hes1 negative feedback while the Hes1 oscillations disappear. So Stat3 oscillations block the Hes1 oscillations. It is clear that Hes1 oscillations run normally to prove that Stat3-Socs3 oscillations inhibit the Hes1 oscillations.

In the previous dimerisation model, the Hes1 dimers have a lower degradation rate than Hes1 monomers. Momiji and Monk (2008) assumed that Stat3 has an equivalent effect on the degradation of both monomeric and dimeric forms of Hes1 and so they set the time dependent Hes1 protein degradation rate to observe the effect of oscillatory Stat3 on Hes1:

$$\mu_p = \mu_p^{`} + d\mu_p sin(\frac{2\pi t}{T}) \tag{5.43}$$

where μ_p is the decay rate of the protein and T is the period of Stat3 oscillation (120 min).

This functional form for the time dependence of the Hes1 protein degradation rate was chosen to observe the effect of oscillatory Stat3 on Hes1, and plays the role of a periodic forcing term in the equations describing Hes1 regulation. Therefore, we modify our system by writing the Hes1 protein degradation rate $\mu 3$,$\mu 4$ as suggested by Momiji and Monk (2008).

We assume that the degradation rate of Hes1 protein dimers $\mu 3$ have a lower degradation rate than Hes1 monomers $\mu 4$. Furthermore, we assume that Stat3 has an equivalent effect on the degradation of both monomeric and dimeric forms of Hes1. We therefore set the time-dependent Hes1 protein degradation rates to be:

$$\mu_3 = \mu_3^{`} + d\mu_3 sin(\frac{2\pi t}{T}) \tag{5.44}$$

$$\mu_4 = \mu_4^{`} + d\mu_4 sin(\frac{2\pi t}{T}) \tag{5.45}$$

The equations for Hes1 and Stat3 are now:

$$
\begin{aligned}
\frac{\partial y_{1n}^*}{\partial t^*} &= D_{y_{1n}}^* \nabla^2 y_{1n}^* - \mu_1^* y_{1n}^* + k_1^* \left(\frac{1}{(1+\alpha 1^* y_{4n}^*)^{n1}} \right) \\
\frac{\partial y_{1c}^*}{\partial t^*} &= D_{y_{1c}}^* \nabla^2 y_{1c}^* - \mu_1^* y_{1c}^* \\
\frac{\partial y_{3c}^*}{\partial t^*} &= D_{y_{3c}}^* \nabla^2 y_{3c}^* - (\mu_3' + d\mu_3 sin(\frac{2\pi t}{T})) y_{3c}^* + k_3^* H_1(x,y) y_{1c}^* - 2k_4^* y_{3c}^{*2} \\
\frac{\partial y_{4c}^*}{\partial t^*} &= D_{y_{4c}}^* \nabla^2 y_{4c}^* - (\mu_4' + d\mu_4 sin(\frac{2\pi t}{T})) y_{4c}^* + k_4^* y_{3c}^{*2} \\
\frac{\partial y_{4n}^*}{\partial t^*} &= D_{y_{4n}}^* \nabla^2 y_{4n}^* - (\mu_4' + d\mu_4 sin(\frac{2\pi t}{T})) y_{4n}^* \\
\frac{\partial y_{5n}}{\partial t} &= D_{y_{5n}} \nabla^2 y_{5n} + \frac{\alpha 5}{1+(y_{6n}/P_0)^{n2}} - \mu_5 y_{5n} \\
\frac{\partial y_{5c}}{\partial t} &= D_{y_{5c}} \nabla^2 y_{5c} - \mu_5 y_{5c} \\
\frac{\partial y_{6c}}{\partial t} &= D_{y_{6c}} \nabla^2 y_{6c} + \alpha 6 y_{6c} - \mu_6 y_{6c} \\
\frac{\partial y_{6n}}{\partial t} &= D_{y_{6n}} \nabla^2 y_{6n} - \mu_6 y_{6n}
\end{aligned}
\tag{5.46}
$$

5.4.1 Numerical Simulations

We apply zero initial conditions, zero-flux boundary condition at the cell membrane and flux continuity boundary conditions across the nucleus membrane:

$$
\begin{aligned}
D_{y_{1n}}\frac{\partial[y_{1n}]}{\partial n} &= D_{y_{1c}}\frac{\partial[y_{1c}]}{\partial n}\ and\ [y_{1n}]=[y_{1c}]\ at\ the\ nuclear\ membrane\\
D_{y_{3c}}\frac{\partial[y_{3c}]}{\partial n} &= 0\ and\ [y_{3c}]=0\ at\ the\ nuclear\ membrane\\
D_{y_{4n}}\frac{\partial[y_{4n}]}{\partial n} &= D_{y_{4c}}\frac{\partial[y_{4c}]}{\partial n}\ and\ [y_{4n}]=[y_{4c}]\ at\ the\ nuclear\ membrane\\
D_{y_{5n}}\frac{\partial[y_{5n}]}{\partial n} &= D_{y_{5c}}\frac{\partial[y_{5c}]}{\partial n}\ and\ [y_{5n}]=[y_{5c}]\ at\ the\ nuclear\ membrane\\
D_{y_{6n}}\frac{\partial[y_{6n}]}{\partial n} &= D_{y_{6c}}\frac{\partial[y_{6c}]}{\partial n}\ and\ [y_{6n}]=[y_{6c}]\ at\ the\ nuclear\ membrane\\
\frac{\partial[y_{1c}]}{\partial n} &= 0,\ at\ the\ cell\ membrane\\
\frac{\partial[y_{3c}]}{\partial n} &= 0,\ at\ the\ cell\ membrane\\
\frac{\partial[y_{4c}]}{\partial n} &= 0,\ at\ the\ cell\ membrane\\
\frac{\partial[y_{5c}]}{\partial n} &= 0,\ at\ the\ cell\ membrane\\
\frac{\partial[y_{6c}]}{\partial n} &= 0,\ at\ the\ cell\ membrane
\end{aligned}
\tag{5.47}
$$

Fig 5.14 shows the results from a numerical simulation of the equation (5.45) when we make the value of Hes1 dimer and monomer degradation rate a function of time.

In an extension to their original, basic model, Momiji and Monk (2008) considered the parameters μ_3 and μ_4 as functions of Stat3 concentration. Arguing that Stat3 oscillated, they then simply made these parameters depend on time in a sinusoidal manner as follows:

$$\begin{aligned}\mu_* &= \mu_*^{\grave{}} + d\mu_* sin(\frac{2\pi t}{T}) \\ &= 0.03 + d\mu_* sin(\frac{2\pi t}{T})\end{aligned} \tag{5.48}$$

with parameter values taken from the work of Yoshiura et al. (2007), $d\mu_p$=1.1, μ_p=1.6 and $\mu_p^{\grave{}}$=1.9.

We now modify our system to make the parameters μ_3 and μ_4 explicitly depend on Stat3 concentration (details given in Appendix A) and hence the modified equations for Hes1 and Stat3 are:

$$\begin{aligned}
\frac{\partial y_{1n}^*}{\partial t^*} &= D_{y_{1n}}^* \nabla^2 y_{1n}^* - \mu_1^* y_{1n}^* + k_1^* \left(\frac{1}{(1+\alpha 1^* y_{4n}^*)^{n1}} \right) \\
\frac{\partial y_{1c}^*}{\partial t^*} &= D_{y_{1c}}^* \nabla^2 y_{1c}^* - \mu_1^* y_{1c}^* \\
\frac{\partial y_{3c}^*}{\partial t^*} &= D_{y_{3c}}^* \nabla^2 y_{3c}^* - (\mu_3^{\grave{}} + (-0.004 + 0.00348 * y_{6c}) y_{3c}^* + k_3^* H_1(x,y) y_{1c}^* - 2k_4^* y_{3c}^{*2} \\
\frac{\partial y_{4c}^*}{\partial t^*} &= D_{y_{4c}}^* \nabla^2 y_{4c}^* - (\mu_4^{\grave{}} + (-0.004 + 0.00348 * y_{6c}) y_{4c}^* + k_4^* y_{3c}^{*2} \\
\frac{\partial y_{4n}^*}{\partial t^*} &= D_{y_{4n}}^* \nabla^2 y_{4n}^* - (\mu_4^{\grave{}} + (-0.004 + 0.00348 * y_{6c}) y_{4n}^* \\
\frac{\partial y_{5n}}{\partial t} &= D_{y_{5n}} \nabla^2 y_{5n} + \frac{\alpha 5}{1+(y_{6n}/P_0)^{n2}} - \mu_5 y_{5n} \\
\frac{\partial y_{5c}}{\partial t} &= D_{y_{5c}} \nabla^2 y_{5c} - \mu_5 y_{5c} \\
\frac{\partial y_{6c}}{\partial t} &= D_{y_{6c}} \nabla^2 y_{6c} + \alpha 6 y_{6c} - \mu_6 y_{6c} \\
\frac{\partial y_{6n}}{\partial t} &= D_{y_{6n}} \nabla^2 y_{6n} - \mu_6 y_{6n}
\end{aligned} \tag{5.49}$$

Alternative equations for Hes1 and Stat3 where the parameters μ_3 and μ_4 explicitly depend on Stat3 concentration (details given in Appendix A) are:

$$
\begin{aligned}
\frac{\partial y^*_{1n}}{\partial t^*} &= D^*_{y_{1n}} \nabla^2 y^*_{1n} - \mu^*_1 y^*_{1n} + k^*_1 \left(\frac{1}{(1+\alpha 1^* y^*_{4n})^{n1}} \right) \\
\frac{\partial y^*_{1c}}{\partial t^*} &= D^*_{y_{1c}} \nabla^2 y^*_{1c} - \mu^*_1 y^*_{1c} \\
\frac{\partial y^*_{3c}}{\partial t^*} &= D^*_{y_{3c}} \nabla^2 y^*_{3c} - (\mu^{`}_3 + (-0.015 + 0.00463 * y_{6c}) y^*_{3c} + k^*_3 H_1(x,y) y^*_{1c} - 2k^*_4 y^{*2}_{3c} \\
\frac{\partial y^*_{4c}}{\partial t^*} &= D^*_{y_{4c}} \nabla^2 y^*_{4c} - (\mu^{`}_4 + (-0.015 + 0.00463 * y_{6c}) y^*_{4c} + k^*_4 y^{*2}_{3c} \\
\frac{\partial y^*_{4n}}{\partial t^*} &= D^*_{y_{4n}} \nabla^2 y^*_{4n} - (\mu^{`}_4 + (-0.015 + 0.00463 * y_{6c}) y^*_{4n} \\
\frac{\partial y_{5n}}{\partial t} &= D_{y_{5n}} \nabla^2 y_{5n} + \frac{\alpha 5}{1 + (y_{6n}/P_0)^{n2}} - \mu_5 y_{5n} \\
\frac{\partial y_{5c}}{\partial t} &= D_{y_{5c}} \nabla^2 y_{5c} - \mu_5 y_{5c} \\
\frac{\partial y_{6c}}{\partial t} &= D_{y_{6c}} \nabla^2 y_{6c} + \alpha 6 y_{6c} - \mu_6 y_{6c} \\
\frac{\partial y_{6n}}{\partial t} &= D_{y_{6n}} \nabla^2 y_{6n} - \mu_6 y_{6n}
\end{aligned} \tag{5.50}
$$

Table 5.4: *Parameters value*

Parameters	Values	Parameters	Values
D	7.5×10^{-4}	α_1	1
μ_1	0.03	α_5	1
μ_3	0.03	α_6	1
μ_4	0.03	k_1	2
μ_5	0.03	k_3	5
μ_6	0.03	k_4	2
$d\mu_3$	0.015	n_1	2
$d\mu_4$	0.015	n_5	5
T	200	p_0	1

5.5 Modelling Different Intracellular Phenomena

In this section we solve model (5.46) numerically to obtain the simulation result of the system with some modifications representing possible intracellular phenomena that could affect the spatio-temporal dynamics of the model. We first change the model system to take account of the effect of adding noise to the diffusion in the cell and examine the effect on the oscillations of the model.

Most physical systems which respond to the concentration of a signalling molecule will exhibit noise due to the random movement of the molecules (diffusion) and variability in the processes of transcription and translation. Recent large scale surveys of noise suggested that the noise in most protein levels can be understood in terms of the components of noise that derive from the translation of mRNA into protein, or the components that arise from noise in the transcription and degradation of the mRNA itself (Gasper 2008).

To understand the effect that noise had on the oscillations of the intracellular network, we add Gaussian Noise to our system by modifying the diffusion coefficient in the Hes1-Stat3 System (5.45) i.e. $D = D + sin(0.01*t + awgn(sin(0.01*t), 25))/5000)$ (For the simulation result see Fig. 5.17).

We now consider a second change of the model system to examine the effect of adding a nuclear membrane with zero flux boundary condition in the cell domain to the oscillation of the model. A nuclear membrane is the double lipid bilayer membrane called the inner membrane and the outer membrane which surrounds the genetic material and divides the cell into two compartments (Martin 2010). During the intracellular signal transaction the nucleus membrane control the diffusion from the cytoplasm through the nucleus pore complex (NPC) to the nucleus and from the nucleus to the cytoplasm (Weis 2003).

When the molecule binds to the surface of the outer membrane it can diffuse through the nuclear pore and then diffuses into the inner membrane. The whole process takes time which depends on the size of the molecule itself and the size of the nuclear pore. Hence, larger molecules, such as proteins, will diffuse more slowly than smaller molecules, such as mRNA (Sturrock et al. 2011).

To show the effect of the nuclear membrane on the oscillations of the Hes1-Stat3 system, we consider the nuclear membrane to be of thickness d (which is also the depth of the NPC of the nucleus membrane) in the system of equations (5.46). The nuclear membrane thickness has been estimated to be approximately 100nm (Sturrock et al. 2011). Also, we assume that diffusion across it is slower than in the cytoplasm or nucleus, with protein diffusion slower than mRNA diffusion across the membrane. We simply choose $D_m = D_{ij}/5$ and $D_p = D_{ij}/15$ for the nuclear membrane diffusion for mRNA for Hes1 and Stat3 and protein for Hes1 and Stat3, respectively (for the simulation result see Fig. 5.18).

Finally we replace the previous continuity of flux boundary conditions with the following boundary conditions which considers the nuclear membrane thickness:

$$
\begin{aligned}
D_{y1_n}\frac{\partial[y1_n]}{\partial n} &= \frac{D_{y1}([y1_n]-[y1_c])}{d}\\
D_{y1_c}\frac{\partial[y1_c]}{\partial n} &= \frac{D_{y1}([y1_c]-[y1_n])}{d}\\
D_{y3_c}\frac{\partial[y3_c]}{\partial n} &= \frac{D_{y3}([y3_c]-[y3_n])}{d}\\
D_{y4_n}\frac{\partial[y4_n]}{\partial n} &= \frac{D_{y4}([y1_n]-[y4_c])}{d}\\
D_{y4_c}\frac{\partial[y4_c]}{\partial n} &= \frac{D_{y4}([y1_c]-[y4_n])}{d}\\
D_{y5_n}\frac{\partial[y5_n]}{\partial n} &= \frac{D_{y5}([y5_n]-[y1_c])}{d}\\
D_{y5_c}\frac{\partial[y5_c]}{\partial n} &= \frac{D_{y5}([y5_c]-[y1_n])}{d}\\
D_{y6_n}\frac{\partial[y6_n]}{\partial n} &= \frac{D_{y6}([y1_n]-[y6_c])}{d}\\
D_{y6_c}\frac{\partial[y6_c]}{\partial n} &= \frac{D_{y6}([y1_c]-[y6_n])}{d}
\end{aligned} \tag{5.51}
$$

The boundary conditions (5.51) describe the flux across the nuclear membrane. This flux can be thought of as a permeability coefficient (defined as the diffusion coefficient of the species in the nuclear membrane divided by the membrane thickness) multiplied by the concentration difference of the species across the nucleocytoplasmic boundary.

Next, we alter the composition of the cell cytoplasm to examine the effect of introducing some regions in the cytoplasm where molecular movement/transport is inhibited for some reason and examine its effect on the oscillations of the model.

Finally we modify the model system to examine the effect of molecular convection on the oscillations of the model. To achieve this, we consider active transport of the proteins which is very important to shift the transcriptional factor quickly from the cytoplasm to the nucleus. Active transport of the proteins can be achieved by attachment to microtubules in the cytoplasm. The microtubules (MTs) are hollow cylindrical filaments. During most of the life of the cell (interphase), the MTs are organized within the cytoplasm as an aster originating from a microtubule organizing center (MTOC) located in the proximity of the nucleus (Cangiani and Natalini 2010).

The role of MTs is that of enhancing intracellular trafficking. The size of macromolecules and intracellular organelles limits their diffusion speed to the cytoplasm, so MTs resort with active transport in order to reach their target location. Active transport is not essential to trafficking processes. Rather it must be seen as a way to improve their efficiency. Active transport along the MTs is achieved by binding to a motor protein, which possesses a mechanism for moving along the MT at a speed of about $0.5\mu\mathrm{m}s^1$ (Sturrock et al. 2012).

We shall model active transport of the transcription factor Hes1 as always being directed towards the nucleus. We do this by adding a convection term to the cytoplasmic Hes1 equation in equation system (5.45), which becomes:

$$\begin{aligned} \frac{\partial y_{3c}^*}{\partial t^*} &= D_{y_{3c}}^* \nabla^2 y_{3c}^* - (\mu_3^{\backslash} + d\mu_3 sin(\frac{2\pi t}{T}))y_{3c}^* \\ &\quad + k_3^* y_{1c}^* - \nabla \cdot (\mathbf{a}[y_{3c}]) - 2k_4^* y_{3c}^{*2}, \end{aligned} \tag{5.52}$$

where $-\nabla \cdot (\mathbf{a}[y_{3c}])$ is active transport and $\mathbf{a}$ is the convective velocity given by

$$\mathbf{a} = [\frac{-ax}{\sqrt{x^2+y^2}}, \frac{-ay}{\sqrt{x^2+y^2}}] \tag{5.53}$$

and the parameter a is the convection speed.

We run the simulation for the system of equations (5.46) and (5.52) while we still considering the nuclear membrane effects.

Fig (5.17) shows the effect of adding a noise to the diffusion ($D = D + \sin(0.01t + awang(\sin(0.01t), 25)/5000$), where $D = 0.00075$). The plot shows that all the variables of the model (Hes1 mRNA, Hes1 protein dimer, Hes1 protein, Stat3 mRNA and Stat3 protein) have oscillations. By comparing the results of fig (5.18) to the original simulation fig (5.14), we note the diffusion noise affects the concentration level of the variables in the cytoplasm and causes some delay in the diffusion between the nucleus and the cytoplasm. This result is similar to simulations of the system when we add a nuclear membrane with width d and zero flux boundary condition in fig (5.18) where the molecules take a longer time to move between the two parts of the domain.

In figs. (5.19) and (5.20) we consider the cell with a nuclear membrane. However we also added some holes in the cytoplasm in fig (5.19) and considered convection (i.e. motion along microtubules) in fig (5.20). In both figures we have oscillations but in fig(5.19) the diffusion between the two domains still has the same delay while in fig (5.20) convection helps to move the molecules faster between the nucleus and the cytoplasm.

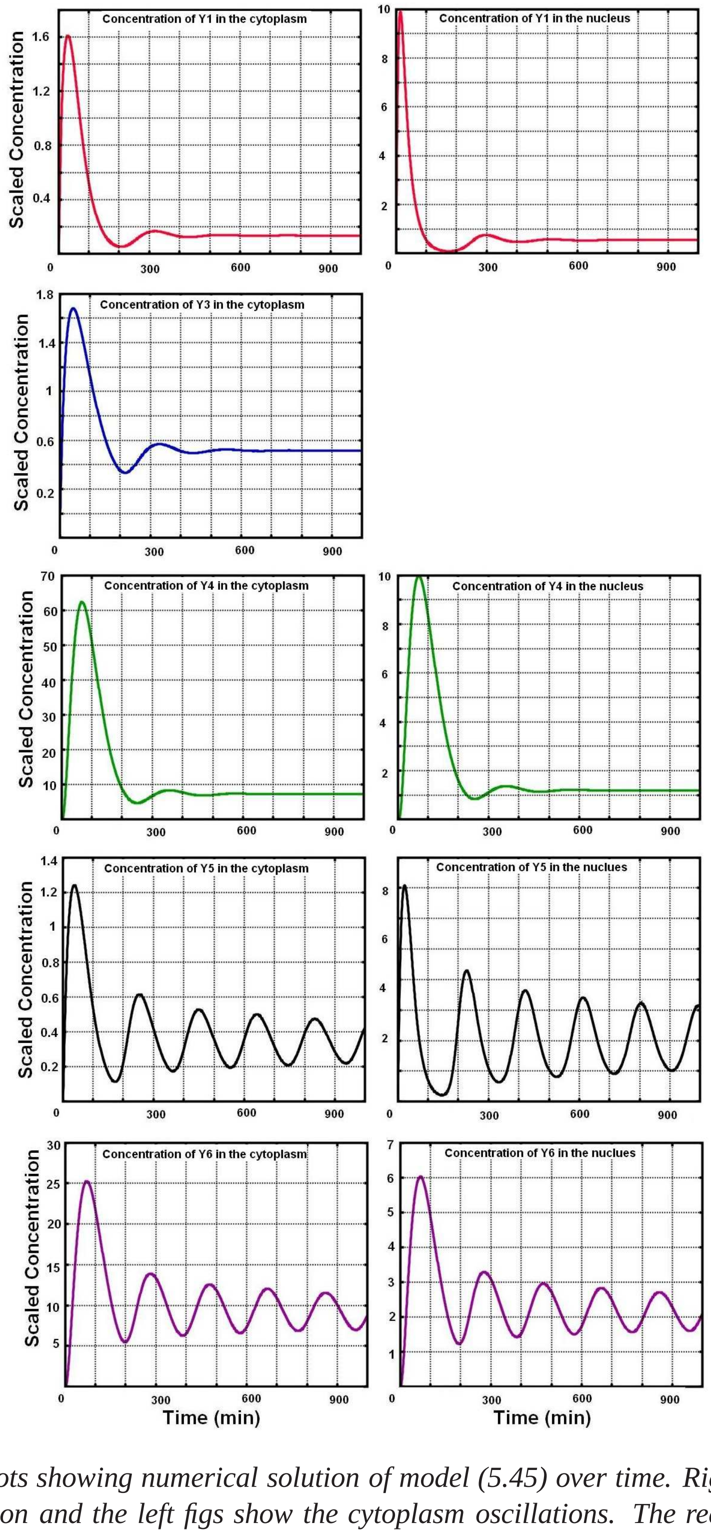

Figure 5.13: *Plots showing numerical solution of model (5.45) over time. Right figs show the nucleus oscillation and the left figs show the cytoplasm oscillations. The red lines represent the Hes1 mRNA (y1), the blue lines represent the Hes1 protein dimer (y3), the green lines represent the Hes1 protein (y4), the black lines represent the Stat3 mRNA (y5), and the purple lines represent the Stat3 protein (y6).*

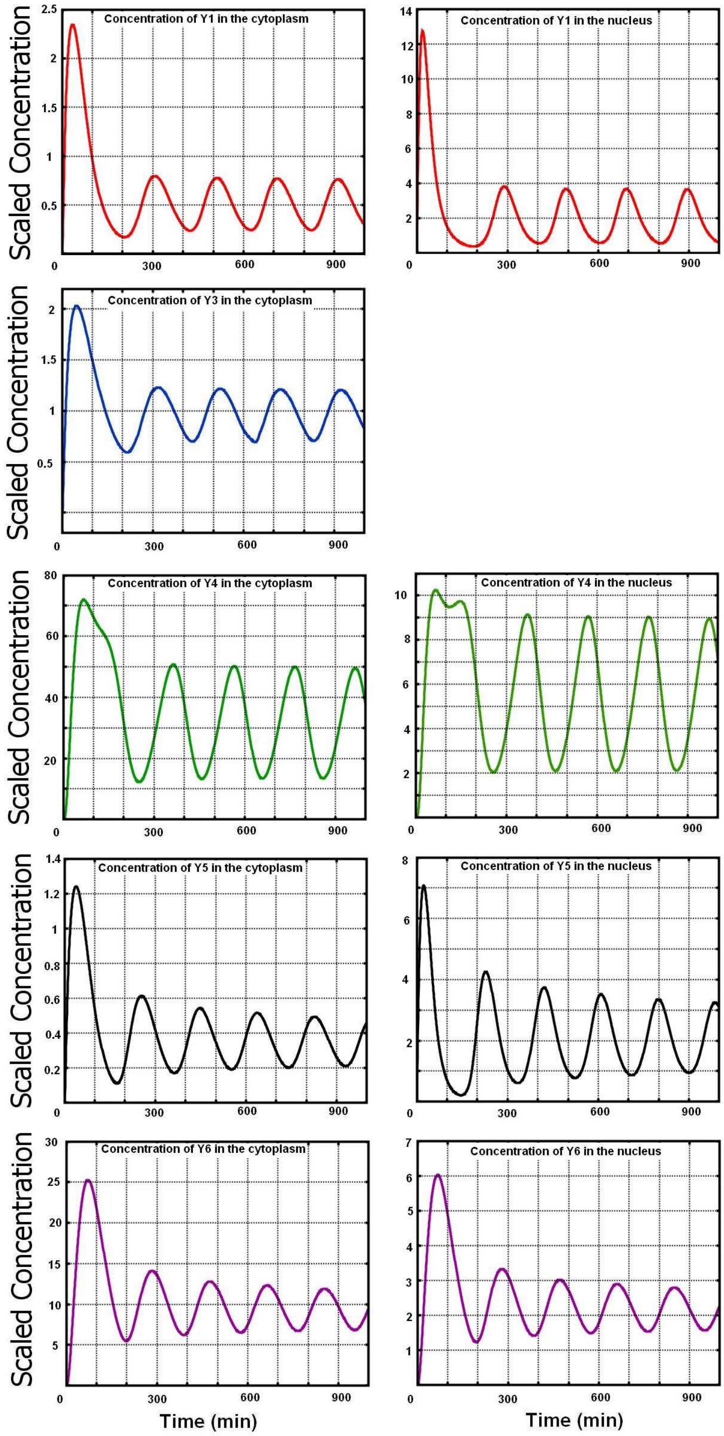

Figure 5.14: *Plots showing numerical solution of model (5.45) over time. The red lines represent the Hes1 mRNA (y1), the blue lines represent the Hes1 protein dimer (y3), the green lines represent the Hes1 protein (y4), the black lines represent the Stat3 mRNA (y5), and the purple lines represent the Stat3 protein (y6).*

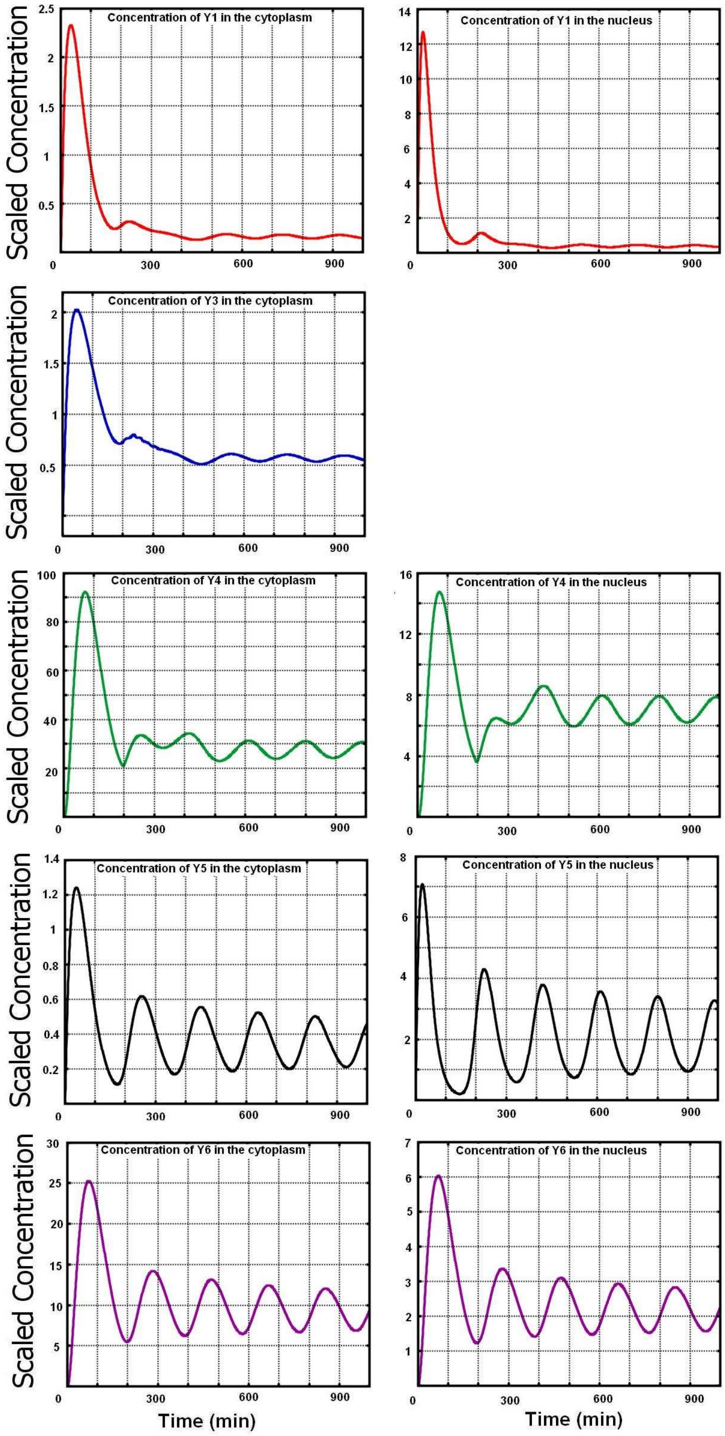

Figure 5.15: *Plots showing numerical solution of model (5.45) over time. The red lines represent the Hes1 mRNA (y1), the blue lines represent the Hes1 protein dimer (y3), the green lines represent the Hes1 protein (y4), the black lines represent the Stat3 mRNA (y5), and the purple lines represent the Stat3 protein (y6). The Figure shows the effect of remapping the value of protein degradation rate in the model (5.45) with the new value present in eq.(5.47)*

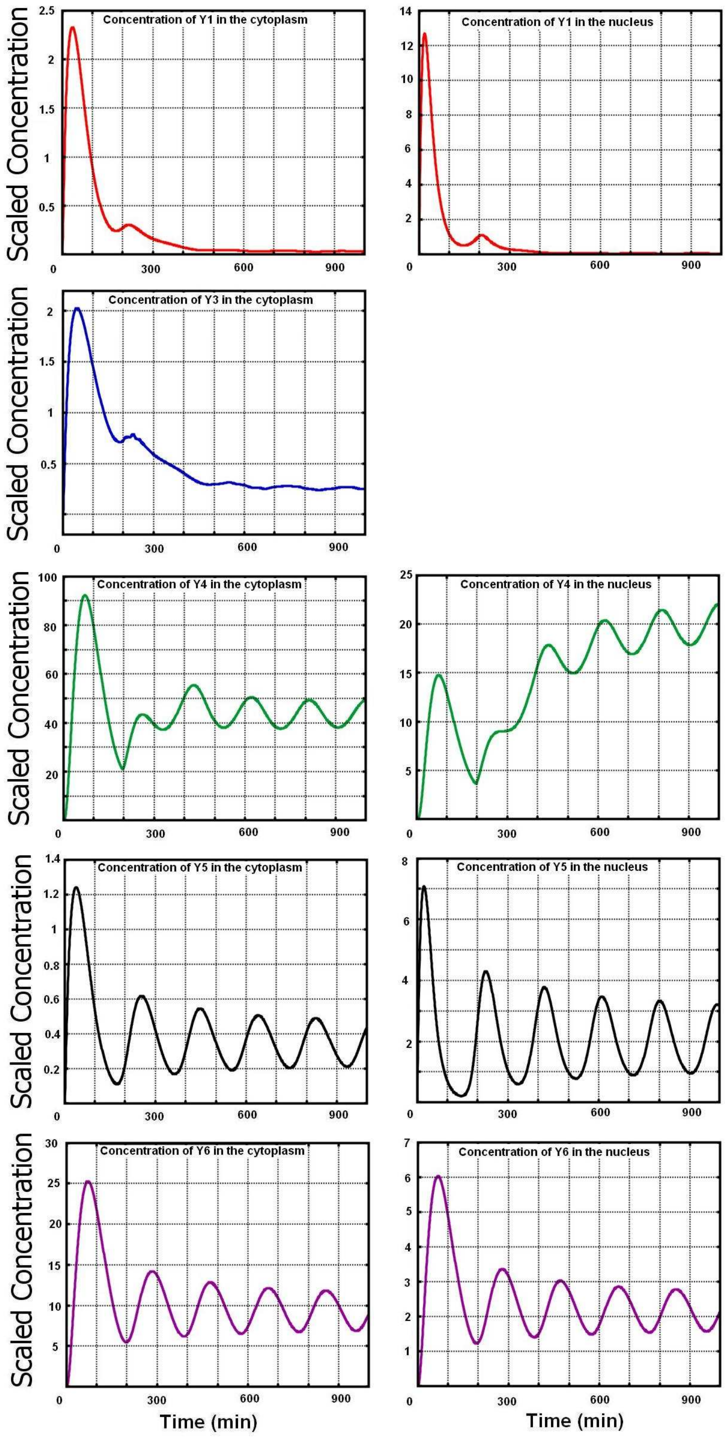

Figure 5.16: *Plots showing numerical solution of model (5.45) over time. The red lines represent the Hes1 mRNA (y1), the blue lines represent the Hes1 protein dimer (y3), the green lines represent the Hes1 protein (y4), the black lines represent the Stat3 mRNA (y5), and the purple lines represent the Stat3 protein (y6). The Fig show the affect of remapping the value of protein degradation rate in the model (5.45) with the new value present in eq. (5.48).*

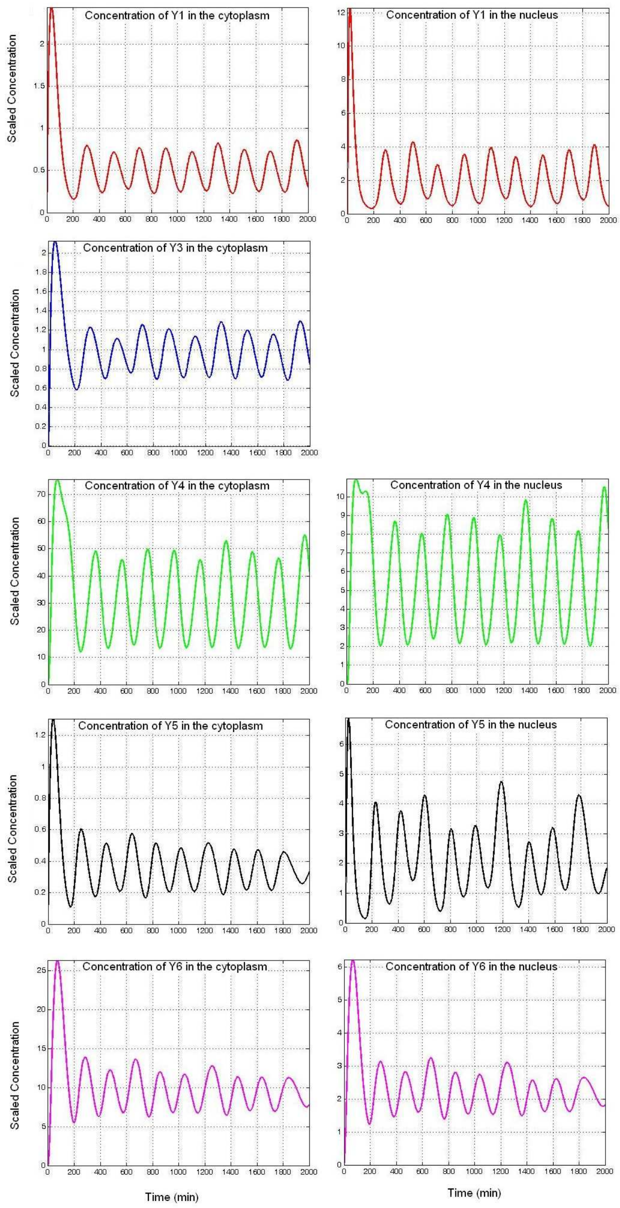

Figure 5.17: *Plots showing n umerical solution of model (5.45) over time. The red lines represent the Hes1 mRNA (y1), the blue lines represent the Hes1 protein dimer (y3), the green lines represent the Hes1 protein (y4), the black lines represent the Stat3 mRNA (y5), and the purple lines represent the Stat3 protein (y6). The plots show the effect of modifying the diffusion D by adding white Gaussian noise* $D + awng$ *and using it in the model (5.45).*

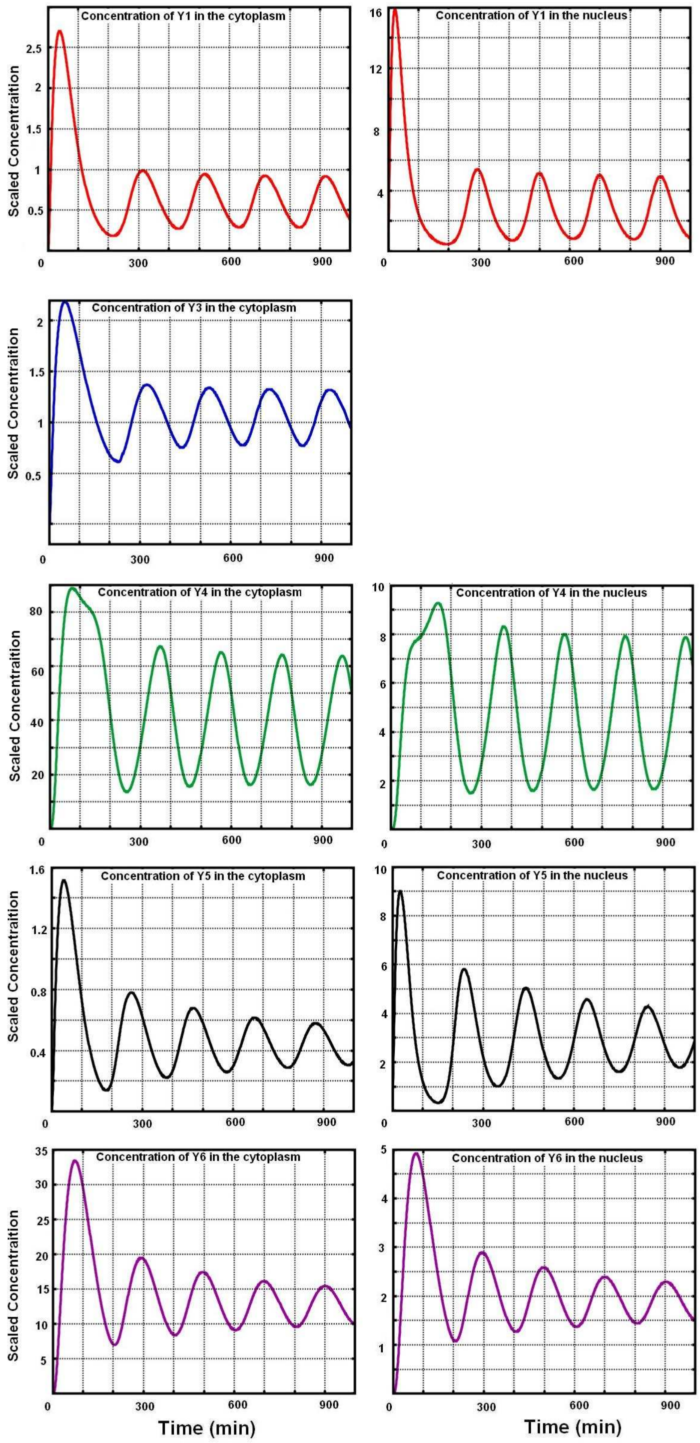

Figure 5.18: *Plots showing Numerical solution of model (5.45) over time which is consider the Nucleus membrane. The red lines represent the Hes1 mRNA (y1), the blue lines represent the Hes1 protein dimer (y3), the green lines represent the Hes1 protein (y4), the black lines represent the Stat3mRNA (y5), and the purple lines represent the Stat3 protein (y6).*

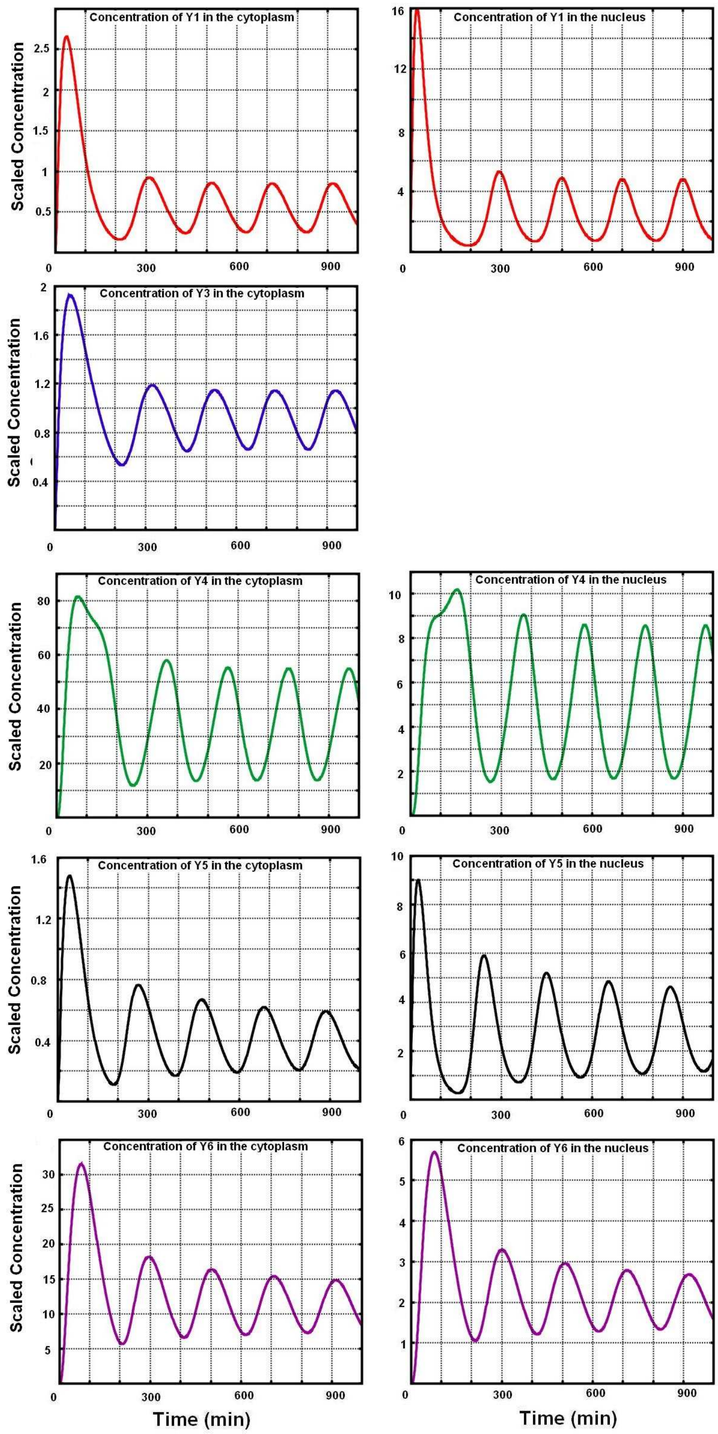

Figure 5.19: *Plots showing Numerical solution of model (5.45) over time. The red lines represent the Hes1mRNA (y1), the blue lines represent the Hes1 protein dimer (y3), the green lines represent the Hes1 protein (y4), the black lines represent the Stat3mRNA (y5), and the purple lines represent the Stat3 protein (y6). The Fig show the affect of making some hole with zero flux boundary condition in the cytoplasm.*

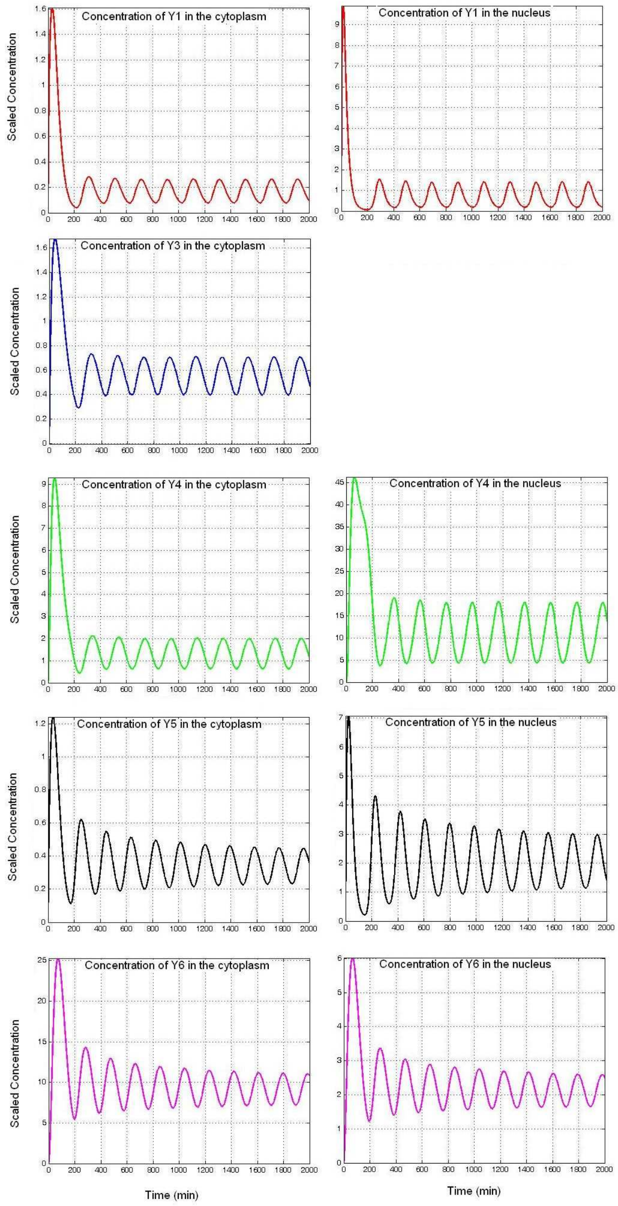

Figure 5.20: *Plots showing Numerical solution of model (5.46) over time. The red lines represent the Hes1 mRNA (y1), the blue lines represent the Hes1 protein dimer (y3), the green lines represent the Hes1 protein (y4), the black lines represent the Stat3mRNA (y5), and the purple lines represent the Stat3 protein (y6). The model (5.46) show the effect of convection*

Chapter 6

Modelling the p53–Mdm2 System

6.1 A Spatio-Temporal Model of the p53-Mdm2 System

In this chapter we extend the previous model of the p53-Mdm2 system and consider spatial interactions within the cell as shown in figure (4.13) in chapter 4. We consider nucleus and cytoplasm domains as two spatial compartments separated by the nuclear membrane and the cytoplasm has zero flux boundary condition with the out side cell membrane. Also, we couple the reaction kinetics from ODE model (4.32), (4.33) and (4.34) in chapter 4, with diffusion to model the protein and mRNA transport within the cell.

p53 transcription takes place in the nucleus to produce p53 mRNA then transfers to the cytoplasm where the p53 protein synthesis occurs and the same process goes with the Mdm2 protein and Mdm2 mRNA. Then, we assume that the mechanism governing the spatial movement of the mRNA and the protein between the nucleus and the cytoplasm is diffusion.

Therefore, we now consider the spatial interactions explicitly, allowing for diffusion within the cell, and arrive at the following system of PDEs:

$$\frac{\partial [P_c]}{\partial t} = D_{P_c}\nabla^2[P_c] + H_2(x,y)\beta - (\mu + \nu(\frac{[M_c]^{h1}}{\widehat{M}^{h1} + [M_c]^{h1}}))[P_c] \tag{6.1}$$

$$\frac{\partial [P_n]}{\partial t} = D_{P_n}\nabla^2[P_n] - (\mu + \nu(\frac{[M_n]^{h1}}{\widehat{M}^{h1} + [M_n]^{h1}}))[P_n] \tag{6.2}$$

$$\frac{\partial [Mm_n]}{\partial t} = D_{Mm_n}\nabla^2[Mm_n] + \alpha + \eta(\frac{[P_n]^{h2}}{\widehat{P}^{h2} + [P_n]^{h2}}) - \phi[Mm_n] \tag{6.3}$$

$$\frac{\partial [Mm_c]}{\partial t} = D_{Mm_c}\nabla^2[Mm_c] - \phi[Mm_c] \tag{6.4}$$

$$\frac{\partial [M_c]}{\partial t} = D_{M_c}\nabla^2[M_c] + H_1(x,y)\gamma[Mm_c] - \rho[M_c] \tag{6.5}$$

$$\frac{\partial [M_n]}{\partial t} = D_{M-n}\nabla^2[M_n] - \rho[M_n] \tag{6.6}$$

where ,$[P_n]$, $[P_c]$, $[Mm_n]$, $[Mm_c]$, $[M_n]$ and $[M_c]$ are the concentrations of the nuclear and the cytoplasmic p53, the nuclear and the cytoplasmic Mdm2 mRNA and the nuclear and the cytoplasmic Mdm2 protein respectively. $[D_i]$ denote the diffusion coefficients for each species.

To model the transportation of both mRNA and the protein within the cell, we coupled the ODE model (4.32), (4.33) and (4.34) with diffusion which enables us to model the molecules moving from the nucleus to the cytoplasm and from the cytoplasm to the nucleus across the nuclear membrane. Eqs.(6.1)-(6.6) represent a PDE system of reaction-diffusion equations modelling the spatio-temporal evolution of the p53-Mdm2 system. $H_1(x,y)$ and $H_2(x,y)$ are functions localising the protein production whose specific form will be given after the nondimensionalisation of the system.

We consider the continuity of flux boundary conditions for the nuclear membrane to allow import and export of mRNA and the protein, and zero flux boundary conditions at the cytoplasm membrane to ensure that all molecules remain within the cell membrane.

$$D_{P_n}\frac{\partial[P_n]}{\partial n} = D_{P_c}\frac{\partial[P_c]}{\partial n} \text{ and } [P_n]=[P_c] \text{ at the nuclear membrane} \tag{6.7}$$

$$D_{Mm_n}\frac{\partial[Mm_n]}{\partial n} = D_{Mm_c}\frac{\partial[Mm_c]}{\partial n} \text{ and } [Mm_n]=[Mm_c] \text{ at the nuclear membrane} \tag{6.8}$$

$$D_{M_n}\frac{\partial[M_n]}{\partial n} = D_{M_c}\frac{\partial[M_c]}{\partial n} \text{ and } [M_n]=[M_c] \text{ at the nuclear membrane} \tag{6.9}$$

$$\frac{\partial[P_c]}{\partial n} = 0, \text{ at the cell membrane} \tag{6.10}$$

$$\frac{\partial[Mm_c]}{\partial n} = 0, \text{ at the cell membrane} \tag{6.11}$$

$$\frac{\partial[M_c]}{\partial n} = 0, \text{ at the cell membrane} \tag{6.12}$$

where n is a unit normal.

We nondimensionalise Eqs. (6.1)-(6.6) with appropriate reference values as follows (see Appendix D):

$$
\begin{aligned}
\overline{[P_n]} &= \frac{[P_n]}{p_0}\ ,\ \overline{[P_c]} = \frac{[P_c]}{p_0}\ ,\ \overline{[Mm_n]} = \frac{[Mm_n]}{mm_0}\ ,\ \overline{[Mm_c]} = \frac{[Mm_c]}{mm_0} \\
\overline{[M_n]} &= \frac{[M_n]}{m_0}\ ,\ \overline{[M_c]} = \frac{[M_c]}{m_0} \\
\bar{t} &= \frac{t}{\tau}\ ,\ \overline{X} = \frac{x}{L}\ ,\ \overline{Y} = \frac{y}{L}
\end{aligned}
\tag{6.13}
$$

where $[p_0]$, $[mm_0]$ and $[m_0]$ are reference concentrations, τ is reference time, and L is a reference length ($10\mu m$ as with the Hes1 system). Using this scaling Eq. (6.1)-(6.6) become:

$$
\frac{\partial\overline{[P_c]}}{\partial t} = D^*_{Pc}\nabla^2\overline{[P_c]} + H_2(x,y)\beta^* - (\mu^* + \nu^*(\frac{\overline{[M_c]}^{h1}}{M^* + \overline{[M_c]}^{h1}}))\overline{[P_c]} \tag{6.14}
$$

$$
\frac{\partial\overline{[P_n]}}{\partial t} = D^*_{P_n}\nabla^2\overline{[P_n]} - (\mu^* + \nu^*(\frac{\overline{[M_n]}^{h1}}{M^* + \overline{[M_n]}^{h1}}))\overline{[P_n]} \tag{6.15}
$$

$$
\frac{\partial\overline{[Mm_n]}}{\partial t} = D^*_{Mm_n}\nabla^2\overline{[Mm_n]} + \alpha^* + \eta^*(\frac{\overline{[P_n]}^{h2}}{P^* + \overline{[P_n]}^{h2}}) - \phi^*\overline{[Mm_n]} \tag{6.16}
$$

$$
\frac{\partial\overline{[Mm_c]}}{\partial t} = D^*_{Mm_c}\nabla^2\overline{[Mm_c]} - \phi^*\overline{[Mm_c]} \tag{6.17}
$$

$$
\frac{\partial\overline{[M_c]}}{\partial t} = D^*_{M_c}\nabla^2\overline{[M_c]} + H_1(x,y)\gamma^*\overline{[Mm_c]} - \rho^*\overline{[M_c]} \tag{6.18}
$$

$$
\frac{\partial\overline{[M_n]}}{\partial t} = D^*_{M_n}\nabla^2\overline{[M_n]} - \rho^*\overline{[M_n]} \tag{6.19}
$$

where

$$
\begin{aligned}
D^*_{P_n} &= \frac{\tau D_{P_n}}{L^2}\ ,\ D^*_{P_c} = \frac{\tau D_{P_c}}{L^2} \\
D^*_{Mm_n} &= \frac{\tau D_{Mm_n}}{L^2}\ ,\ D^*_{Mm_c} = \frac{\tau D_{Mm_c}}{L^2} \\
D^*_{M_n} &= \frac{\tau D_{M_n}}{L^2}\ ,\ D^*_{M_c} = \frac{\tau D_{M_c}}{L^2} \\
M^* &= \frac{\widehat{Mm^{h1}}}{[Mm_0]^{h1}}\ ,\ P^* = \frac{\widehat{p}^{h2}}{[P_0]^{h2}} \\
\beta^* &= \frac{\tau\beta}{p_0}\ ,\ \eta^* = \frac{\tau\eta}{mm_0}\mu^* = \tau\mu\ ,\ \nu^* = \tau\nu \\
\phi^* &= \tau\phi\ ,\ \gamma^* = \frac{\tau\gamma[Mm_0]}{m_0}\ ,\ \alpha^* = \frac{\tau\alpha}{mm_0}\rho^* = \tau\rho
\end{aligned}
\tag{6.20}
$$

and

$$
H_1(\bar{x},\bar{y}) = \begin{cases} 0 & \text{if } \frac{\bar{x}^2}{2} + \bar{y}^2 \leq 0.25, \\ 1 & \text{if } \frac{\bar{x}^2}{2} + \bar{y}^2 > 0.25. \end{cases}
$$

and

$$
H_2(\bar{x},\bar{y}) = \begin{cases} 0 & \text{if } \frac{\bar{x}^2}{2} + \bar{y}^2 \leq 0.25, \\ 1 & \text{if } 0.25 < \frac{\bar{x}^2}{2} + \bar{y}^2 < 0.375, \\ 0 & \text{if } \frac{\bar{x}^2}{2} + \bar{y}^2 \geq 0.375, \end{cases}
$$

The function $H_1(x,y)$ is such that in a region close to the nucleus (representing the location of the ER), the function is zero, meaning there is no protein synthesis in this region. In a region further away from the nucleus (outside the ER) the function takes the value of one, modelling the translation of protein in this region of the cytoplasm. The function $H_2(x,y)$ is such that in a region close to the nucleus the function is zero, meaning there is no protein synthesis here. However, it is now assumed that the function takes the value of one in an annular region outside of the ER (again modelling the translation of protein). An annular region is chosen because we assume p53 is produced at a constant rate in the cytoplasm. This prevents p53 from being produced close to the plasma membrane, where mRNA is unlikely to reach in sufficient quantities. The

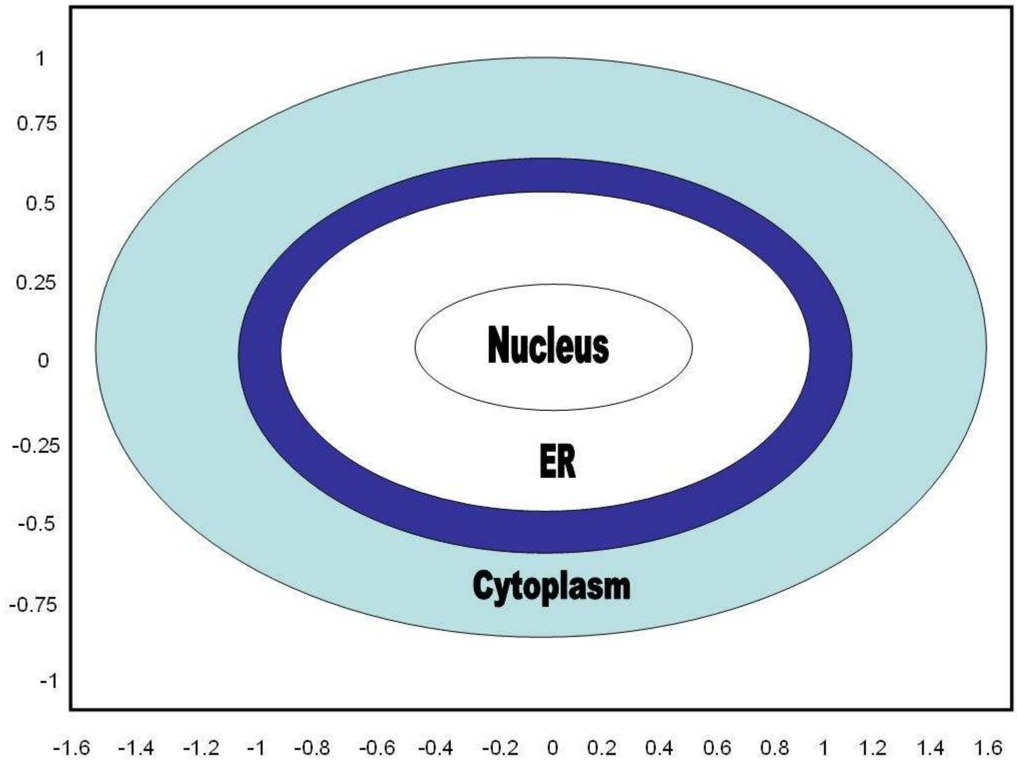

Figure 6.1: *Schematic diagram showing the regions where the two functions $H_1(x,y)$ and $H_2(x,y)$ are non-zero. The blue region of the cytoplasm depicts where we allow constant protein synthesis to occur, i.e., this represents the rectangular function $H_2(x,y)$. The blue and red regions together depict where we allow protein translation via mRNA, i.e., this represents the function $H_1(x,y)$. In the white region representing the ER and nucleus, no protein synthesis takes place.*

two functions are illustrated graphically in Fig 6.1.

We apply zero initial conditions, zero-flux boundary conditions at the cell membrane and flux continuity boundary conditions across the nuclear membrane:

$$[\overline{P}_n] = [\overline{P}_c] = [\overline{Mm}_n] = [\overline{Mm}_c] = [\overline{M}_n] = [\overline{M}_c] = 0, \ at\ t = 0 \tag{6.21}$$

$$D^{*}_{P_n}\frac{\partial[\overline{P_n}]}{\partial n} = D^{*}_{P_c}\frac{\partial[\overline{P_c}]}{\partial n} \; and \; [\overline{P_n}] = [\overline{P_c}] \; at\ the\ nuclearmembrane \tag{6.22}$$

$$D^{*}_{Mm_n}\frac{\partial[\overline{Mm_n}]}{\partial n} = D^{*}_{Mm_c}\frac{\partial[\overline{Mm_c}]}{\partial n} \; and \; [\overline{Mm_n}] = [\overline{Mm_c}] \; at\ the\ nuclearmembrane \tag{6.23}$$

$$D^{*}_{M_n}\frac{\partial[\overline{M_n}]}{\partial n} = D^{*}_{M_c}\frac{\partial[\overline{M_c}]}{\partial n} \; and \; [\overline{M_n}] = [\overline{M_c}] \; at\ the\ nuclearmembrane \tag{6.24}$$

$$\frac{\partial[\overline{P_c}]}{\partial n} = 0, \; at\ the\ cell\ membrane \tag{6.25}$$

$$\frac{\partial[\overline{Mm_c}]}{\partial n} = 0, \; at\ the\ cell\ membrane \tag{6.26}$$

$$\frac{\partial[\overline{M_c}]}{\partial n} = 0, \; at\ the\ cell\ membrane \tag{6.27}$$

We take reference concentrations to be $[P_0] = 0.05, \mu M$ and estimated reference concentrations for $[Mm_0]$=0.05μM and $[M_0]$=2μM. Ma et al. (2005). Fig (6.1), (6.2) show the simulations of Eqs.(6.14)-(6.19). It was noticed that the period of oscillation was approximately 400 time units. Hence, knowing that the period of oscillation of p53 is approximately 3h Monk (2003), as result of this, we have the reference time τ as follows: 400τ = 3 h which mean τ= 27 s.

Parameter estimation

The following parameter values were used in our simulations of the non-dimensional p53-Mdm2 system:

$$
\begin{aligned}
D^*_{P_c} &= D^*_{P_n} = D^*_{Mm_c} = D^*_{Mm_n} = D^*_{M_c} = D^*_{M_n} = 9 \times 10^{-4} \\
\beta^* &= 0.5\ ,\ \mu^* = 0.003\ ,\ \nu^* = 1\ ,\ \alpha^* = 0.0175 \\
\eta^* &= 1\ ,\ \phi^* = 0.0175.\ ,\ \gamma^* = 0.5\ ,\ \rho^* = 0.025 \\
h1 &= 2\ ,\ h2 = 4\ ,\ M^* = 16\ ,\ P^* = 5
\end{aligned}
\tag{6.28}
$$

By using (6.20) and (6.28) to estimate the parameter values of the dimensional p53-Mdm2 model (6.1)-(6.6).

$$
\begin{aligned}
D_{P_c} &= D_{P_n} = D_{Mm_c} = D_{Mm_n} = D_{M_c} = D_{M_n} = 3.33 \times 10^{-11} cm^2 s^{-1} \\
\beta &= 9.26 \times 10^{-3} Ms^{-1}\ ,\ \mu = 1.11 \times 10^{-4} s^{-1} \\
\nu &= 0.04 s^{-1}\ ,\ \alpha = 3.24 \times 10^{-11} Ms^{-1} \\
\eta &= 1.85 \times 10^{-9} Ms^{-1}\ ,\ \phi = 6.48 \times 10^{-4} s^{-1} \\
\gamma &= 0.74 s^{-1}\ ,\ \rho = 9.26 \times 10^{-4} s^{-1} \\
\widehat{M} &= 8 \times 10^{-6} M\ ,\ \widehat{P} = 7.48 \times 10^{-7} M \\
h1 &= 2\ ,\ h2 = 4
\end{aligned}
\tag{6.29}
$$

6.2 Computational Simulation Results

Once again we solved the PDE system (6.14)(6.19) numerically using the finite element package COMSOL/FEMLAB (with the same basis elements and basis functions and time-stepping as previously). For all our simulations we used a 2-dimensional cell domain of two ellipses to represent the nucleus and cytoplasm to show the oscillatory dynamics results of the P53-Mdm2 system.

Figs. (6.1) and (6.2) show the concentrations of p53 and Mdm2 in the nucleus and cytoplasm. We can see from these p53 simulations that the mRNA concentration is higher in the nucleus compared to the protein concentrations in the cytoplasm. while, Mdm2 mRNA concentrations higher in the cytoplasm and Mdm2 protein is higher in the nucleus.

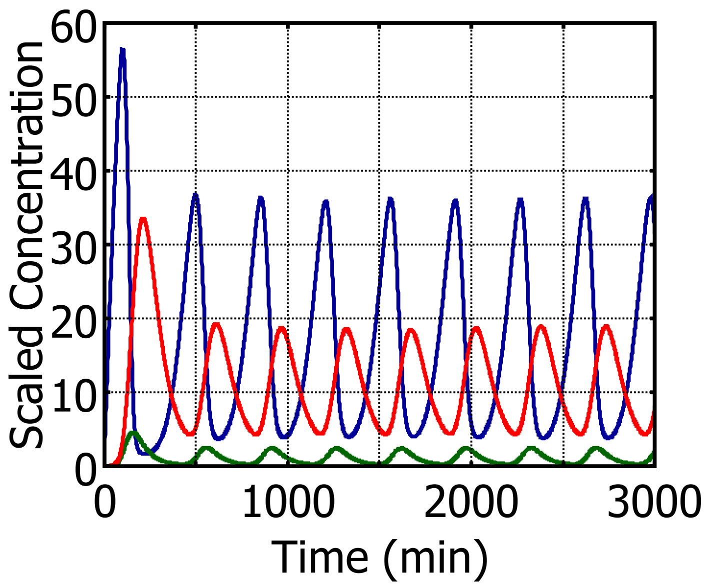

Figure 6.2: *Plots showing the concentrations of p53 (blue), Mdm2 mRNA (green) and Mdm2 (red) in the cytoplasm. The period of oscillations is approximately 180 min. Parameter values as per (60).*

Figs. (6.3), (6.4), and (6.5) show how the dynamics of the p53-Mdm2 system (evolve in space as well as time) vary spatially throughout the cell over the period of the oscillations in figures (6.1) and (6.2).

In Fig (6.3), we see that p53 has accumulated in the cytoplasm around $t = 50$, then begins to diffuse across the nucleus membrane entering the nucleus by $t = 100$ while

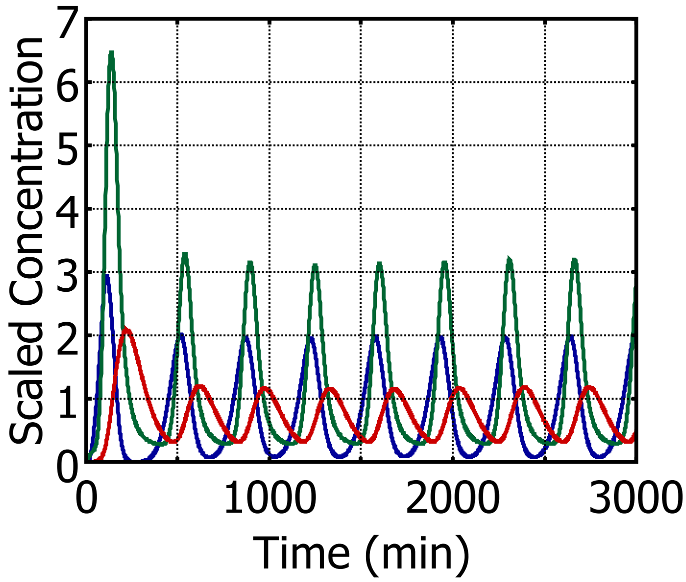

Figure 6.3: *Plots showing the concentrations of p53 (blue), Mdm2 mRNA (green) and Mdm2 (red) in the nucleus. The period of oscillations is approximately 180 min. Parameter values as per (60).*

the Mdm2 mRNA in Fig (6.4) shows in the nucleus at the same time where the Mdm2 binds to the p53 to prevent p53 transcription. At $t = 150$ the Mdm2 shuttles p53 from the nucleus to the cytoplasm for degradation, Fig(6.5). By time 400 the level of p53 begins to increase again in the cytoplasm. Figs. (6.4), (6.5) show the plots of Mdm2 concentration over time. In Fig (6.5) the Mdm2 protein is produced between $t = 100$ to $t = 250$ min, the same time as the Mdm2 mRNA is exported from the nucleus and translation occurs in the cytoplasm.

In order to investigate the influence of spatial effects, we carried out number of simulations on system (6.14)-(6.19), where we consider varying the thickness of the nuclear membrane, varying the values of the diffusion coefficients of p53, Mdm2 protein and Mdm2 mRNA, while all other parameters remaining unchanged and adding noise to the diffusion coefficients.

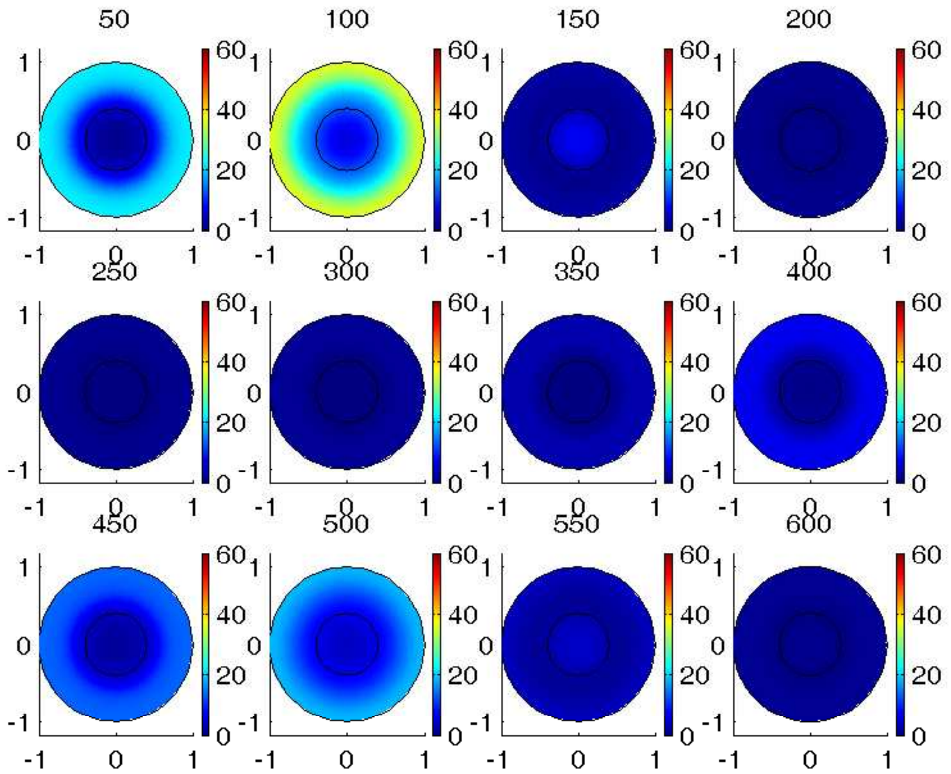

Figure 6.4: *Plots showing the spatio-temporal evolution of p53 protein concentration within the cell from times t = 0 to 450 min. The concentration oscillates in both time and space. Parameter values as per (60).*

6.3 Model extension incorporating the effect of the nuclear membrane

We now examine the effect of adding a nuclear membrane with zero flux boundary condition in the cell domain to the oscillation of the model. A nuclear membrane is the double lipid bilayer membrane called the inner membrane and outer membrane which surrounds the genetic material and divides the cell into two compartments (Martin 2010). During the intracellular signal transaction the nuclear membrane controls the diffusion from the cytoplasm through the nuclear pore complex (NPC) to the nucleus and from the nucleus to the cytoplasm (Weis 2003).

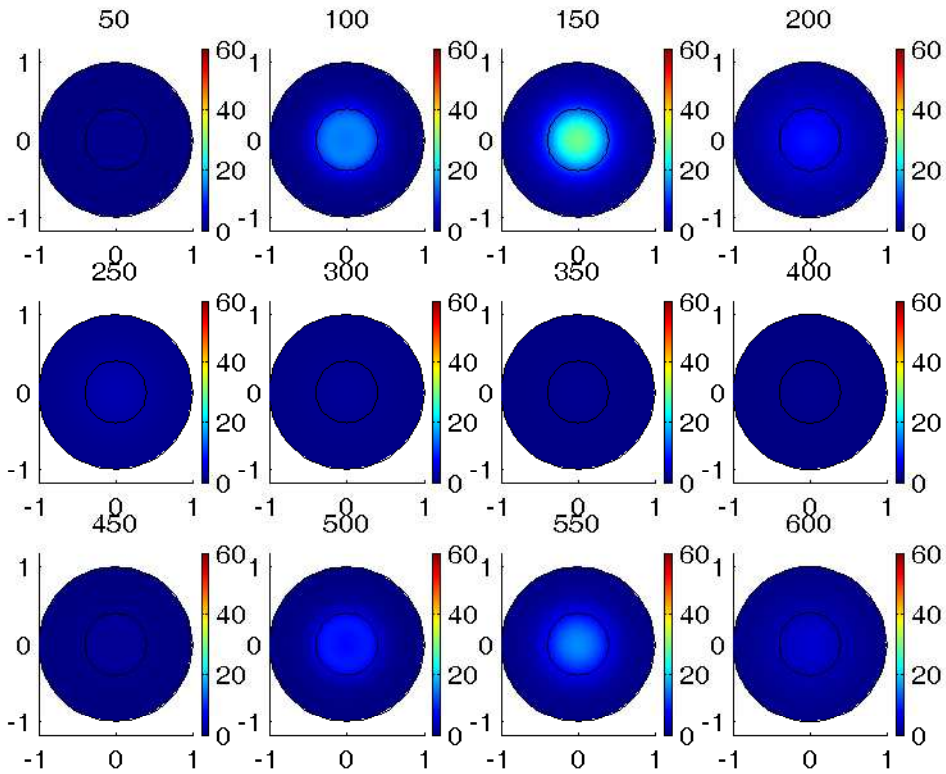

Figure 6.5: *Plots showing the spatio-temporal evolution of Mdm2 mRNA concentration within the cell from times t = 0 to 450 min. The concentration oscillates in both time and space. Parameter values as per (60).*

When the molecule binds to the surface of the outer membrane it can diffuse through the nuclear pore and then diffuses into the inner membrane. The whole process takes time which depends on the size of the molecule itself and the size of the nuclear pore. Hence, larger molecules, such as proteins, will diffuse more slowly than smaller molecules, such as mRNA (Sturrock et al. 2011).

To show the effect of the nuclear membrane on the oscillations of the p53-Mdm2 system, we consider some additional points such as introducing a thickness d to the nuclear membrane (which is also the depth of the NPC of the nuclear membrane) to

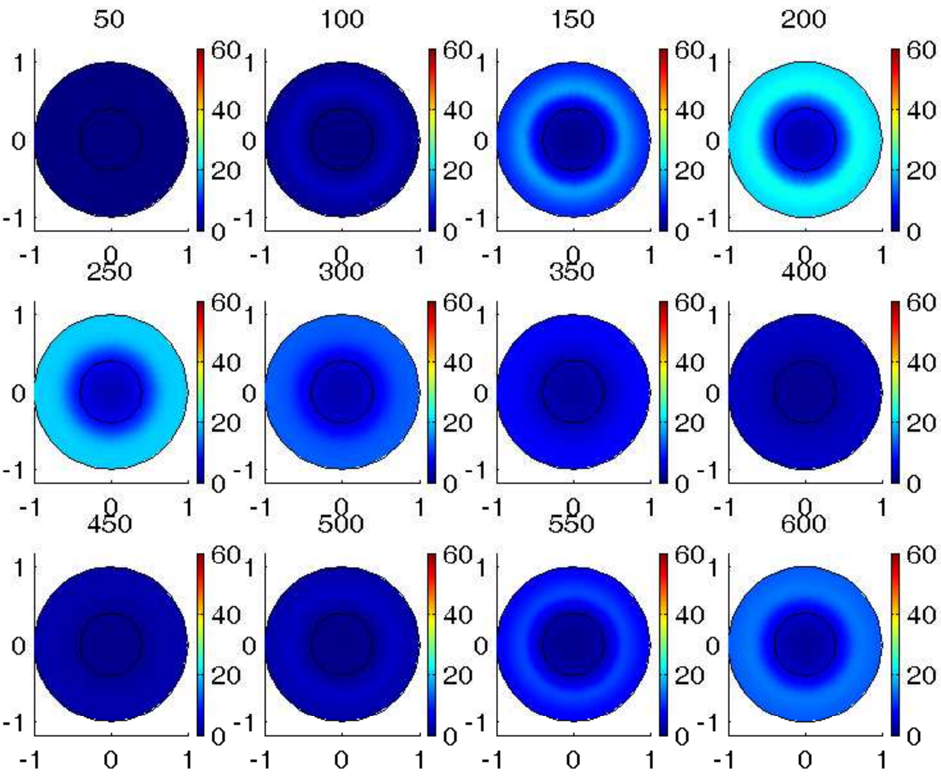

Figure 6.6: *Plots showing the spatio-temporal evolution of Mdm2 protein concentration within the cell from times t = 0 to 450 min. The concentration oscillates in both time and space. Parameter values as per (60).*

equations (6.14)-(6.19). The nuclear membrane thickness has been estimated to be approximately 100nm (Sturrock et al. 2011). Also, we assume that diffusion across it is slower than in the cytoplasm or nucleus, with protein diffusion slower than mRNA diffusion across the membrane. We simply choose $D_m = D_{ij}/5$ and $D_p = D_{ij}/15$ for the nuclear membrane diffusion for mRNA for p53 and Mdm2 and protein for p53 and Mdm2, respectively. Finally we replace the previous continuity of flux boundary condition at the nuclear membrane with the following boundary condition which considers the nuclear membrane thickness:

$$
\begin{aligned}
D_{P53_n}\frac{\partial[P53_n]}{\partial n} &= \frac{D_{P53}([P53_n]-[P53_c])}{d}\\
D_{P53_c}\frac{\partial[P53_c]}{\partial n} &= \frac{D_{P53}([P53_c]-[P53_n])}{d}\\
D_{Mdm2m_n}\frac{\partial[Mdm2m_n]}{\partial n} &= \frac{D_{Mdm2m}([Mdm2m_n]-[Mdm2m_c])}{d}\\
D_{Mdm2m_c}\frac{\partial[Mdm2m_c]}{\partial n} &= \frac{D_{Mdm2m}([Mdm2m_c]-[Mdm2m_n])}{d}\\
D_{Mdm2_n}\frac{\partial[Mdm2_n]}{\partial n} &= \frac{D_{Mdm2}([Mdm2_n]-[Mdm2_c])}{d}\\
D_{Mdm2_c}\frac{\partial[Mdm2_c]}{\partial n} &= \frac{D_{Mdm2}([Mdm2_c]-[Mdm2_n])}{d}
\end{aligned}
\tag{6.30}
$$

The boundary conditions (6.30) describe the flux across the nuclear membrane. This flux can be thought of as a permeability coefficient (defined as the diffusion coefficient of the species in the nuclear membrane divided by the membrane thickness) multiplied by the concentration difference of the species across the nucleocytoplasmic boundary.

We ran the numerical simulation of the model system twice, the first one with no change in the diffusion values (see Fig 6.7), while the second figure shows the effects of nuclear membrane and the diffusion of the variables varies and are not equal (see Figure 6.8).

The simulation result of Fig 6.7 and Fig 6.8 show clearly that the nuclear membrane thickness could stop the diffusion of molecules between the two parts of the domain, the nucleus and the cytoplasm.

6.4 Modelling the effects of noise on the system

Most physical systems which respond to the concentration of a signalling molecule will exhibit noise due to the random movement of molecules (diffusion) and delays in the processes of transcription and translation. Recent large scale surveys of noise suggested that the noise in most protein levels can be understood in terms of the components of noise that derive from the translation of mRNA into protein, or the components that arise from noise in the transcription and degradation of the mRNA itself (Gasper 2008).

To understand the effect that noise coused to the oscillation of the intracellular network, we add Gaussian Noise to the simulation code by modifying the diffusion coefficients in the p53-Mdm2 System (6.14)-(6.19) to $D = D + \sin(0.01 * t + awgn(sin(0.01 * t), 25))/5000$.

We ran the numerical simulation of the model system twice. First with no change in the diffusion values (see Fig 6.9), and second showing the effects of the nuclear membrane and the diffusion coefficients of the variables not equal. (see Figure 6.10).

By comparing the simulation result of the p53-Mdm2 system including noise in the molecular diffusion to the result of the main model system (6.30), we see clearly how the noise caused the component concentration in the cytoplasm to reach a higher value than in the nucleus where are the concentration is lower than the concentration in the main model results, shown in Fig.6.2 and 6.3.

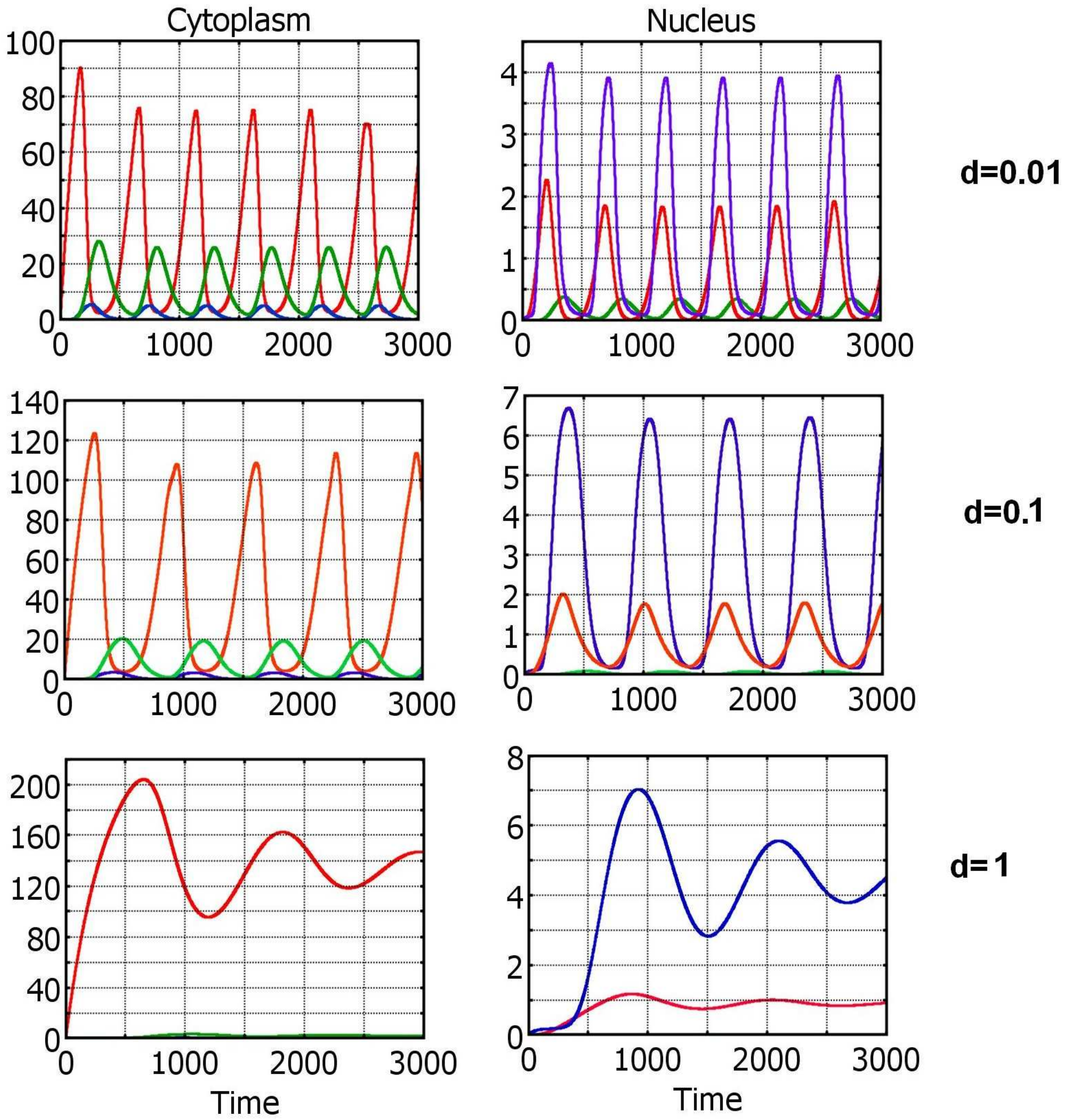

Figure 6.7: *Plots showing numerical simulation of model (6.14)-(6.19) over time. The red lines represent the p53 (y1), the blue lines represent the Mdm2 mRNA (y2), the green lines represent the Mdm2 protein (y3). The Fig shows the effect of considering the different nucleus membrane thickness d values (d=0.01, d=0.1, d=1), whereas the diffusion for the variables is equal.*

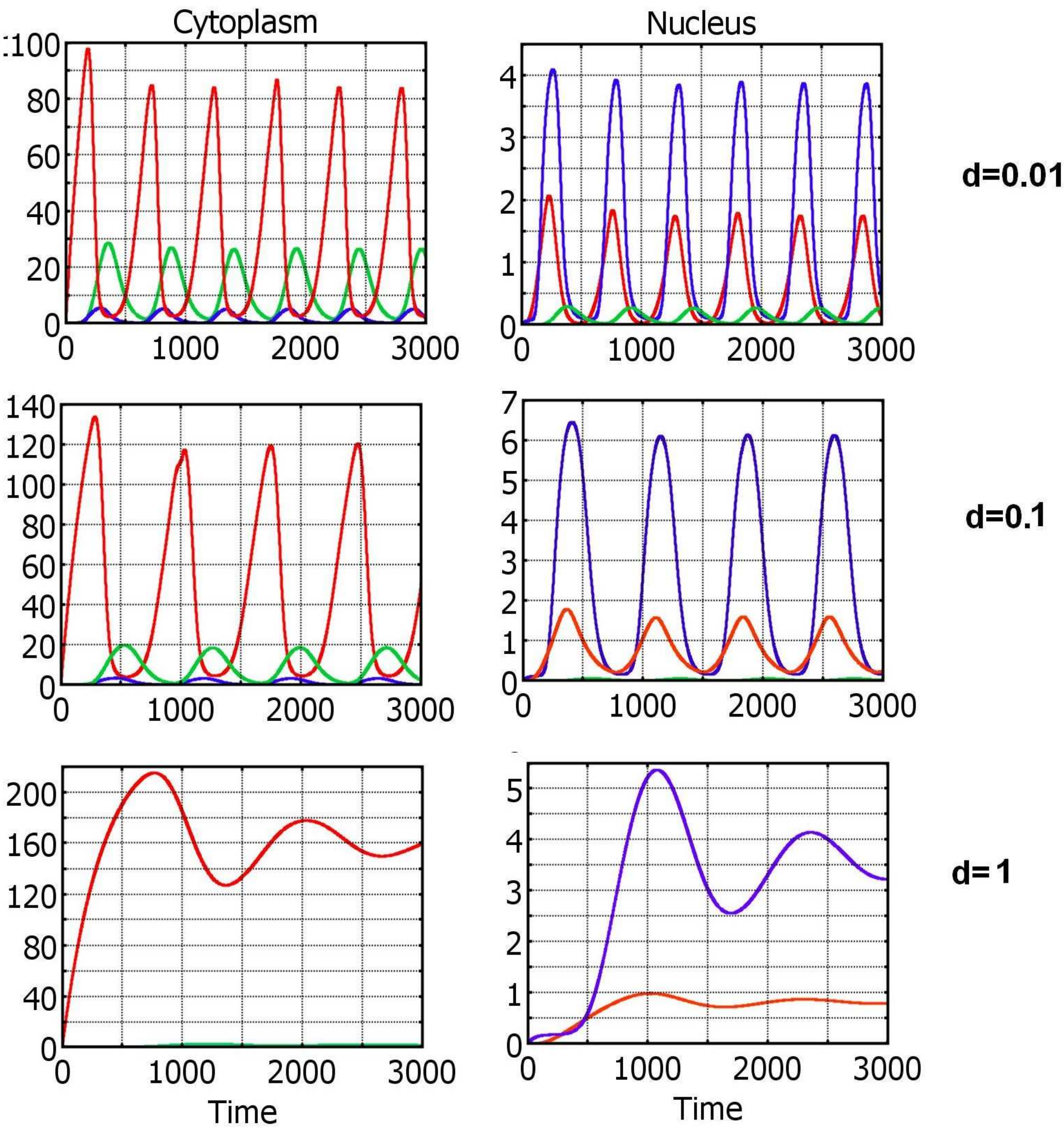

Figure 6.8: *Plots showing numerical simulation of model (6.14)-(6.19) over time. The red lines represent the p53 (y1), the blue lines represent the Mdm2 mRNA (y2), the green lines represent the Mdm2 protein (y3). The Fig show the effect of considering the different nucleus membrane thickness d values (d=0.01, d=0.1, d=1), whereas the diffusion for the variables varies and is not equal.*

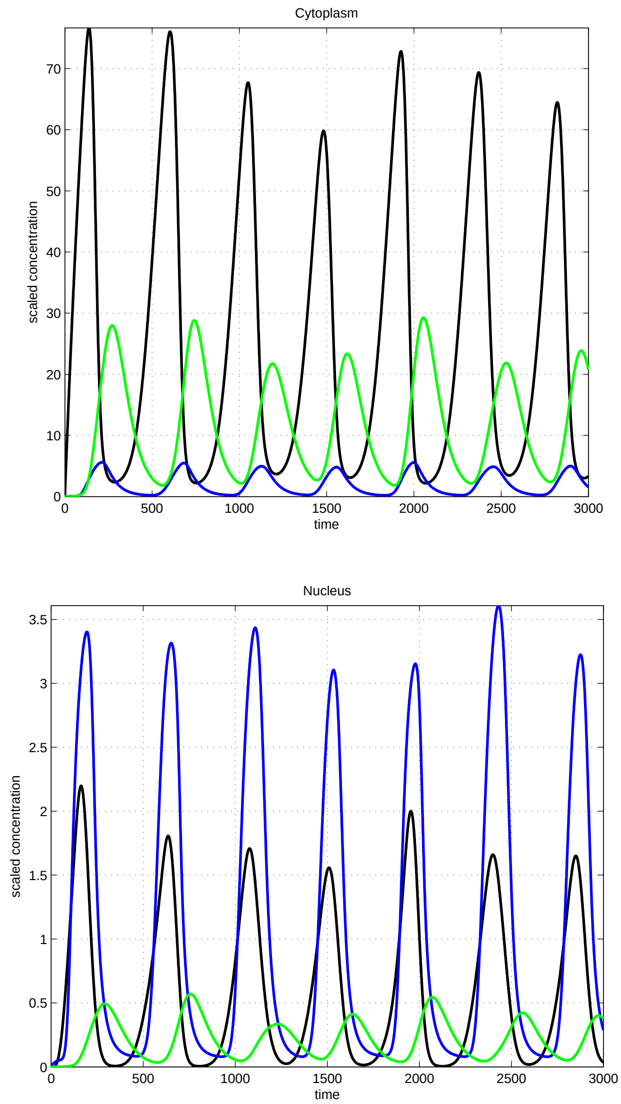

Figure 6.9: *Plots showing numerical simulation of model (6.14)-(6.19) over time. The black lines represent the p53 (y1), the blue lines represent the Mdm2 mRNA (y2), the green lines represent the Mdm2 protein (y3). The Fig show the effect of modifying the diffusion coefficient D by adding additive white Gaussian noise D+awng. The diffusion for all variables is equal and the nuclear membrane thickness = 0.01*

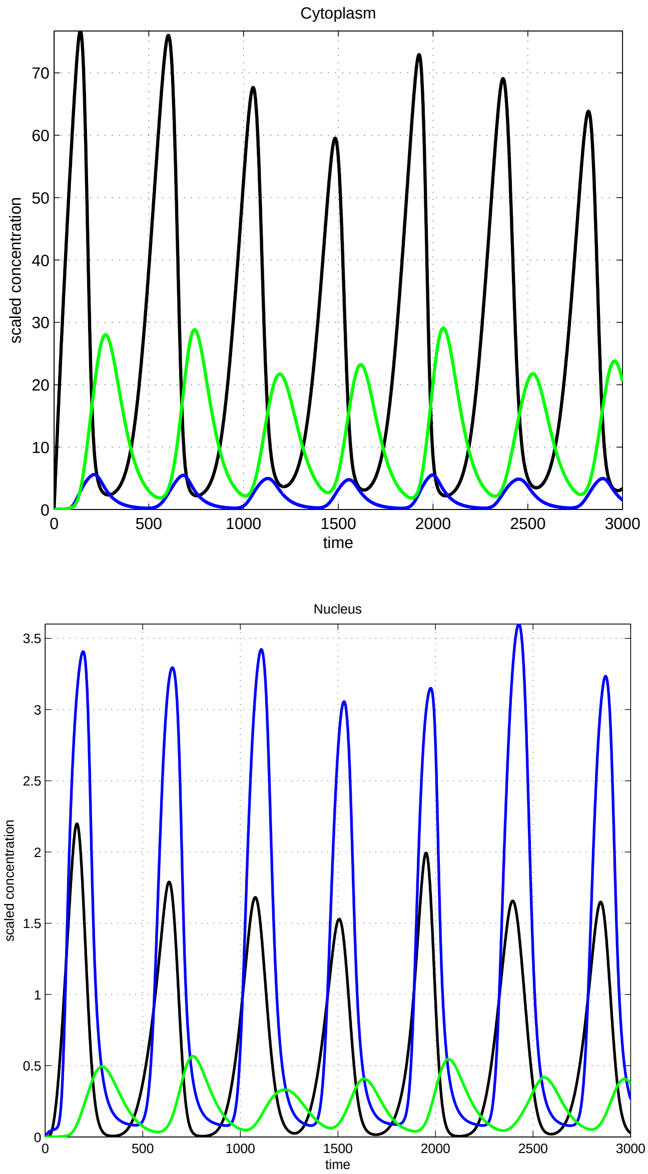

Figure 6.10: *Plots showing numerical simulation of model (6.14)-(6.19) over time. The black lines represent the p53 (y1), the blue lines represent the Mdm2 mRNA (y2), the green lines represent the Mdm2 protein (y3). The Fig show the effect of modifying the diffusion D by adding additive white Gaussian noise D+awng. The diffusion for the variables varies and is not equal and the nucleus membrane thickness = 0.01*

Chapter 7

Conclusions and Future Work

We conclude this thesis with a brief summary of the major points and some possible avenues of future exploration. Of course, this is by no means exhaustive, and we refer the reader to the appropriate chapters for a more detailed account.

In the framework of this thesis we have studied the correct spatial localisation of transcription factors where it is vitally important for the proper functioning of many intracellular signalling pathways. Also we have showed that negative feedback loops are important components of many intracellular signal transduction processes. In this thesis we have built on previous mathematical modelling approaches, and we have derived systems of partial differential equations to capture the evolution in space and time of the variables in the two pathways of the Hes1 and p53-Mdm2 feedback loops (gene regulatory networks, GRN).

In the first model, we examined a detailed model of the Hes1 system, incorporating a number of basic biochemical processes neglected in previous models using a combination of mathematical analysis and numerical simulation. We developed and extended the Hes1 model system of Momiji and Monk (2008) by using partial differential equations (PDEs) in order to be able to model the aspects of intracellular signalling pathways. Also, we showed that Hes1 oscillations are in fact dependent on a post-translational oscillation in the phosphorylation state of the protein Stat3. Oscillations in the level of pStat3 provide an extrinsic driving force to the Hes1 auto-regulatory network, by regulating the degradation rate of Hes1 protein (Yoshiura et al. 2007). We have developed an extended model of the pStat3-driven Hes1 network by incorporating transcriptional delay and Hes1 dimerisation. However, simulation of the driven network shows that the Hes1 network can respond to pStat3 oscillations by generating oscillations in Hes1 mRNA and Hes1 protein without the inclusion of transcriptional delay (Yoshiura et al. 2007).

The second model discussed in this thesis is a mathematical model of the p53-Mdm2 pathway where we use a system of PDEs to model the aspects this intracellular signalling pathway. The simulation results of our models demonstrated the existence of oscillatory dynamics in negative feedback systems for the p53-Mdm2 pathways and have been able to focus on reactions occurring both in the cell nucleus and in the cytoplasm.

In both the Hes1 and p53-Mdm2 systems, we varied the diffusion coefficients of the mRNAs and proteins and found a range of values for these diffusion coefficients where the system exhibits oscillatory dynamics. By varying the diffusion coefficients of the molecules, we can vary the flux rates across the nuclear membrane (equivalent to varying nuclear import and export rates), thus granting greater control and allowing a much more in depth analysis of the systems. Similar results were obtained by varying the mRNA degradation rates, protein degradation rates and Hill coefficients, further demonstrating that the oscillations are robust to parameter changes. Exploiting the explicitly spatial nature of PDEs, we were also able to manipulate mathematically the location of the ribosomes, thus controlling where the proteins were synthesized within the cytoplasm. For both the Hes1 and the p53-Mdm2 systems, we carried out a number of numerical simulations where we investigated the effect of varying the two functions $H_1(x,y)$ and $H_2(x,y)$, controlling constant protein synthesis and protein translation via mRNA in the cytoplasm, respectively. For both model systems, the simulation results revealed an optimum distance outside the nucleus for protein production for which sustained (undamped) oscillations of large amplitude were observed.

Future work arising from this thesis could extend the current models by considering the active transport of proteins and mRNA within the cell as mechanisms of movement in addition to diffusion (Cangiani and Natalini 2010). One could also model the nuclear membrane in more detail and take into account its thickness. This would allow one to model differences in the rate of transport of mRNA and protein across the nuclear membrane more accurately. Additional complexities of post-transcriptional mRNA and post-translational protein modifications could also be examined. Future models with the developments just noted, would enable us to drill down into the fundamental differences between cancer cells and normal cells. As an exemplar, using the p53-Mdm2 pathway we would be able to model the effects of different therapeutic approaches, including the temporal and spatial distributions of targeted disruption of p53 or Mdm2 interactions by non-genotoxic mechanisms.

Finally, one could consider extending the Hes1 GRN in some detail using the spatial stochastic models in various ways. In particular, one could investigate nuclear transport in more detail and begin to account for the ran-cycle. Many transcription factors are known to be actively transported towards the nucleus along microtubules and this aspect of intracellular molecular transport should be investigated in more detail

(Lomakin and Nadezhdina 2010). One should also conduct a global sensitivity analysis of the model using data clustering techniques. One may also consider cell-cell communication in future work to see if this acts to stabilise and synchronise oscillatory behaviour as Masamizu et al. (2006) found. Naturally, our approach is readily applicable to many other pathways and future work should also investigate the intricacies of the p53-Mdm2 negative feedback loop in more detail and perhaps consider pathway cross-talk e.g. interactions with other gene regulatory networks such as the NF-κB pathway.

Appendix

Appendix A

The Non-Dimensional Hes1 System:

$$\begin{aligned}
\frac{\partial[M_n]}{\partial t} &= D_{M_n}\nabla^2[M_n] + \frac{\alpha_M}{1+(\frac{[P_n]}{\widehat{p}})^h} - \mu_M[M_n] \\
\frac{\partial[M_c]}{\partial t} &= D_{M_c}\nabla^2[M_c] - \mu_M[M_c] \\
\frac{\partial[P_c]}{\partial t} &= D_{P_c}\nabla^2[P_c] + \alpha_P[M_c] - \mu_P[P_c] \\
\frac{\partial[P_n]}{\partial t} &= D_{P_n}\nabla^2[P_n] - \mu_P[P_n]
\end{aligned} \tag{7.1}$$

Nondimensionalisation: Reference concentrations: $m0$, $p0$

Reference time: τ (the period of oscillation in the Hes1 system)

Reference length: L (0.4 times the length of a cell)

Normalising variables in terms of appropriate reference parameters:

$$\begin{aligned} [M_n] &= [\overline{M_n}]m_0 \ , \ [M_c] = [\overline{M_c}]m_0 \\ t &= \bar{t}\tau \ , \ x = L\overline{X} \ , \ y = L\overline{Y} \end{aligned} \tag{7.2}$$

Nondimensionalise the 5 equations using the scaling variables:

first equation:

$$\begin{aligned} \frac{\partial[M_n]}{\partial t} &= D_{M_n}\nabla^2[M_n] + \frac{\alpha_M}{1+(\frac{[P_n]}{\widehat{p}})^h} - \mu_M[M_n] \\ \frac{\partial[M_n]}{\partial t} &= \frac{\partial m_0.[\overline{M_n}]}{\partial t} = m_0\frac{[\overline{M_n}]}{\partial\bar{t}}\cdot\frac{\partial\bar{t}}{\partial t} = \frac{m_0}{\tau}\cdot\frac{\partial[\overline{M_n}]}{\partial\bar{t}} \end{aligned} \tag{7.3}$$

$$\begin{aligned} D_{M_n}\nabla^2[M_n] &= D_{\overline{M_n}\cdot m_0}\left(\frac{\partial^2 m_0\cdot[\overline{M_n}]}{\partial x^2} + \frac{\partial^2 m_0\cdot[\overline{M_n}]}{\partial y^2}\right) \\ &= D_{\overline{M_n}\cdot m_0}\left(\frac{\partial}{\partial x}\left(\frac{\partial m_0\cdot[\overline{M_n}]}{\partial x}\right) + \frac{\partial}{\partial y}\left(\frac{\partial m_0\cdot[\overline{M_n}]}{\partial y}\right)\right) \\ &= D_{\overline{M_n}\cdot m_0}\left(\left(\frac{\partial}{\partial\overline{X}}\cdot\frac{\partial\overline{X}}{\partial x}\right)\left(\frac{\partial m_0\cdot[\overline{M_n}]}{\partial\overline{X}}\cdot\frac{\partial\overline{X}}{\partial x}\right) + \left(\frac{\partial}{\partial\overline{Y}}\cdot\frac{\partial\overline{Y}}{\partial y}\right)\left(\frac{\partial m_0\cdot[\overline{M_n}]}{\partial\overline{Y}}\cdot\frac{\partial\overline{Y}}{\partial y}\right)\right) \\ &= D_{\overline{M_n}\cdot m_0}\left(\left(\frac{\partial}{\partial\overline{X}}\cdot\frac{1}{L}\right)\left(\frac{\partial m_0\cdot[\overline{M_n}]}{\partial\overline{X}}\cdot\frac{1}{L}\right) + \left(\frac{\partial}{\partial\overline{Y}}\cdot\frac{1}{L}\right)\left(\frac{\partial m_0\cdot[\overline{M_n}]}{\partial\overline{Y}}\cdot\frac{1}{L}\right)\right) \\ &= D_{\overline{M_n}\cdot m_0}\left(\frac{m_0}{L^2}\left(\frac{\partial^2[\overline{M_n}]}{\partial\overline{X}^2}\right) + \frac{m_0}{L^2}\left(\frac{\partial^2[\overline{M_n}]}{\partial\overline{Y}^2}\right)\right) \\ &= D_{\overline{M_n}\cdot m_0}\frac{m_0}{L^2}\cdot\left(\frac{\partial^2}{\partial\overline{X}^2} + \frac{\partial^2}{\partial\overline{Y}^2}\right)\cdot[\overline{M_n}] \\ &= \frac{m_0}{L^2}D_{\overline{M_n}\cdot m_0}\nabla^2[\overline{M_n}] \end{aligned} \tag{7.4}$$

$$(\frac{[P_n]}{\widehat{p}})^h = (\frac{p_0[\overline{P_n}]}{\widehat{p}})^h \ , \ [M_n] = [\overline{M_n}]m_0 \tag{7.5}$$

So the equation has the new form:

$$
\begin{aligned}
\frac{m_0}{\tau}\cdot\frac{\partial[\overline{M_n}]}{\partial\bar{t}} &= \frac{m_0}{L^2}D_{\overline{M_n}\cdot m_0}\nabla^2[\overline{M_n}]+\frac{\alpha_M}{1+(\frac{p_0[\overline{P_n}]}{\widehat{p}})^h}-\mu_{M\cdot}[\overline{M_n}] \\
\frac{\partial[\overline{M_n}]}{\partial\bar{t}} &= \frac{\tau}{L^2}D_{\overline{M_n}\cdot m_0}\nabla^2[\overline{M_n}]+\frac{\tau}{m_0}\frac{\alpha_M}{1+(\frac{p_0[\overline{P_n}]}{\widehat{p}})^h}-\frac{\tau\mu_{M\cdot}}{m_0}[\overline{M_n}]
\end{aligned}
\tag{7.6}
$$

Where

$$
\frac{\tau}{L^2}D_{\overline{M_n}\cdot m_0} = D^*_{\overline{M_n}}\ ,\ \frac{\tau\mu_{M\cdot}}{m_0}=\mu^*_M\ ,\ \frac{\tau\alpha_M}{m_0}=\alpha^*_M\ ,\ p^*=\frac{p_0}{\widehat{p}}
\tag{7.7}
$$

Also similarly:

$$
\begin{aligned}
D^*_{\overline{M_c}} &= \frac{\tau}{L^2}D_{\overline{M_c}\cdot m_0}\ ,\ D^*_{\overline{P_n}}=\frac{\tau}{L^2}D_{\overline{P_n}\cdot p_0}\ ,\ D^*_{\overline{P_c}}=\frac{\tau}{L^2}D_{\overline{P_c}\cdot p_0} \\
\mu^*_P &= \frac{\tau\mu_{P\cdot}}{p_0}\ ,\ \alpha^*_P=\frac{\tau\alpha_P}{p_0}
\end{aligned}
\tag{7.8}
$$

The following parameter values were used in our simulations of the non-dimensional Hes1 system:

$$
\begin{gathered}
D^*_{M_n}=D^*_{M_c}=D^*_{P_n}=D^*_{P_c}=7.5\times10^{-4} \\
\alpha^*_M=1\ ,\ \alpha^*_P=2\ ,\ h=5\ ,\ p^*=1\ ,\ \mu^*_M=\mu^*_P=0.03
\end{gathered}
\tag{7.9}
$$

$$
\begin{aligned}
\frac{\partial\left([\overline{M_n}]m_0\right)}{\partial\left(\bar{t}\tau\right)} &= \frac{D_{M_n}}{L^2}\nabla^2[\overline{M_n}]m_0+\frac{\alpha_M}{1+(\frac{[\overline{P_n}]p_0}{\widehat{p}})^h}-\mu_M[\overline{M_n}]m_0 \\
\frac{\partial\left([\overline{M_c}]m_0\right)}{\partial\left(\bar{t}\tau\right)} &= \frac{D_{M_c}}{L^2}\nabla^2[\overline{M_c}]m_0-\mu_M[\overline{M_c}]m_0 \\
\frac{\partial\left([\overline{P_c}]p_0\right)}{\partial\left(\bar{t}\tau\right)} &= \frac{D_{P_c}}{L^2}\nabla^2[\overline{P_c}]p_0+\alpha_P[M_c]-\mu_P[\overline{P_c}]p_0 \\
\frac{\partial\left([\overline{P_n}]p_0\right)}{\partial\left(\bar{t}\tau\right)} &= \frac{D_{P_n}}{L^2}\nabla^2[\overline{P_n}]p_0-\mu_P[\overline{P_n}]p_0
\end{aligned}
\tag{7.10}
$$

$$
\begin{aligned}
\frac{\partial[\overline{M_n}]}{\partial\bar{t}} &= \left(\frac{\tau D_{M_n}}{L^2}\right)\nabla^2[\overline{M_n}] + \frac{\left(\frac{\tau\alpha_M}{m_0}\right)}{1+(\frac{[\overline{P_n}]p_0}{\widehat{p}})^h} - (\tau\mu_M)\,[\overline{M_n}] \\
\frac{\partial[\overline{M_c}]}{\partial\bar{t}} &= \left(\frac{\tau D_{M_c}}{L^2}\right)\nabla^2[\overline{M_c}] - (\tau\mu_M)\,[\overline{M_c}] \\
\frac{\partial[\overline{P_c}]}{\partial\bar{t}} &= \left(\frac{\tau D_{P_c}}{L^2}\right)\nabla^2[\overline{P_c}] + \left(\frac{\tau m_0\alpha_P}{p_0}\right)[M_c] - (\tau\mu_P)\,[\overline{P_c}] \\
\frac{\partial[\overline{P_n}]}{\partial\bar{t}} &= \left(\frac{\tau D_{P_n}}{L^2}\right)\nabla^2[\overline{P_n}] - (\tau\mu_P)\,[\overline{P_n}]
\end{aligned}
\tag{7.11}
$$

$$
\begin{aligned}
\frac{\partial[\overline{M_n}]}{\partial\bar{t}} &= D^*_{M_n}\nabla^2[\overline{M_n}] + \frac{\alpha^*_M}{1+(p^*[\overline{P_n}])^h} - \mu^*_M[\overline{M_n}] \\
\frac{\partial[\overline{M_c}]}{\partial\bar{t}} &= D^*_{M_c}\nabla^2[\overline{M_c}] - \mu^*_M[\overline{M_c}] \\
\frac{\partial[\overline{P_c}]}{\partial\bar{t}} &= D^*_{P_c}\nabla^2[\overline{P_c}] + \alpha^*_P[M_c] - \mu^*_P[\overline{P_c}] \\
\frac{\partial[\overline{P_n}]}{\partial\bar{t}} &= D^*_{P_n}\nabla^2[\overline{P_n}] - \mu^*_P[\overline{P_n}]
\end{aligned}
\tag{7.12}
$$

Where

$$
\begin{aligned}
D^*_{M_n} &= \frac{\tau D_{M_n}}{L^2}\ ,\ D^*_{M_c} = \frac{\tau D_{M_c}}{L^2}\ ,\ D^*_{P_n} = \frac{\tau D_{P_n}}{L^2}\ ,\ D^*_{P_c} = \frac{\tau D_{P_c}}{L^2} \\
\alpha^*_M &= \frac{\tau\alpha_M}{[m_0]}\ ,\ \alpha^*_P = \frac{\tau[m_0]\alpha_P}{[p_0]} \\
\mu^*_M &= \tau\mu_M\ ,\ \mu^*_P = \tau\mu_P\ ,\ p^* = \frac{p_0}{\widehat{p}}
\end{aligned}
\tag{7.13}
$$

As a first approximation we assume all diffusion coefficients are equal.

Calculating the effective diffusion coefficient, D:

$$\begin{aligned} L &= 10\mu m \\ &= 10 \times 10^{-6} m \\ &= 10 \times 10^{-4} cm \end{aligned} \tag{7.14}$$

$$\begin{aligned} 200\tau &= 2hrs \\ \tau &= \frac{7200s}{200} = 36s \end{aligned} \tag{7.15}$$

$$\begin{aligned} D^* &= \frac{\tau D}{L^2} \\ D = \frac{L^2 D^*}{\tau} & \\ &= \frac{10 \times 10 \times \left(10^{-6}\right)^2 m^2 \times D^*}{\tau} \\ &= \frac{10 \times 10 \times \left(10^{-4}\right)^2 cm^2 \times D^*}{\tau} \\ &= \frac{100 \times 10^{-8} cm^2 \times D^*}{\tau} \\ &= \frac{1 \times 10^{-6} cm^2 \times 7.5 \times 10^{-4}}{36s} \\ &= 2.0833333333 \times 10^{-11} cm^2 s^{-1} \end{aligned} \tag{7.16}$$

Calculating the transcription rate α_M.

$$\begin{aligned}
m_0 &= 0.05\mu m \\
\tau &= 36s \\
\alpha_M^* &= \frac{\tau\alpha_M}{m_0} \\
\alpha_M &= \frac{m_0\alpha_M^*}{\tau} \\
&= \frac{0.05\times 10^{-6}M\times 1}{36s} \\
&= 1.388888889\times 10^{-9}ms^{-1} \qquad (7.17)
\end{aligned}$$

Calculating the repression threshold, $\widehat{p}$:

$$\begin{aligned}
p^* &= \frac{p_0}{\widehat{p}} \\
\widehat{p} &= \frac{p_0}{p^*} \\
&= \frac{1\times 10^{-6}m}{1} \\
&= 1\times 10^{-6}m \qquad (7.18)
\end{aligned}$$

Calculating the degradation rate of hes1 mRNA, μ_M:

$$\tau = 36s$$

$$\begin{aligned}
\mu_M^* &= \tau\mu_M \\
\mu_M &= \frac{\mu_M^*}{\tau} \\
&= \frac{0.03}{36s} \\
&= 8.3333333\times 10^{-4}s^{-1} \qquad (7.19)
\end{aligned}$$

Calculating the translation rate, α_P:

$$\begin{aligned} m_0 &= 0.05\mu m \\ p_0 &= 1\mu m \\ \tau &= 36s \\ \alpha_P^* &= \frac{\tau[m_0]\alpha_P}{[p_0]} \\ \alpha_P &= \frac{\alpha_P^*[p_0]}{\tau[m_0]} \\ &= \frac{2 \times 1 \times 10^{-6} m}{0.05 \times 10^{-6} m \times 36s} \\ &= 1.11111111111 s^{-1} \end{aligned} \tag{7.20}$$

Calculating the degradation rate of Hes1 protein, μ_P:

$$\tau = 36s$$

$$\begin{aligned} \mu_P^* &= \tau\mu_P \\ \mu_P &= \frac{\mu_P^*}{\tau} \\ &= \frac{0.03}{36s} \\ &= 8.3333333 \times 10^{-4} s^{-1} \end{aligned} \tag{7.21}$$

Appendix B

Functional Dependence of the Parameters μ_3 and μ_4 on Stat3 Concentration

In this section we provide details of how we modified the parameters μ_3 and μ_4 to have them explicitly depend on the concentration of Stat3. This was done to match the model extension of Momiji and Monk (2008) where the two parameters μ_3 and μ_4

were oscillatory values over time.

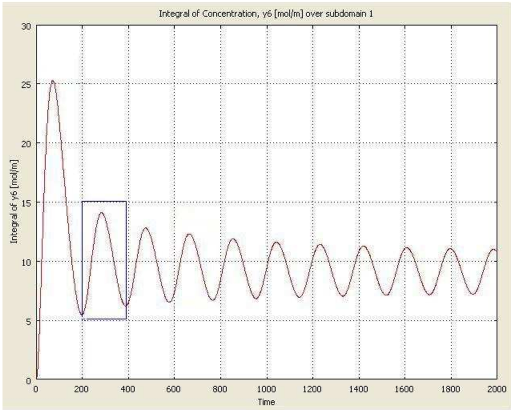

Figure 7.1: *Plot of the total concentration of Stat3 showing the maximum and minimum values which are used to modify the parameters μ_3 and μ_4.*

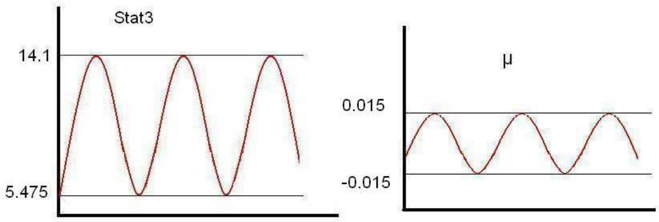

Figure 7.2: *Plot of the Stat3 concentration use to map to the parameters μ_3 and μ_4*

We made the parameters μ_3 and μ_4 functions of Stat3 concentration (i.e. to ensure both parameters varied over time in an oscillatory manner as per Stat3 concentration, but to also ensure they remained positive) via a simple mapping as follows:

$$
\begin{aligned}
[5.475, 14.1] &\longrightarrow [-0.015, 0.015] \\
\mu &= a + b * Stat3 \\
0.015 &= a + b * 14.1 \\
-0.015 &= a + b * 5.475 \\
0.03 &= 8.625 * b \\
b &= 0.00348 \\
a &= -0.034
\end{aligned} \tag{7.22}
$$

So

$$
\begin{aligned}
\mu &= a + b * y_{6c} \\
&= -0.034 + 0.00348 * y_{6c} \\
\mu &= 0.03 - 0.034 + 0.00348 * y_{6c} \\
&= -0.004 + 0.00348 * y_{6c}
\end{aligned} \tag{7.23}
$$

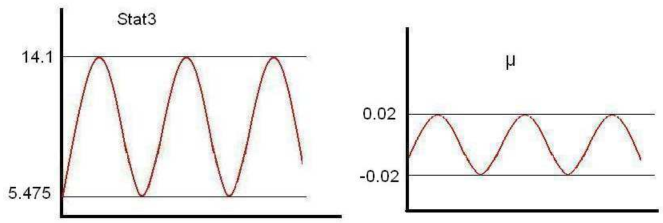

Figure 7.3: *Plot of the Stat3 concentration use to map to the parameters μ_3 and μ_4*

Once again we made the parameters μ_3 and μ_4 functions of Stat3 concentration (i.e. to ensure both parameters varied over time in an oscillatory manner as per Stat3 concentration, but to also ensure they remained positive) via a simple mapping as follows:

$$
\begin{aligned}
[5.475, 14.1] &\longrightarrow [-0.02, 0.02] \\
\mu &= a + b * Stat3 \\
0.02 &= a + b * 14.1 \\
-0.02 &= a + b * 5.475 \\
0.04 &= 8.625 * b \\
b &= 0.00463 \\
a &= -0.045
\end{aligned}
\tag{7.24}
$$

So

$$
\begin{aligned}
\mu &= a + b * y_{6c} \\
&= -0.045 + 0.00463 * y_{6c} \\
\mu &= 0.03 - 0.045 + 0.00463 * y_{6c} \\
&= -0.015 + 0.00463 * y_{6c}
\end{aligned}
\tag{7.25}
$$

Appendix C

The Non-Dimensional Hes1 System Extended model:

$$
\begin{aligned}
\frac{\partial[y_{1n}]}{\partial t} &= D_{y_{1n}}\nabla^2[y_{1n}] - \mu_1[y_{1n}] + k_1\left[\frac{1}{(1+[y_{4n}])^n}\right] \\
\frac{\partial[y_{1c}]}{\partial t} &= D_{y_{1c}}\nabla^2[y_{1c}] - \mu_1[y_{1c}] \\
\frac{\partial[y_{3c}]}{\partial t} &= D_{y_{3c}}\nabla^2[y_{3c}] - \mu_3[y_{3c}] + k_3[y_{1c}] - 2k_4[y_{3c}]^2 \\
\frac{\partial[y_{4c}]}{\partial t} &= D_{y_{4c}}\nabla^2[y_{4c}] - \mu_4[y_{4c}] + k_4[y_{3c}]^2 \\
\frac{\partial[y_{4n}]}{\partial t} &= D_{y_{4n}}\nabla^2[y_{4n}] - \mu_4[y_{4n}]
\end{aligned}
\tag{7.26}
$$

scaling variables:

$$
\begin{aligned}
y_{1n}^* &= \frac{y_{1n}}{y_0}\ ,\ y_{1c}^* = \frac{y_{1c}}{y_0}\ ,\ y_{3c}^* = \frac{y_{3c}}{y_0}\ ,\ y_{4n}^* = \frac{y_{4n}}{y_0}\ ,\ y_{4c}^* = \frac{y_{4c}}{y_0} \\
t^* &= \frac{t}{\tau}\ ,\ X^* = \frac{x}{L}\ ,\ Y^* = \frac{y}{L}
\end{aligned}
\tag{7.27}
$$

So:

$$
\begin{aligned}
\frac{\partial y_{1n}}{\partial t} &= D_{y_{1n}}\nabla^2 y_{1n} - \mu_1 y_{1n} + k_1[\frac{1}{1+y_{4n}}] \\
\frac{\partial y_{1n}}{\partial t} &= \frac{\partial y_0 . y_{1n}^*}{\partial t} = y_0\frac{\partial y_{1n}^*}{\partial t^*}\cdot\frac{\partial t^*}{\partial t} = \frac{y_0}{\tau}\cdot\frac{\partial y_{1n}^*}{\partial t^*} \\
D_{y_{1n}}\nabla^2 y_{1n} &= D_{y_{1n}^*\cdot y_0}\left(\frac{\partial^2 y_0\cdot y_{1n}^*}{\partial x^2} + \frac{\partial^2 y_0\cdot y_{1n}^*}{\partial y^2}\right) \\
&= D\left(\frac{\partial}{\partial x}\left(\frac{\partial y_0\cdot y_{1n}^*}{\partial x}\right) + \frac{\partial}{\partial y}\left(\frac{\partial y_0\cdot y_{1n}^*}{\partial y}\right)\right) \\
&= D_{y_{1n}^*\cdot y_0}\left(\left(\frac{\partial}{\partial X^*}\cdot\frac{\partial X^*}{\partial x}\right)\left(\frac{\partial y_0\cdot y_{1n}^*}{\partial X^*}\cdot\frac{\partial X^*}{\partial x}\right) + \left(\frac{\partial}{\partial Y^*}\cdot\frac{\partial Y^*}{\partial y}\right)\left(\frac{\partial y_0\cdot y_{1n}^*}{\partial Y^*}\cdot\frac{\partial Y^*}{\partial y}\right)\right) \\
&= D_{y_{1n}^*\cdot y_0}\left(\left(\frac{\partial}{\partial X^*}\cdot\frac{1}{L}\right)\left(\frac{\partial y_0\cdot y_{1n}^*}{\partial x^*}\cdot\frac{1}{L}\right) + \left(\frac{\partial}{\partial Y^*}\cdot\frac{1}{L}\right)\left(\frac{\partial y_0\cdot y_{1n}^*}{\partial Y^*}\cdot\frac{1}{L}\right)\right) \\
&= D\left(\frac{y_0}{L^2}\left(\frac{\partial^2 y_{1n}^*}{\partial X^{*2}}\right) + \frac{y_0}{L^2}\left(\frac{\partial^2 y_{1n}^*}{\partial Y^{*2}}\right)\right) \\
&= D\frac{y_0}{L^2}\cdot\left(\frac{\partial^2}{\partial X^{*2}} + \frac{\partial^2}{\partial Y^{*2}}\right)\cdot y_{1n}^* \\
&= \frac{y_0}{L^2} D_{y_{1n}^*\cdot y_0}\nabla^2 y_{1n}^* \qquad (7.28)
\end{aligned}
$$

$$
\begin{aligned}
\frac{y_0}{\tau}\cdot\frac{\partial y_{1n}^*}{\partial t^*} &= \frac{y_0}{L^2} D_{y_{1n}^*\cdot y_0}\nabla^2 y_{1n}^* - \mu_1 . y_{1n}^* + k_1\left(\frac{1}{1+\alpha y_0\cdot y_{4n}^*}\right) \\
\frac{\partial y_{1n}^*}{\partial t^*} &= \frac{\tau}{L^2} D_{y_{1n}^*\cdot y_0}\nabla^2 y_{1n}^* - \frac{\tau\mu_1 .}{y_0} y_{1n}^* + \frac{\tau k_1}{y_0}\left(\frac{1}{1+\alpha y_0\cdot y_{4n}^*}\right) \\
\frac{\partial y_{1n}^*}{\partial t^*} &= D_{y_{1n}}^*\nabla^2 y_{1n}^* - \mu_1^* y_{1n}^* + k_1^*\left(\frac{1}{1+\alpha^* y_{4n}^*}\right) \qquad (7.29)
\end{aligned}
$$

$$
\begin{aligned}
\frac{y_0}{\tau}\frac{\partial y^*_{1n}}{\partial t^*} &= \frac{y_0}{L^2} D_{y^*_{1n} \cdot y_0} \nabla^2 y^*_{1n} - y_0 \mu_1 y^*_{1n} + k_1 \left(\frac{1}{1 + y_0 \alpha y^*_{4n}} \right) \\
\frac{y_0}{\tau}\frac{\partial y^*_{1c}}{\partial t^*} &= \frac{y_0}{L^2} D_{y^*_{1c} \cdot y_0} \nabla^2 y^*_{1c} - y_0 \mu_1 y^*_{1c} \\
\frac{y_0}{\tau}\frac{\partial y^*_{3c}}{\partial t^*} &= \frac{y_0}{L^2} D_{y^*_{3c} \cdot y_0} \nabla^2 y^*_{3c} - \mu_3 y^*_{3c} + k_3 y^*_{1c} - 2 k_4 y^{*2}_{3c} \\
\frac{y_0}{\tau}\frac{\partial y^*_{4c}}{\partial t^*} &= \frac{y_0}{L^2} D_{y^*_{4c} \cdot y_0} \nabla^2 y^*_{4c} - y_0 \mu_4 y^*_{4c} + y_0^2 k_4 y^{*2}_{3c} \\
\frac{y_0}{\tau}\frac{\partial y^*_{4n}}{\partial t^*} &= \frac{y_0}{L^2} D_{y^*_{4n} \cdot y_0} \nabla^2 y^*_{4n} - y_0 \mu_4 y^*_{4n} \qquad (7.30)
\end{aligned}
$$

$$
\begin{aligned}
\frac{\partial y^*_{1n}}{\partial t^*} &= \frac{\tau}{L^2} D_{y^*_{1n} \cdot y_0} \nabla^2 y^*_{1n} - \tau \mu_1 y^*_{1n} + \frac{\tau k_1}{y_0} \left(\frac{1}{1 + y_0 \alpha y^*_{4n}} \right) \\
\frac{\partial y^*_{1c}}{\partial t^*} &= \frac{\tau}{L^2} D_{y^*_{1c} \cdot y_0} \nabla^2 y^*_{1c} - \tau \mu_1 y^*_{1c} \\
\frac{\partial y^*_{3c}}{\partial t^*} &= \frac{\tau}{L^2} D_{y^*_{3c} \cdot y_0} \nabla^2 y^*_{3c} - \tau \mu_3 y^*_{3c} + \tau k_3 y^*_{1c} - 2 \tau y_0 k_4 y^{*2}_{3c} \\
\frac{\partial y^*_{4c}}{\partial t^*} &= \frac{\tau}{L^2} D_{y^*_{4c} \cdot y_0} \nabla^2 y^*_{4c} - \tau \mu_4 y^*_{4c} + \tau y_0 k_4 y^{*2}_{3c} \\
\frac{\partial y^*_{4n}}{\partial t^*} &= \frac{\tau}{L^2} D_{y^*_{4n} \cdot y_0} \nabla^2 y^*_{4n} - \tau \mu_4 y^*_{4n} \qquad (7.31)
\end{aligned}
$$

$$
\begin{aligned}
\frac{\partial y^*_{1n}}{\partial t^*} &= D^*_{y_{1n}} \nabla^2 y^*_{1n} - \mu^*_1 y^*_{1n} + k^*_1 \left(\frac{1}{1 + \alpha^* y^*_{4n}} \right) \\
\frac{\partial y^*_{1c}}{\partial t^*} &= D^*_{y_{1c}} \nabla^2 y^*_{1c} - \mu^*_1 y^*_{1c} \\
\frac{\partial y^*_{3c}}{\partial t^*} &= D^*_{y_{3c}} \nabla^2 y^*_{3c} - \mu^*_3 y^*_{3c} + k^*_3 y^*_{1c} - 2 k^*_4 y^{*2}_{3c} \\
\frac{\partial y^*_{4c}}{\partial t^*} &= D^*_{y_{4c}} \nabla^2 y^*_{4c} - \mu^*_4 y^*_{4c} + k^*_4 y^{*2}_{3c} \\
\frac{\partial y^*_{4n}}{\partial t^*} &= D^*_{y_{4n}} \nabla^2 y^*_{4n} - \mu^*_4 y^*_{4n} \qquad (7.32)
\end{aligned}
$$

Where,

$$
\begin{aligned}
\frac{\tau}{L^2} D_{y^*_{1n}} \cdot y_0 &= D^*_{y_{1n}} \, , \; \frac{\tau}{L^2} D_{y^*_{1c}} \cdot y_0 = D^*_{y_{1c}} \, , \; \frac{\tau}{L^2} D_{y^*_{3c}} \cdot y_0 = D^*_{y_{3c}} \\
\frac{\tau}{L^2} D_{y^*_{4n}} \cdot y_0 &= D^*_{y_{4n}} \, , \; \frac{\tau}{L^2} D_{y^*_{4c}} \cdot y_0 = D^*_{y_{4c}} \, , \; \alpha y_0 = \alpha^* \\
\tau \mu_1 &= \mu_1^* \, , \; \tau \mu_3 = \mu_3^* \, , \; \tau \mu_4 = \mu_4^* \\
\frac{\tau k_1}{y_0} &= k_1^* \, , \; \tau k_3 = k_3^* \, , \; \tau y_0 k_4 = k_4^* \qquad (7.33)
\end{aligned}
$$

The following parameter values were used in our simulations of the non-dimensional Hes1 system:

$$
\begin{aligned}
D^*_{y_{1n}} &= D^*_{y_{1c}} = D^*_{y_{3c}} = D^*_{y_{4n}} = D^*_{y_{4c}} = 7.5 \times 10^{-4} \\
\mu_1^* &= \mu_3^* = \mu_4^* = 0.03 \\
k_1^* &= k_3^* = k_4^* = 5 \\
\alpha^* &= 1 \, , \; n^* = 5 \qquad (7.34)
\end{aligned}
$$

As a first approximation we assume all diffusion coefficients are equal.

Calculating the effective diffusion coefficient, D:

$$
\begin{aligned}
L &= 10 \mu m \\
&= 10 \times 10^{-6} m \\
&= 10 \times 10^{-4} cm \qquad (7.35)
\end{aligned}
$$

$$
\begin{aligned}
225 \tau &= 2 hrs \\
\tau &= \frac{7200 s}{225} = 32 s \qquad (7.36)
\end{aligned}
$$

$$
\begin{aligned}
D^* &= \frac{\tau D}{L^2} \\
D = \frac{L^2 D^*}{\tau} & \\
&= \frac{10 \times 10 \times \left(10^{-6}\right)^2 m^2 \times D^*}{\tau} \\
&= \frac{10 \times 10 \times \left(10^{-4}\right)^2 cm^2 \times D^*}{\tau} \\
&= \frac{100 \times 10^{-8} cm^2 \times D^*}{\tau} \\
&= \frac{1 \times 10^{-6} cm^2 \times 7.5 \times 10^{-4}}{32s} \\
&= 2.34375 \times 10^{-11} cm^2 s^{-1} \qquad (7.37)
\end{aligned}
$$

Calculating the degradation rates, μ_1,μ_3 and μ_4

$$
\begin{aligned}
\mu_1 &= \mu_3 = \mu_4 \\
\tau &= 32s \\
\mu^* &= \tau\mu \\
\mu &= \frac{\mu^*}{\tau} \\
&= \frac{0.03}{32s} \\
&= 9.4 \times 10^{-4} s^{-1} \qquad (7.38)
\end{aligned}
$$

Calculating the production rates, k_1,k_3 and k_4

$$\begin{aligned}
\frac{\tau k_1}{y_0} &= k_1^* \, , \; \tau k_3 = k_3^* \, , \; \tau y_0 k_4 = k_4^* \\
k_1 &= \frac{y_0 k_1^*}{\tau} \, , \; k_3 = \frac{k_3^*}{\tau} \, , \; k_4 = \frac{k_4^*}{\tau y_0} \\
y_0 &= 1m\mu \\
k_1 &= \frac{y_0 k_1^*}{\tau} \\
&= \frac{1 \times 5}{32s^{-1}} \\
&= 1.56 \times 10^{-1} s^{-1} \\
k_3 &= \frac{k_3^*}{\tau} \\
&= \frac{1 \times 5}{32s^{-1}} \\
&= 1.56 \times 10^{-1} s^{-1} \\
k_4 &= \frac{k_4^*}{\tau y_0} \\
&= \frac{1 \times 5}{32s^{-1}} \\
&= 1.56 \times 10^{-1} s^{-1} \\
\alpha^* &= y_0 \alpha \\
\alpha &= \frac{\alpha^*}{y_0} \\
&= 1ms^{-1} \qquad (7.39)
\end{aligned}$$

Appendix D

The Non-Dimensional P53-Mdm2 System:

$$\frac{\partial[P_c]}{\partial t} = D_{P_c}\nabla^2[P_c]+\beta-(\mu+\nu(\frac{[M_c]^{h1}}{\widehat{M}^{h1}+[M_c]^{h1}}))[P_c] \tag{7.40}$$

$$\frac{\partial[P_n]}{\partial t} = D_{P_n}\nabla^2[P_n]-(\mu+\nu(\frac{[M_n]^{h1}}{\widehat{M}^{h1}+[M_n]^{h1}}))[P_n] \tag{7.41}$$

$$\frac{\partial[Mm_n]}{\partial t} = D_{Mm_n}\nabla^2[Mm_n]+\alpha+\eta(\frac{[P_n]^{h2}}{\widehat{P}^{h2}+[P_n]^{h2}})-\phi[Mm_n] \tag{7.42}$$

$$\frac{\partial[Mm_c]}{\partial t} = D_{Mm_c}\nabla^2[Mm_c]-\phi[Mm_c] \tag{7.43}$$

$$\frac{\partial[M_c]}{\partial t} = D_{M_c}\nabla^2[M_c]+\gamma[Mm_c]-\rho[M_c] \tag{7.44}$$

$$\frac{\partial[M_n]}{\partial t} = D_{M-n}\nabla^2[M_n]-\rho[M_n] \tag{7.45}$$

Where ,$[P_n]$, $[P_c]$, $[Mm_n]$,$[Mm_c]$, $[M_n]$ and $[M_c]$ are the concentration of the nuclear and the cytoplasmic P53, the nuclear and the cytoplasmic Mdm2 mRNA and the nuclear and the cytoplasmic Mdm2 protein respectively.$[D_i]$ denote the diffusion coefficients for each species.

We nondimensionalise equations with appropriate reference values as follows:

$$\begin{aligned}
[\overline{P_n}] &= \frac{[P_n]}{p_0}\ ,\ [\overline{P_c}] = \frac{[P_c]}{p_0}\ ,\ [\overline{Mm_n}] = \frac{[Mm_n]}{mm_0}\ ,\ [\overline{Mm_c}] = \frac{[Mm_c]}{mm_0} \\
\overline{M_n}] &= \frac{[M_n]}{m_0}\ ,\ [\overline{M_c}] = \frac{[M_c]}{m_0} \\
\bar{t} &= \frac{t}{\tau}\ ,\ \overline{X} = \frac{x}{L}\ ,\ \overline{Y} = \frac{y}{L}
\end{aligned} \tag{7.46}$$

Where $[p_0]$, $[mm_0]$ and $m_0]$ are reference concentration, τ is reference time, and L is a reference length ($10\mu m$as with Hes1 system).

$$\begin{aligned}
\frac{\partial\left[P_c\right]}{\partial t} &= p_0\frac{\partial\left[\overline{P}_c\right]}{\partial t^*}\cdot\frac{\partial t^*}{\partial t} = \frac{p_0}{\tau}\cdot\frac{\partial\left[\overline{P}_c\right]}{\partial t^*} \\
D_{P_n}\nabla^2 P_n &= D_{\overline{P}_n\cdot p_0}\left(\frac{\partial^2 p_0\cdot\overline{P}_n}{\partial x^2}+\frac{\partial^2 p_0\cdot\overline{P}_n}{\partial y^2}\right) \\
&= D_{\overline{P}_n\cdot p_0}\left(\frac{\partial}{\partial x}\left(\frac{\partial p_0\cdot\left[\overline{P}_n\right]}{\partial x}\right)+\frac{\partial}{\partial y}\left(\frac{\partial p_0\cdot\left[\overline{P}_n\right]}{\partial y}\right)\right) \\
&= D_{\overline{P}_n\cdot p_0}\left(\left(\frac{\partial}{\partial\overline{X}}\cdot\frac{\partial\overline{X}}{\partial x}\right)\left(\frac{\partial p_0\cdot\left[\overline{P}_n\right]}{\partial\overline{X}}\cdot\frac{\partial\overline{X}}{\partial x}\right)+\left(\frac{\partial}{\partial\overline{Y}}\cdot\frac{\partial\overline{Y}}{\partial y}\right)\left(\frac{\partial p_0\cdot\left[\overline{P}_n\right]}{\partial\overline{Y}}\cdot\frac{\partial\overline{Y}}{\partial y}\right)\right) \\
&= D_{\overline{P}_n\cdot p_0}\left(\left(\frac{\partial}{\partial\overline{X}}\cdot\frac{1}{L}\right)\left(\frac{\partial p_0\cdot\left[\overline{P}_n\right]}{\partial\overline{X}}\cdot\frac{1}{L}\right)+\left(\frac{\partial}{\partial\overline{Y}}\cdot\frac{1}{L}\right)\left(\frac{\partial p_0\cdot\left[\overline{P}_n\right]}{\partial\overline{Y}}\cdot\frac{1}{L}\right)\right) \\
&= D_{\overline{P}_n\cdot p_0}\left(\frac{p_0}{L^2}\left(\frac{\partial^2\left[\overline{P}_n\right]}{\partial\overline{X}^2}\right)+\frac{p_0}{L^2}\left(\frac{\partial^2\left[\overline{P}_n\right]}{\partial\overline{Y}^2}\right)\right) \\
&= D_{\overline{P}_n\cdot p_0}\frac{p_0}{L^2}\cdot\left(\frac{\partial^2}{\partial\overline{X}^2}+\frac{\partial^2}{\partial\overline{Y}^2}\right)\cdot\overline{P}_n \\
&= \frac{p_0}{L^2}D_{\overline{P}_n\cdot p_0}\nabla^2\overline{P}_n
\end{aligned} \tag{7.47}$$

As well:

$$\begin{aligned}
\frac{\partial\left[P_c\right]}{\partial t} &= \frac{p_0}{\tau}\cdot\frac{\partial\left[\overline{P}_c\right]}{\partial t^*},\frac{\partial\left[P_n\right]}{\partial t} = \frac{p_0}{\tau}\cdot\frac{\partial\left[\overline{P}_n\right]}{\partial t^*} \\
\frac{\partial\left[Mm_c\right]}{\partial t} &= \frac{mm_0}{\tau}\cdot\frac{\partial\left[\overline{Mm}_c\right]}{\partial t^*},\frac{\partial\left[Mm_n\right]}{\partial t} = \frac{mm_0}{\tau}\cdot\frac{\partial\left[\overline{Mm}_n\right]}{\partial t^*} \\
\frac{\partial\left[M_c\right]}{\partial t} &= \frac{m_0}{\tau}\cdot\frac{\partial\left[\overline{M}_c\right]}{\partial t^*},\frac{\partial\left[M_n\right]}{\partial t} = \frac{m_0}{\tau}\cdot\frac{\partial\left[\overline{M}_n\right]}{\partial t^*}
\end{aligned} \tag{7.48}$$

1

$$
\begin{aligned}
\frac{\partial[P_c]}{\partial t} &= D_{P_c}\nabla^2[P_c]+\beta-(\mu+\nu(\frac{[M_c]^{h1}}{\widehat{M}^{h1}+[M_c]^{h1}}))[P_c] \\
\frac{p_0}{\tau}\cdot\frac{\partial\left[\overline{P}_c\right]}{\partial t^*} &= \frac{p_0}{L^2}D_{\overline{P}_c\cdot p_0}\nabla^2\overline{P}_c+\beta-(\mu+\nu(\frac{([\overline{M}_c]m_0)^{h1}}{\widehat{M}^{h1}+([\overline{M}_c]m_0)^{h1}}))([\overline{P_c}]p_0) \\
\frac{\partial\left[\overline{P}_c\right]}{\partial t^*} &= \frac{\tau}{L^2}D_{\overline{P}_n\cdot p_0}\nabla^2\overline{P}_c+\frac{\tau}{p_0}\beta-(\tau\mu+(\tau\nu)(\frac{([\overline{M}_c]m_0)^{h1}}{\widehat{M}^{h1}+([\overline{M}_c]m_0)^{h1}}))([\overline{P_c}]) \\
\frac{\partial\left[\overline{P}_c\right]}{\partial t^*} &= \frac{\tau}{L^2}D_{\overline{P}_n\cdot p_0}\nabla^2\overline{P}_c+\frac{\tau}{p_0}\beta-(\tau\mu+(\tau\nu)(\frac{[\overline{M}_c]^{h1}}{\left(\frac{\widehat{M}}{m_0}\right)^{h1}+[\overline{M}_c]^{h1}}))([\overline{P_c}]) \\
\frac{\partial\left[\overline{P}_c\right]}{\partial t^*} &= D^*_{\overline{P}_n\cdot}\nabla^2\overline{P}_c+\beta^*-(\mu^*+\nu^*(\frac{[\overline{M}_c]^{h1}}{M^{*h1}+[\overline{M}_c]^{h1}}))([\overline{P_c}]) \qquad (7.49)
\end{aligned}
$$

2

$$
\begin{aligned}
\frac{\partial[P_n]}{\partial t} &= D_{P_n}\nabla^2[P_n]-(\mu+\nu(\frac{[M_n]^{h1}}{\widehat{M}^{h1}+[M_n]^{h1}}))[P_n] \\
\frac{p_0}{\tau}\cdot\frac{\partial\left[\overline{P}_n\right]}{\partial t^*} &= \frac{p_0}{L^2}D_{\overline{P}_n\cdot p_0}\nabla^2\overline{P}_n-(\mu+\nu(\frac{([\overline{M}_c]m_0)^{h1}}{\widehat{M}^{h1}+([\overline{M}_c]m_0)^{h1}}))([\overline{P_n}]p_0) \\
\frac{\partial\left[\overline{P}_n\right]}{\partial t^*} &= \frac{\tau}{L^2}D_{\overline{P}_n\cdot p_0}\nabla^2\overline{P}_n-(\tau\mu+(\tau\nu)(\frac{([\overline{M}_c]m_0)^{h1}}{\widehat{M}^{h1}+([\overline{M}_c]m_0)^{h1}}))([\overline{P_n}]) \\
\frac{\partial\left[\overline{P}_n\right]}{\partial t^*} &= \frac{\tau}{L^2}D_{\overline{P}_n\cdot p_0}\nabla^2\overline{P}_n-(\tau\mu+(\tau\nu)(\frac{[\overline{M}_c]^{h1}}{\left(\frac{\widehat{M}}{m_0}\right)^{h1}+[\overline{M}_c]^{h1}}))([\overline{P_n}]) \\
\frac{\partial\left[\overline{P}_n\right]}{\partial t^*} &= D^*_{\overline{P}_n\cdot}\nabla^2\overline{P}_n-(\mu^*+\nu^*(\frac{[\overline{M}_c]^{h1}}{M^{*h1}+[\overline{M}_c]^{h1}}))([\overline{P_n}]) \qquad (7.50)
\end{aligned}
$$

3

$$
\begin{aligned}
\frac{\partial[Mm_n]}{\partial t} &= D_{Mm_n}\nabla^2[Mm_n]+\alpha+\eta\left(\frac{[P_n]^{h2}}{\widehat{P}^{h2}+[P_n]^{h2}}\right)-\phi[Mm_n] \\
\frac{mm_0}{\tau}\cdot\frac{\partial\left[\overline{Mm_n}\right]}{\partial t^*} &= \frac{mm_0}{L^2}D_{\overline{Mm_n}\cdot mm_0}\nabla^2\left[\overline{Mm_n}\right]+\alpha+\eta\left(\frac{(p_0\overline{[P_n]})^{h2}}{\widehat{P}^{h2}+(p_0\overline{[P_n]})^{h2}}\right)-\phi([\overline{Mm_n}]mm_0) \\
\frac{mm_0}{\tau}\cdot\frac{\partial\left[\overline{Mm_n}\right]}{\partial t^*} &= \frac{\tau}{L^2}D_{\overline{Mm_n}\cdot mm_0}\nabla^2\left[\overline{Mm_n}\right]+\frac{\tau}{mm_0}\alpha+\frac{\tau}{mm_0}\eta\left(\frac{(p_0\overline{[P_n]})^{h2}}{\widehat{P}^{h2}+(p_0\overline{[P_n]})^{h2}}\right)-\tau\phi[\overline{Mm_n}] \\
\frac{\partial\left[\overline{Mm_n}\right]}{\partial t^*} &= \frac{\tau}{L^2}D_{\overline{Mm_n}\cdot mm_0}\nabla^2\left[\overline{Mm_n}\right]+\frac{\tau}{mm_0}\alpha+\frac{\tau}{mm_0}\eta\left(\frac{\overline{[P_n]}^{h2}}{\left(\frac{\widehat{P}}{p_0}\right)^{h2}+\overline{[P_n]}^{h2}}\right)-\tau\phi[\overline{Mm_n}] \\
\frac{\partial\left[\overline{Mm_n}\right]}{\partial t^*} &= D^*_{\overline{Mm_n}\cdot}\nabla^2\left[\overline{Mm_n}\right]+\alpha^*+\eta*\left(\frac{\overline{[P_n]}^{h2}}{p^{*h2}+\overline{[P_n]}^{h2}}\right)-\tau\phi[\overline{Mm_n}] \qquad (7.51)
\end{aligned}
$$

4

$$
\begin{aligned}
\frac{\partial[Mm_c]}{\partial t} &= D_{Mm_c}\nabla^2[Mm_c]-\phi[Mm_c] \\
\frac{mm_0}{\tau}\cdot\frac{\partial\left[\overline{Mm_c}\right]}{\partial t^*} &= \frac{mm_0}{L^2}D_{\overline{Mm_c}\cdot mm_0}\nabla^2\left[\overline{Mm_c}\right]-\phi\left(\left[\overline{Mm_c}\right]mm_0\right) \\
\frac{\partial\left[\overline{Mm_c}\right]}{\partial t^*} &= \frac{\tau}{L^2}D_{\overline{Mm_c}\cdot mm_0}\nabla^2\left[\overline{Mm_c}\right]-\tau\phi\left[\overline{Mm_c}\right] \\
\frac{\partial\left[\overline{Mm_c}\right]}{\partial t^*} &= D^*_{\overline{Mm_c}\cdot}\nabla^2\left[\overline{Mm_c}\right]-\phi^*\left[\overline{Mm_c}\right] \qquad (7.52)
\end{aligned}
$$

5

$$
\begin{aligned}
\frac{\partial[M_c]}{\partial t} &= D_{M_c}\nabla^2[M_c]+\gamma[Mm_c]-\rho[M_c] \\
\frac{m_0}{\tau}\cdot\frac{\partial\left[\overline{M}_c\right]}{\partial t^*} &= \frac{m_0}{L^2}D_{\overline{M}_c\cdot m_0}\nabla^2\left[\overline{M}_c\right]+\gamma([\overline{Mm_c}]mm_0)-\rho([\overline{M}_c]m_0) \\
\frac{\partial\left[\overline{M}_c\right]}{\partial t^*} &= \frac{\tau}{L^2}D_{\overline{M}_c\cdot m_0}\nabla^2\left[\overline{M}_c\right]+\frac{\tau}{m_0}\gamma([\overline{Mm_c}]mm_0)-\frac{\tau}{m_0}\rho([\overline{M}_c]m_0) \\
\frac{\partial\left[\overline{M}_c\right]}{\partial t^*} &= \frac{\tau}{L^2}D_{\overline{M}_c\cdot m_0}\nabla^2\left[\overline{M}_c\right]+\frac{\tau mm_0}{m_0}\gamma[\overline{Mm_c}]-\tau\rho[\overline{M}_c] \\
\frac{\partial\left[\overline{M}_c\right]}{\partial t^*} &= D^*_{\overline{M}_c\cdot}\nabla^2\left[\overline{M}_c\right]+\gamma^*[\overline{Mm_c}]-\rho^*[\overline{M}_c] \qquad (7.53)
\end{aligned}
$$

$$\begin{aligned}
\frac{\partial[M_n]}{\partial t} &= D_{M-n}\nabla^2[M_n]-\rho[M_n]\\
\frac{m_0}{\tau}\cdot\frac{\partial\left[\overline{M}_n\right]}{\partial t^*} &= \frac{m_0}{L^2}D_{\overline{M}_n\cdot m_0}\nabla^2\left[\overline{M}_n\right]-\rho([\overline{M}_n]m_0)\\
\frac{\partial\left[\overline{M}_n\right]}{\partial t^*} &= \frac{\tau}{L^2}D_{\overline{M}_n\cdot m_0}\nabla^2\left[\overline{M}_n\right]-\frac{\tau}{m_0}\rho([\overline{M}_n]m_0)\\
\frac{\partial\left[\overline{M}_n\right]}{\partial t^*} &= \frac{\tau}{L^2}D_{\overline{M}_n\cdot m_0}\nabla^2\left[\overline{M}_n\right]-\tau\rho[\overline{M}_n]\\
\frac{\partial\left[\overline{M}_n\right]}{\partial t^*} &= D^*_{\overline{M}_n\cdot}\nabla^2\left[\overline{M}_n\right]+\gamma^*[\overline{Mm_n}]-\rho^*[\overline{M}_n]
\end{aligned} \tag{7.54}$$

where

$$\begin{aligned}
D^*_{P_n} &= \frac{\tau D_{P_n}}{L^2}\ ,\ D^*_{P_c}=\frac{\tau D_{P_c}}{L^2}\\
D^*_{Mm_n} &= \frac{\tau D_{Mm_n}}{L^2}\ ,\ D^*_{Mm_c}=\frac{\tau D_{Mm_c}}{L^2}\\
D^*_{M_n} &= \frac{\tau D_{M_n}}{L^2}\ ,\ D^*_{M_c}=\frac{\tau D_{M_c}}{L^2}\\
M^* &= \frac{\widehat{Mm^{h1}}}{[Mm_0]^{h1}}\ ,\ P^*=\frac{\widehat{p}^{h2}}{[P_0]^{h2}}\\
\beta^* &= \frac{\tau\beta}{p_0}\ ,\ \eta^*=\frac{\tau\eta}{mm_0}\mu^*=\tau\mu\ ,\ \nu^*=\tau\nu\\
\phi^* &= \tau\phi\ ,\ \gamma^*=\frac{\tau\gamma[Mm_0]}{m_0}\ ,\ \alpha^*=\frac{\tau\alpha}{mm_0}\rho^*=\tau\rho
\end{aligned} \tag{7.55}$$

The following parameter values were used in our simulations of the non-dimensional P53-Mdm2 system:

$$
\begin{aligned}
D^*_{P_c} &= D^*_{P_n} = D^*_{Mm_c} = D^*_{Mm_n} = D^*_{M_c} = D^*_{M_n} = 9 \times 10^{-4} \\
\beta^* &= 0.5\ ,\ \mu^* = 0.003\ ,\ \nu^* = 1\ ,\ \alpha^* = 0.0175 \\
\eta^* &= 1\ ,\ \phi^* = 0.0175.\ ,\ \gamma^* = 0.5\ ,\ \rho^* = 0.025 \\
h1 &= 2\ ,\ h2 = 4\ ,\ M^* = 16\ ,\ P^* = 5 \qquad (7.56)
\end{aligned}
$$

Calculating the effective diffusion coefficient, D:

$$
\begin{aligned}
L &= 10\mu m \\
&= 10 \times 10^{-6} m \\
&= 10 \times 10^{-4} cm \qquad (7.57)
\end{aligned}
$$

$$
\begin{aligned}
400\tau &= 3hrs \\
\tau &= \frac{10800s}{400} = 27s \qquad (7.58)
\end{aligned}
$$

$$
\begin{aligned}
D^* &= \frac{\tau D}{L^2} \\
D &= \frac{L^2 D^*}{\tau} \\
&= \frac{10 \times 10 \times \left(10^{-6}\right)^2 m^2 \times D^*}{\tau} \\
&= \frac{10 \times 10 \times \left(10^{-4}\right)^2 cm^2 \times D^*}{\tau} \\
&= \frac{100 \times 10^{-8} cm^2 \times D^*}{\tau} \\
&= \frac{1 \times 10^{-6} cm^2 \times 9 \times 10^{-4}}{27s} \\
&= 0.33333333 \times 10^{-10} cm^2 s^{-1} \\
&= 3.3333333 \times 10^{-11} cm^2 s^{-1} \qquad (7.59)
\end{aligned}
$$

Calculating the production rate of P53, β:

$$
\begin{aligned}
p_0 &= 0.05 \mu m \Longrightarrow p_0 = 0.05 \times 10^{-6} M \\
\tau &= 27s \\
\beta^* &= \frac{\tau}{p_0} \beta \\
\beta &= \frac{p_0 \beta^*}{\tau} \\
&= \frac{0.05 \times 10^{-6} M \times 0.5}{27s} \\
&= 0.000925939 \times 10^{-6} M s^{-1} \\
&= 9.25939 \times 10^{-10} M s^{-1} \qquad (7.60)
\end{aligned}
$$

Calculating the degradation rate of P53, μ:

$$\begin{aligned}
\mu^* &= \tau\mu \\
\mu &= \frac{\mu^*}{\tau} \\
&= \frac{0.003}{27s} \\
&= 1.11 \times 10^{-4} s^{-1} \qquad (7.61)
\end{aligned}$$

Calculating the degradation rate of P53 dependent on Mdm2 concentration, ν:

$$\begin{aligned}
\nu^* &= \tau\nu \\
\nu &= \frac{\nu^*}{\tau} \\
&= \frac{1}{27s} \\
&= 0.03703704 s^{-1} \\
&= 0.04 s^{-1} \qquad (7.62)
\end{aligned}$$

Calculating the natural transcription rate of Mdm2 mRNA, α:

$$\begin{aligned}
mm_0 &= 0.05\mu m \\
\alpha^* &= \frac{\tau\alpha}{mm_0} \\
\alpha &= \frac{mm_0\alpha^*}{\tau} \\
&= \frac{0.05 \times 10^{-6} M \times 0.0175}{27s} \\
&= 0.00003241 \times 10^{-6} M s^{-1} \\
&= 3.241 \times 10^{-11} M s^{-1} \qquad (7.63)
\end{aligned}$$

Calculating the enhanced natural transcription rate of Mdm2 mRNA dependent on the concentration of P53, η:

$$\begin{aligned}
mm_0 &= 0.05\mu m \\
\eta^* &= \frac{\tau\eta}{mm_0} \\
\eta &= \frac{mm_0\eta^*}{\tau} \\
&= \frac{0.05 \times 10^{-6}M \times 1}{27s} \\
&= 0.00185185 \times 10^{-6}Ms^{-1} \\
&= 1.85 \times 10^{-9}Ms^{-1} \qquad (7.64)
\end{aligned}$$

Calculating the natural degradation rate of Mdm2 mRNA, ϕ:

$$\begin{aligned}
\phi^* &= \tau\phi \\
\phi &= \frac{\phi^*}{\tau} \\
&= \frac{0.0175}{27s} \\
&= 0.00064815s^{-1} \\
&= 6.4815 \times 10^{-4}s^{-1} \qquad (7.65)
\end{aligned}$$

Calculating the translation rate of Mdm2, γ:

$$\begin{aligned}
mm_0 &= 0.05\mu m \\
m_0 &= 2\mu m \\
\gamma^* &= \frac{\tau\gamma mm_0}{m_0} \\
\gamma &= \frac{m_0\gamma^*}{\tau mm_0} \\
&= \frac{0.5 \times 2 \times 10^{-6}M}{0.05 \times 10^{-6}M \times 27s} \\
&= 0.740s^{-1} \qquad (7.66)
\end{aligned}$$

Calculating the natural degradation rate of Mdm2, ρ

$$\begin{aligned}
\rho^* &= \tau\rho \\
\rho &= \frac{\rho^*}{\tau} \\
&= \frac{0.025}{27s} \\
&= 0.00092593s^{-1} \\
&= 9.2593 \times 10^{-4}s^{-1} \qquad (7.67)
\end{aligned}$$

Calculating the activation threshold of P53 degradation dependent on Mdm2, $\widehat{Mdm2}$: $\widehat{M}$:

$$\begin{aligned}
m_0 &= 2\mu m \\
h_1 &= 2 \\
M^* &= \frac{\widehat{M}^2}{m_0^2} \\
\widehat{M} &= \sqrt{M^* \times m_0^2} \\
\widehat{M} &= \sqrt{16 \times (2\mu m)^2} \\
&= 8 \times 10^{-6}\mu M \qquad (7.68)
\end{aligned}$$

Calculating the activation threshold for transcription of Mdm2 mRNA dependent on

P53,$\widehat{P53}$: $\widehat{P}$:

$$\begin{aligned} p_0 &= 0.5\mu m \\ h_2 &= 4 \\ P^* &= \frac{\widehat{P}^{\,4}}{p_0^4} \\ \widehat{P} &= \sqrt[4]{P^* \times p_0^4} \\ &= \sqrt[4]{5 \times (0.5\mu m)^4} \\ &= 0.74 \times 10^{-7}\mu M \end{aligned} \tag{7.69}$$

Bibliography

Alam-Nazki, A. and Krishnan, H. (2012). An investigation of spatial signal transduction in cellular networks. *BMC Systems Biology*, 6:83.

Alberts, B., Bray, D., Lewis, J., Raff, M., Roberts, K., and Watson, J. (1994). *Molecular Biology of the Cell.*, volume 3rd edition. New York: Garland Science.

Baek, J. H., Hatakeyama, J., Sakamoto, S., Ohtsuka, T., and Kageyama, R. (2006). Persistent and high levels of hes1 expression regulate boundary formation in the developing central nervous system. *Development*, 133:2467–2476.

Bar-Or, R. L., Maya, R., Segel, L. A., Alon, U., Levine, A. J., and Oren, M. (2000). Generation of oscillations by the p53-mdm2 feedback loop: A theoretical and experimental study. *PNAS*, 97(21):1125011255.

Bennett, I., Gattas, M., and Teh, B. (1999). The genetic basis of breast cancer and its clinical implications. *Aust. NZ J. Surg.*, 69(2):95–105.

Berg JM, T. J. (2002). *Biochemistry*. New York: W H Freeman.

Bernard, S., Čajavec, B., Pujo-Menjouet, L., Mackey, M., and Herzel, H. (2006). Modelling transcriptional feedback loops: the role of Gro/TLE1 in Hes1 oscillations. *Phil. Trans. Roy. Soc. A*, 364:1155–1170.

Bose, I. and Ghosh, B. (2007). The p53-mdm2 network: from oscillations to apoptosis. *J. Biosci.*, 32:991–997.

Brown, G. C. and Kholodenko, B. N. (1999). Spatial gradients of cellular phosphoproteins. *Federation of European Biochemical Societies.*, 457:452–454.

Busenberg, S. and Mahaffy, J. (1985). Interaction of spatial diffusion and delays in models of genetic control by repression. *Journal of Mathematical Biology*, 22:313–33.

Cangiani, A. and Natalini, R. (2010). A spatial model of cellular molecular trafficking including active transport along microtubules. *J. Theor. Biol.*, 267:614–625.

Ciliberto, A., Novak, B., and Tyson, J. J. (2005). Steady states and oscillation in p53/mdm2 network. *Cell Cycle*, 4(3):488–493.

Davidson, E. (2005). Gene regulatory networks. *PNAS*, 102:4935.

Dawson, S., Turner, D., Weintraub, H., and Parkhurst, S. (1995). Specificity for the hairy/enhancer of split basic helix-loop-helix (bhlh) proteins maps outside the bhlh domain and suggests two separable modes of transcriptional repression. *Mol. Cell. Biol.*, 15:6923–6931.

DeJong, H. (2002). Modeling and simulation of genetic regulatory systems: A literature review. *J. Comp. Biol.*, 9(1):67–103.

Feki, A. and Irminger-Finger, I. (2004). Mutational spectrum of p53 mutations inprimary breast and ovarian tumors. *Crit. Rev. Oncol. Hematol.*, 52:103–116.

Freedman, D. and Levine, A. (1998). Nuclear export is required for degradation of endogenous p53 by mdm2 and human papillomavirus e6. *Mol. Cell. Biol.*, 18:72887293.

Freeman, M. (2000). Feedback control of intercellular signalling in development. *Nature.*, 408:313–319.

Fridman, J. and Lowe, S. (2003). Control of apoptosis by p53. *Oncogene*, 22:9030–9040.

Gasper, Tkacik. Thomas, G. W. B. (2008). The role of input noise in transcriptional reaction. *PLoS ONE*, 3(7):2774–2785.

Geva-Zatorsky, N., Rosenfeld, N., Itzkovitz, S., Milo, R., Sigal, A., Dekel, E., Yarnitzky, T., Liron, Y., Polak, P., Lahav, G., and Alon, U. (2006). Oscillations and variability in the p53 system. *Mol. Syst. Biol.*, 2:E1–E13.

Goodwin, B. (1965). Oscillatory behaviour in enzymatic control processes. *Adv. Enzyme Reg.*, 3:425–428.

Gordon, K., van Leeuwen, I., Lane, S., and Chaplain, M. (2009). Spatio-temporal modelling of the p53-mdm2 oscillatory system. *Math. Model. Nat. Phenom.*, 4(3):97–116.

Griffith, J. S. (1968a). Mathematics of cellular control process i. negative feedback to one gene. *J. Theor. Biol.*, 20:202–208.

Griffith, J. S. (1968b). Mathematics of cellular control process ii. positive feedback to one gene. *J. Theor. Biol.*, 20:209–216.

Grima, R., Schmidt, D., and Newman, T. (2012). Steady-state fluctuations of a genetic feedback loop: An exact solution. *J. Chem. Phys.*, 137:035104.

Hainaut, P. and Hollstein, M. (2000). p53 and human cancer: the first ten thousand mutations. *Adv. Cancer Res.*, 77:81–137.

Hanahan, D. and Weinberg, R. (2000). The hallmarks of cancer. *Cell*, 100 (1):57–70.

Hengartner, M. (2000). The biochemistry of apoptosis. *Nature*, 407(6805):770–776.

Hirata, H., Yoshiura, S., Ohtsuka, T., Bessho, Y., Harada, T., Yoshikawa, K., and Kageyama, R. (2003). Oscillatory expression of the bhlh factor hes1 regulated by a negative feedback loop. *Science*, 298:840–843.

Hornos, J., Schultz, D., Innocentini, G., Wang, J., Walczak, A., Onuchic, J., and Wolynes, P. (2005). Self-regulating gene: an exact solution. *Phys. Rev. E*, 72:051907.

Istvan Petak, J. A. H. and Kopper., L. (2006). Molecular targeting of cell death signal transduction pathways in cancer. *Current Signal Transduction Therapy*, 1:113–131.

Jing, N. and Tweardy, D. (2005). Targeting stat3 in cancer therapy. *Anticancer Drugs.*, 16(6):601–607.

Kageyama, R.; Ohtsuka, T. (1999). The notch-hes pathway in mammalian neural development. *Cell Research*, 9(3):179–188.

Kamakura, S., Oishi, K., Yoshimatsu, T., Nakafuku, M., Masuyama, N., and Gotoh, Y. (2004). Hes binding to stat3 mediates crosstalk between notch and jak-stat signalling. *Nature Cell Biology*, 6:547–554.

Karlebach, G. and Shamir., R. (2008). Modelling and analysis of gene regulatory networks. *The Blavatnik School of Computer Science.*, 9:770–780.

Katrien Vermeulen, Z. N. B. and Bockstaele, D. R. V. (2003). Cell cycle and apoptosis. *Cell Prolif.*, 36:165–175.

King, K. L. and Cidlowski, J. A. (1998). Cell cycle regulation and apoptosis. *Annu. Rev. Physiol.*, 60:601–617.

Kobayashi, T. and Kageyama, R. (2011). Hes1 oscillations contribute to heterogeneous differentiation responses in embryonic stem cells. *Genes*, 2:219–228.

Kussie, P., Gorina, S., and Marechal, V. (1996). Structure of the mdm2 oncoprotein bound to the p53 tumour suppressor transactivation domain. *Science*, 274:948–953.

Landers, J., Cassel, S., and George, D. (1997). Translational enhancement of mdm2 oncogene expression in human tumor cells containing a stabilized wild-type p53 protein. *Cancer Res.*, 57(16):3562–3568.

Lane, D. and Crawford, L. (1979). Tantigen is bound to a host protein in sv40-transformed cells. *Nature*, 278:261263.

Lawen, A. (2003). Apoptosisan introduction. *BioEssays*, 25:888–896.

Levine, M., Jones, C., Kern, A., Lindfors, H., and Begun, D. (2006). Novel genes derived from noncoding dna in drosophila melanogaster are frequently x-linked and exhibit testis-biased expression. *Proc. Natl. Acad. Sci. USA*, 103:9935–9939.

Li, M., Brooks, C., and F., W.-B. (2003). Mono-versus polyubiquitination: differential control of p53 fate by mdm2. *Science*, 302(5652):1972–1975.

Lomakin, A. and Nadezhdina, E. (2010). Dynamics of nonmembranous cell components: Role of active transport along microtubules. *Biochemistry (Moscow)*, 75(1):7–18.

Lozano, G. and Zambetti, G. (2005). What have animal models taught us about the p53 pathway? *J. Pathol.*, 205(2):206–20.

Lu, H. and Levine, A. (1995). Human tafii31 protein is a transcriptional coactivator of the p53 protein. *Proc. Natl. Acad. Sci. USA*, 92:51545158.

Ma, C., Adjei, A., Salavaggione, O., Coronel, J., Pelleymounter, L., Wang, L., Eckloff, B., Schaid, D., Wieben, E., Adjei, A., and Weinshilboum, R. (2005). Human aromatase: gene resequencing and functional genomics. *Cancer Res.*, 65(23):11071–11082.

Mahaffy, J. and Pao, C. (1984). Models of genetic control by repression with time delays and spatial effects. *J. Math. Biol.*, 20:39–57.

Manfredi, J. (2010). The mdm2-p53 relationship evolves: Mdm2 swings both ways as an oncogene and a tumor suppressor. *Genes Dev.*, 24(15):1580–1589.

Martin, W. H. (2010). The nuclear envelope. *Cold Spring Harbor Perspect. Biol.*, 2(3):1–16.

Masamizu, Y., Ohtsuka, T., Takashima, Y., Nagahara, H., Takenaka, Y., Yoshikawa, K., Okamura, H., and Kageyama, R. (2006). Real-time imaging of the somite segmentation clock: revelation f unstable oscillators in the individual presomitic mesoderm cells. *Proc. Natl. Acad. Sci. USA*, 103:1313–1318.

Melino, G., Lu, X., Gasco, M., Crook, T., and Knight, R. (2003). Functional regulation of p73 and p63: development and cancer. *Trends Biochem. Sci.*, 28:663670.

Miekisz, J. and Szymańska, P. (2013). Gene expression in self-repressing system with multiple gene copies. *Bull. Math. Biol.*, 75:317–330.

Mihalas, G. I., Neamtu, M., Opris, D., and Horhat, F. (2006). A dynamic p53-mdm2 with time delay. *Chaos, Solitons, Fractals*, 30(4):936–945.

Momiji, H. and Monk, N. (2008). Dissecting the dynamics of the hes1 genetic oscillator. *J. Theor. Biol.*, 254:784–798.

Monk, N. (2003). Oscillatory expression of Hes1, p53, and NF-κB driven by transcriptional time delays. *Curr. Biol.*, 13:1409–1413.

Nikol'skii, N. N. and Vasilenko, K. P. (2000). Stat pathway of intracellular signaling. *Journal of Evolutionary Biochemistry and Physiology*, 36(6):655–661.

O'Connell, M. and Cimprich, K. (2005). G2 damage checkpoints: what is the turn on? *J. Cell. Sci.*, 118(1):1–6.

Ohsako, S., Hyer, J., Panganiban, G., Oliver, I., and Caudy, M. (1994). hairy function as a dna binding hlh repressor of drosophila sensory organ formation. *Genes & Dev.*, 8:2743–2755.

Oswald F, Tuber B, D. T. B. S. K. U. A. G. L. S. S. R. (2001). p300 acts as a transcriptional coactivator for mammalian notch-1. *Mol. Cell. Biol*, 21 (22):7761–7774.

Ouhammouch, M., Dewhurst, R., Hausner, W., Thomm, M., and Geiduschek, E. (2003). Activation of archaeal transcription by recruitment of the tata-binding protein. *Proc. Natl. Acad. Sci. USA*, 9:5097–5102.

Puszynski, K., Bertolusso, R., and Lipniacki, T. (2009). Crosstalk between p53 and nuclear factor-kb systems: pro- and anti-apoptotic functions of nf-kb. *IET Syst. Biol.*, 3(5):356367.

Ramos, A., Innocentini, G., and Hornos, J. (2011). Exact time dependent solutions for a self-regulating gene. *Phys. Rev. E*, 83:062902.

Rangamani, P. and Iyengar, R. (2006). Modelling spatio-temporal interactions within the cell. *J. Biosci.*, 32:157167.

Robbins, Cotran, Kumar, Abbas, and Fausto (2004). *Pathological Basis of Disease*, volume 7th Edition. Elsevier.

Roth, J., Knig, C., Wienzek, S., Weigel, S., Ristea, S., and Dobbelstein, M. (1998). Inactivation of p53 but not p73 by adenovirus type 5 e1b 55-kilodalton and e4 34-kilodalton oncoproteins. *J. Virol.*, 72(11):8510–8516.

Ryoichiro, Kageyama, T. O. H. S. and Imayoshi, I. (2008). Dynamic notch signaling in neural progenitor cells and a revised view of lateral inhibition. *NATURE NEUROSCIENCE*, 11(11):1247–1251.

Sang, L., Roberts, J., and Coller, H. (2010). Hijacking HES1: Tumors co-opt the anti-differentiation stategies of queiscent cells. *Trends Mol. Med.*, 16:17–26.

Schindler, C., Shuai, K., Prezioso, V., and J.E. Darnell, J. (1992b). Interferon-dependent tyrosine phosphorylation of a latent cytoplasmic transcription factor. *Science*, 257:809–813.

Schwartz, G. K. and Shah, M. A. (2005). Targeting the cell cycle: A new approach to cancer therapytargeting the cell cycle: A new approach to cancer therapy. *JOURNAL OF CLINICAL ONCOLOGY*, 23(36):9408–9421.

Shi-Wei, Y., Qi, W., Bai-Song, X., and Feng-Shou, Z. (2007). Oscillatory activities in regulatory biological networks and hopf bifurcation. *Chin. Phys. Lett.*, 24(6):1771–1774.

Shimojo, H., Ohtsuka, T., and Kageyama, R. (2008). Oscillations in notch signaling regulate maintenance of neural progenitors. *Neuron*, 58:52–64.

Shymko, R. M. and Glass, L. (1974). Spatial switching in chemical reactions with heterogeneous catalysis. *Journal of Chemical Physics*, 60(3):835–841.

Smithgall, T., Briggs, S., Schreiner, S., Lerner, E., Cheng, H., and Wilson, M. (2000). Control of myeloid differentiation and survival by stats. *Oncogene*, 19:2612–2618.

Solomon, E., Berg, L., and Martin, D. (2007). *Biology*, volume 8th Edition,. Thomson Brooks/Cole.

Stryer and Lubert (2002). *Biochemistry*, volume Fifth edition. W. H. Freeman and Company.

Sturm, T. and Weber, A. (2008). Investigating generic methods to solve hopf bifurcation problems in algebraic biology. *Springer-Verlag.*, 5147.

Sturrock, M., Terry, A., Xirodimas, D., Thompson, A., and Chaplain, M. (2011). Spatio-temporal modelling of the Hes1 and p53–Mdm2 intracellular signalling pathways. *J. Theor. Biol.*, 273:15–31.

Sturrock, M., Terry, A., Xirodimas, D., Thompson, A., and Chaplain, M. (2012). Influence of the nuclear membrane, active transport and cell shape on the Hes1 and p53–Mdm2 pathways: Insights from spatio-temporal modelling. *Bull. Math. Biol.*, 74:1531–1579.

Takahashi, I., Nakanishi, S., Kobayashi, E., Nakano, H., Suzuki, K., and Tamaoki, T. (1989). Hypericin and pseudohypericin specifically inhibit protein kinase c: possible relation to their antiretroviral activity. *Biochem. Biophys. Res. Commun.*, 165(3):1207–1212.

Takebayashi, K., Sasai, Y., Sakai, Y., Watanabe, T., Nakanishi, S., and Kageyama, R. (1994). Structure, chromosomal locus, and promoter analysis of the gene encoding the mouse helix-loop-helix factor HES-1. *J. Biol. Chem.*, 269:5150–5156.

Thut, C., Goodrich, J., and Tjian, R. (1997). Repression of p53-mediated transcription by mdm2: a dual mechanism. *Genes Dev.*, 11(15):1974–1986.

Vassilev, L., Vu, B., and Graves, B. (2004). In vivo activation of the p53 pathway by small-molecule antagonists of mdm2. *Science*, 303:844–8.

Vogelstein, B., Fearon, E., Hamilton, S., Kern, S., Preisinger, A., Leppert, M., Nakamura, Y., White, R., Smits, A., and Bos, J. (1988). Genetic alterations during colorectal-tumor development. *N. Engl. J. Med.*, 319(9):525–532.

Vousden, K. and Lu, X. (2002). Live or let die: the cell's response to p53. *Nat. Rev. Cancer.*, 2:594–604.

Walker, F., Zhang, H.-H., Odorizzi, A., and Burgess, A. (2011). Lgr5 is a negative regulator of tumourigenicity, antagonizes wnt signalling and regulates cell adhesion in colorectal cancer cell lines. *PLoS ONE*, 6(7):e22733.

Wegenka, U., Buschmann, J., Lutticken, C., Heinrich, P., and Horn, F. (1993). Acutephase response factor, a nuclear factor binding to acute-phase response elements, is rapidly activated by interleukin-6 at the posttranslational level. *Mol. Cell Biol.*, 13:276–288.

Weis, K. (2003). Regulating access to the genome: nucleocytoplasmic transport throughout the cell cycle. *Cell*, 112:441–451.

Yoshiura, S., Ohtsuka, T., Takenaka, Y., Nagahara, H., Yoshikawa, K., and Kageyama, R. (2007). Ultradian oscillations of stat, smad, and hes1 expression in response to serum. *Proc. Natl. Acad. Sci. USA*, 104:11292–11297.

Yutaka, H. and Shinji, H. (2011). Time delay effects on oscillation profiles in cyclic gene regulatory networks: Harmonic balance approach. *American Control Conference*, pages 2891–2896.

Zeiser, S., Muller, J., and Liebscher, V. (2007). Modeling the Hes1 oscillator. *J. Comp. Biol.*, 14:984–1000.

Zhang, T., Brazhnik, P., and Tyson, J. J. (2007). Exploring mechanisms of the dna-damage response p53 pulses and their possible relevance to apoptosis. *Cell Cycle*, 6(1):85–94.